

**Identification and Characterisation of MAP4K3 as a Novel Cell Death
Regulator**

Thesis submitted for the degree of
Doctor of Philosophy
at the University of Leicester

by

David Stephen Dickens
MRC Toxicology Unit
University of Leicester

August 2007

UMI Number: U491706

All rights reserved

INFORMATION TO ALL USERS

The quality of this reproduction is dependent upon the quality of the copy submitted.

In the unlikely event that the author did not send a complete manuscript and there are missing pages, these will be noted. Also, if material had to be removed, a note will indicate the deletion.



UMI U491706

Published by ProQuest LLC 2013. Copyright in the Dissertation held by the Author.
Microform Edition © ProQuest LLC.

All rights reserved. This work is protected against
unauthorized copying under Title 17, United States Code.



ProQuest LLC
789 East Eisenhower Parkway
P.O. Box 1346
Ann Arbor, MI 48106-1346

Abstract

Acquired resistance towards apoptosis is widely believed to be a hallmark of most types of cancer (Hanahan and Weinberg 2000). Defects in the apoptotic pathway can make cancer cells resistant to chemotherapy and irradiation. The resistance to apoptosis constitutes an important clinical problem (Igney and Krammer 2002).

To identify novel regulators of apoptosis, a vector based RNAi library screen was performed with UV irradiation used to induce apoptosis. The screen revealed that a shRNA targeting MAP4K3 was the most highly expressed following UV treatment and as such this candidate cell death regulator was selected for further experimentation. MAP4K3 is a Ste20 kinase protein that is activated by UV irradiation and from overexpression experiments it was shown to induce JNK activation (Deiner, Wang et al. 1997).

To confirm the screen results, siRNA experiments revealed that suppression of MAP4K3 conferred increased cell survival following UV and cisplatin induced apoptosis. Ectopic expression showed that MAP4K3 can induce apoptosis with the kinase activity of MAP4K3 required for the maximal induction. From deletion mutants I have determined that the N-terminus kinase domain is sufficient to induce apoptosis. The MAP4K3 induced apoptosis was found to be caspase dependent and induced a conformational change of Bax with the co-overexpression of Bclxl rescuing the cell death phenotype. This suggests that MAP4K3 could activate the intrinsic pathway of apoptosis.

Ectopic expression of MAP4K3 was used to investigate the involvement of signalling transduction pathways and revealed an increase in phosphorylation of JNK and p38 kinases. The MAP4K3 Δ C mutant revealed that the kinase domain induces a phosphorylation cascade resulting in the increase in phosphorylation of the transcription factors, Stat-1 and c-Jun. The regulation of MAP4K3 was investigated and experiments suggest that the 26S proteasome degrades MAP4K3 as a proteasome inhibitor stabilises MAP4K3 expression levels. This degradation could be ubiquitin mediated as co-overexpression studies with HA-ubiquitin reveal that MAP4K3 co-immunoprecipitates with the HA tagged ubiquitin.

Acknowledgments

I would like to thank Dr Miguel Martins, Dr Nicoleta Moiso, Dr Valentina Fedele and Elisabeth Reid for the help and support they have given me throughout my time working in the laboratory and during the writing up of this project. It has been invaluable to me.

Contents

Identification and characterisation of MAP4K3 as a novel cell death regulator..... 1

Abstract 2

Acknowledgments..... 3

Contents..... 4

List of Figures 8

Abbreviations 10

Chapter 1: Introduction 12

 Cancer..... 12

 Apoptosis..... 15

 Intrinsic pathway of apoptosis..... 19

 DNA damage induced apoptosis 21

 The MAP kinase pathways..... 23

 Ste20 type kinases 29

 Ubiquitin mediated proteasomal degradation..... 35

 RNAi interference mechanism 39

Aim..... 45

Chapter 2: Materials and Methods 46

 Materials..... 46

 Table 2.1- Primary antibodies 46

 Table 2.2- Secondary antibodies conjugated to HRP 47

 Table 2.3- DNA Plasmids 48

 Table 2.4- siRNA nucleotides 49

Methods	50
Cell culture	50
Retroviral expression.....	50
Retroviral infection.....	51
Transfections	52
Cell Treatments	54
FACS Analysis	55
Crystal violet assay.....	55
Cell fixation.....	55
Cell Survival assay	56
BrdU proliferation assay	56
Immunocytochemistry	57
Microscopy and cell death counts	57
Amplification of plasmid DNA.....	58
DNA sequencing	58
Recovery of shRNA inserts from infected pRS K330 U2OS cells	58
Generation of MAP4K3 expression plasmids.....	59
RNA extraction.....	66
Quantitative RT-PCR	67
Quantitative PCR.....	68
Protein lysates.....	68
Immunoprecipitation experiments.....	69
Western blotting	69
Chapter 3: Results	71

Chapter 3.1: An RNAi-based library screen to identify regulators of UV induced cell death	71
Generation of a U2OS cell line expressing the K330 RNAi library	72
Establishment of UV assay conditions	73
Cell death suppressor screen	75
Identification of candidate modulators of UV induced cell death	77
Chapter 3.2: The role of MAP4K3 in cell death and proliferation using gain & loss of function analysis	82
Establishment of a system for the siRNA-mediated transient suppression of MAP4K3	83
siRNA mediated suppression of MAP4K3 protects from DNA damage induced cell death	84
MAP4K3 triggers caspase dependent cell death	87
The MAP4K3 Δ 343-874 deletion mutant is sufficient to induce cell death	89
MAP4K3 modulates mitochondria-dependent apoptotic cell death	91
Suppression of MAP4K3 enhances cell proliferation	96
Chapter 3.3: Analysis of MAP4K3 dependent signal transduction pathways	97
Overexpression of MAP4K3 results in enhanced phosphorylation of JNK and p38	99
UV treatment has no effect on MAP4K3-EGFP expression levels	111
siRNA mediated suppression of MAP4K3 or MAP4K3 K45E overexpression does not effect UV-induced phosphorylation of JNK and p38	113
Chapter 3.4: Proteasomal regulation of MAP4K3	116
Proteasomal regulation of MAP4K3	117
Chapter 3.5: Analysis of MAP4K3 levels in normal and tumour tissues	122
In-silico analysis of MAP4K3 in cancer	123
Experimental analysis of MAP4K3 levels in normal and tumour tissues	126

Discussion 129

 An RNAi-based library screen to identify regulators of UV induced cell death..... 129

 The role of MAP4K3 in cell death and proliferation using gain & loss of function analysis
 133

 Analysis of MAP4K3 dependent signal transduction pathways 143

 Proteasomal regulation of MAP4K3 155

 Analysis of MAP4K3 levels in normal and tumour tissues 160

 Final Discussion 163

 Further Work 166

References 170

List of Figures

Figure 1.1: Hallmarks of cancer	14
Figure 1.2: Intrinsic pathway of apoptosis	18
Figure 1.3: Stress response pathways	25
Figure 1.4: Ste20 kinase family	31
Figure 1.5: The involvement of MAP4K3 in the JNK and mTOR pathways	34
Figure 1.6 Ubiquitin proteasome proteolytic pathway	36
Figure 1.7 RNAi mechanism	41
Figure 2.1 pRetrosuper library vector	51
Figure 2.2 Amino acid sequence of MAP4K3	62
Figure 2.3 MAP4K3 fragments subcloned into pcDNA3.1/CT-GFP	63
Figure 2.4 MAP4K3 fragments subcloned into pEGFP N-1 plasmid	66
Figure 3.1.1 Diagram illustrating the strategy for the generation of a human cell line expressing a stable shRNA library.	73
Figure 3.1.2 Establishment of UV assay conditions	75
Figure 3.1.3 Schematic representation of the UV induced cell death suppressor RNAi library screen.	77
Figure 3.1.4: Population of identified hairpin sequences before and after UV treatment	79
Table 3.1.5: Candidate cell death suppressors and cell death sensitizers identified by the UV-induced RNAi screen	81
Figure 3.2.1: siRNA mediated suppression of MAP4K3 protects from DNA damage induced cell death.	84
Figure 3.2.2: Overexpression of MAP4K3 induces caspase dependent cell death	89
Figure 3.2.3: MAP4K3 kinase domain is sufficient to induce cell death	91
Figure 3.2.4: MAP4K3 induces Bax conformational change	94

Figure 3.2.5: MAP4K3 induced cell death is suppressed by BclxL overexpression	95
Figure 3.2.6 siRNA mediated suppression of MAP4K3 induces an increase in DNA synthesis	97
Figure 3.3.1: Confirmation of expression of MAP4K3 EGFP tagged protein fragments	100
Figure 3.3.2: MAP4K3 induces JNK and p38 phosphorylation	103
Figure 3.3.3: MAP4K3 induces phosphorylation of Stat-1	105
Figure 3.3.4: MAP4K3 does not affect expression levels of proteins involved in cell death	107
Figure 3.3.5: MAP4K3 Δ C induces p38 and JNK phosphorylation in U2OS cell line	110
Figure 3.3.6: UV treatment has no effect on MAP4K3-EGFP expression	112
Figure 3.3.7: MAP4K3 K45E does not act as a dominant negative on UV induced stress response pathways	115
Figure 3.3.8: siRNA mediated MAP4K3 knockdown has no effect on UV induced stress response pathways	116
Figure 3.4.1: Proteasome inhibition stabilises MAP4K-EGFP	120
Figure 3.4.2: MAP4K3 IP complex is poly-ubiquitinated	122
Figure 3.5.1 : Gene expression analysis of MAP4K3 in normal tissues versus tumours	126
Figure 3.5.2: Comparison of MAP4K3 mRNA levels in control vs ovarian cancer samples	128
Figure 4.1: Proposed model for MAP4K3 involvement in the regulation of cell death	166

Abbreviations

CAD	Caspase Activated Deoxyribonuclease
cDNA	Complementary Deoxynucleic Acid
CLK3	Cdc-Like Kinase 3
EGFP	Enhanced Green Fluorescent Protein
ES	Embryonic Stem Cells
GCK	Germinal Centre Kinase (MAP4K2)
GCKR	Germinal Centre Kinase-Related (MAP4K5)
GFP	Green Fluorescent Protein
GLK	Germinal Centre-Like Kinase (MAP4K3)
H2B	Histone 2B
HPK1	Hematopoietic Progenitor Kinase 1 (MAP4K1)
iCAD	Caspase Activated Deoxyribonuclease Inhibitor
IP	Immunoprecipitation
JNK	c-Jun Amino Terminal Kinase
kDa	Kilodaltons
MAD2L2	Mitotic Arrest Deficient-Like 2
MAPK	Mitogen Activated Protein Kinase
MAPKAPK2	MAP Kinase Activated Protein Kinase 2
MAPKK	Mitogen Activated Protein Kinase Kinase
MAPKKK	Mitogen Activated Protein Kinase Kinase Kinase
MEFs	Mouse Embryonic Fibroblasts
MOMP	Mitochondrial Outer Membrane Permeabilisation

mTOR	Mammalian Target of Rapamycin
PBS	Phosphate Buffered Saline
PCR	Polymerase Chain Reaction
PTK2B	Protein Tyrosine Kinase 2 Beta
QRT-PCR	Quantitative Reverse Transcriptase PCR
RFP	Red Fluorescent Protein
RISC	RNA Induced Signalling Complex
RNAi	Ribonucleic Acid Interference
ROS	Reactive Oxygen Species
shRNA	Short Hairpin RNA
siRNA	Short Interfering RNA
Stat-1	Signal Transducer and Activator of Transcription 1
TNF α	Tumour Necrosis Factor
zVAD-fmk	Benzyloxycarbonyl-val-ala-asp(Ome)-fluoromethylketone

Chapter 1: Introduction

Cancer

Cancers are diseases in which unremitting clonal expansion of somatic cells causes pathology by invading and colonising within normal tissue, where malignant cells out-compete the local population (Evan and Vousden 2001). In 2003 276,678 people in the UK were diagnosed with malignant tumours and the number of deaths in 2004 was 153,397. Over half of all new cases are localised to breast, lung, colon and prostate (CRUK 2007). The probability of cancer arising in an individual is 1 in 3 worldwide (Evan and Vousden 2001). The risk of developing cancer tends to increase with age, with 64% of cases diagnosed in people aged over 65 and more than a third of cases in people over 75.

The pathological analysis of pre-malignant lesions reveal intermediate steps which occur whilst the cells are progressing towards the invasive cancer (Foulds 1954). This is a multi-step process which is caused by the accumulation of genetic mutations within a cell and its progeny. The accumulation of four to seven mutations are unpredictable, rate-limiting events (Renan 1993). The multi-step process of cancer refers to a series of changes within a population of cells. The tumour cells can acquire upto six essential alterations in their physiology; loss of dependence on growth signals, insensitive to growth inhibitory signals, evasion of apoptosis, limitless replicative potential, sustained angiogenesis and tissue invasion (Hanahan and Weinberg 2000)(Figure 1.1). Cell surface receptors on tumour cells may become deregulated leading to loss of dependence on growth signals, for example many tumours upregulate erbB-2 (Her2). ErbB-2 is a receptor tyrosine kinase that is normally involved in the signal transduction pathways leading to cell growth and differentiation (Olayioye 2001). The upregulation of erbB-2 in tumour cells leads to ligand-independent

signalling (Di Fiore, Pierce et al. 1987). Anti-proliferative signals operate to maintain tissue homeostasis and cellular quiescence. An example of cancer cell avoidance of this signal is the disruption of the pRb pathway in which the cellular transcription factor E2F is liberated from regulation thus allowing proliferation and desensitizing the cells to antigrowth factors (Geng, Eaton et al. 1996; Herrera, Sah et al. 1996). Cell cycle checkpoints and other cellular control mechanisms are in place to limit the growth of cells with genetic damage and initiate cell death, however, tumour cells lose these control mechanisms (Igney and Krammer 2002). The cloning and characterisation of Bcl-2 has shown the importance of apoptosis in tumour development. Bcl-2, an anti-apoptotic protein, is up-regulated in follicular lymphoma cells by a chromosomal translocation that couples the Bcl-2 gene to the immunoglobulin heavy chain (Tsujimoto, Cossman et al. 1985). When co-expressed with *myc* in transgenic mice Bcl-2 gene promotes B-cell lymphomas by enhancing lymphocyte survival (Strasser, Harris et al. 1990). The replicative potential is limited by the telomeres which are situated at the termini of the chromosome. With each replicative cycle the telomeres are shortened until the cells enter a crisis state and undergo cell death. This is overcome in cancer cells by telomere maintenance which is evident in nearly all types of malignancy (Shay and Bacchetti 1997). For tumours to progress to a larger size, they need to develop the ability to induce angiogenesis in order to divert the local nutrient supply (Bouck, Stellmach et al. 1996). Due to the loss of dependency on growth signals from hormones or tissue matrix proteins, tumour cells develop the ability to separate from the initial tumour site and colonise parts of the body that have space and access to nutrients. This process is known as metastatic spreading and is responsible for 90% of human cancer deaths (Sporn 1996).

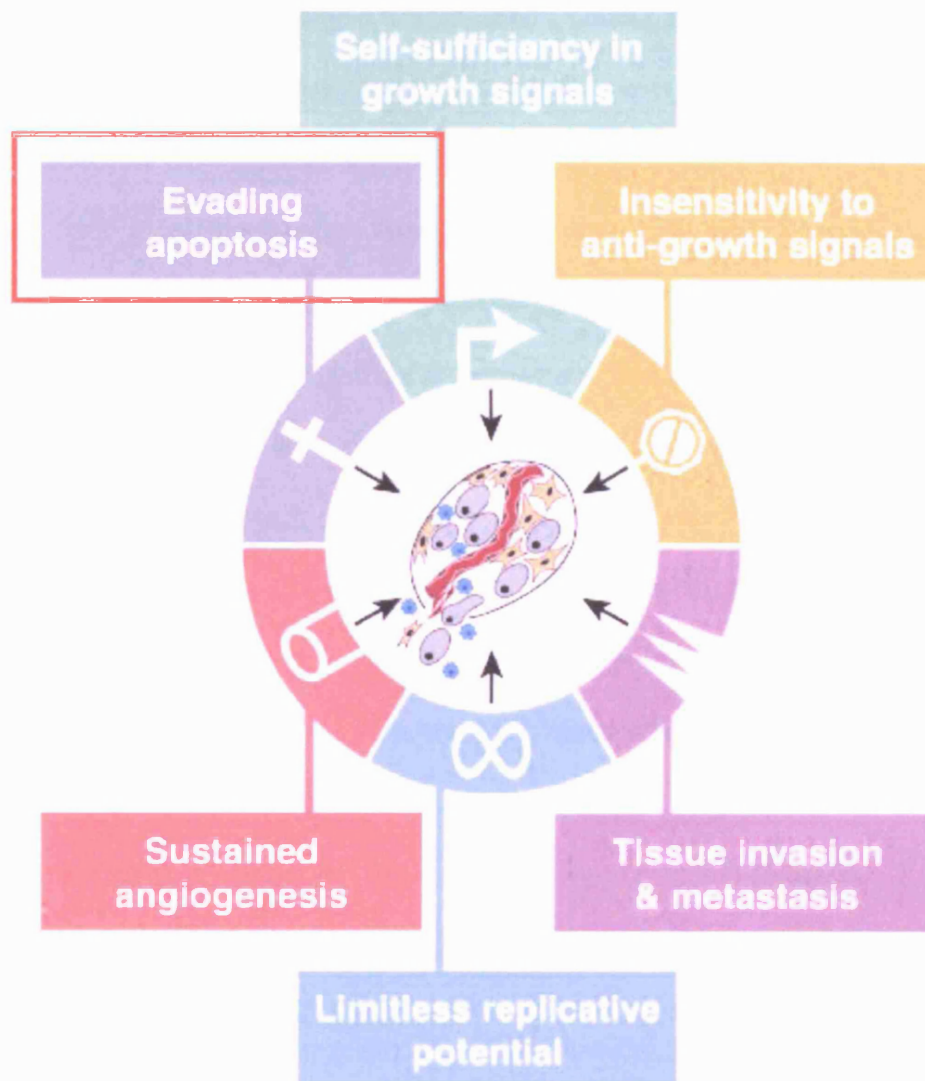


Figure 1.1: Hallmarks of cancer

Tumour cells are thought to acquire six major alterations to their physiology. This multistep process involves loss of growth factor dependence, insensitivity to growth inhibitory signals, evasion of apoptosis, unlimited replicative potential, sustained angiogenesis and tissue invasion. The red box is present to indicate the direction of research in this project. Diagram from (Hanahan and Weinberg, 2000)

The multi-step process is illustrated in humans by colorectal cancer, in which the cancer forms over decades and appears to require at least seven distinct genetic mutations (Kinzler and Vogelstein 1996). If an individual has inherited a genetic mutation (for example the APC gene in colorectal cancer) their risk of acquiring the disease is greatly increased (Kinzler and Vogelstein 1996). *In vitro* models using human primary cells have shown that cells do not readily form tumour cell lines unless there is expression of the telomerase catalytic subunit along with two oncogenes (the simian virus 40 large-T oncoprotein and an oncogenic allele of H-ras) (Hahn, Counter et al. 1999). This causes tumorigenic conversion of the cell. *In vivo* models using transgenic mice have produced mice with a heritable predisposition to develop specific cancers by expression of oncogenes or loss of function of tumour suppressor genes. The cells from the tumours that develop acquire increases in proliferation, decreases in apoptosis and the ability to induce angiogenesis (Bergers, Hanahan et al. 1998). Genetic mutations are caused by genomic instability which occurs on two levels; at the nucleotide level (subtle changes in gene sequences or regulatory domains) or at the chromosome level (changes in chromosome number or translocation of chromosomes) (Lengauer, Kinzler et al. 1998). Genomic instability can be thought of as an enabling characteristic of tumour development (Hanahan and Weinberg 2000).

Apoptosis

Both inactivating mutations in pro-apoptotic genes and increased expression of anti-apoptotic genes can occur in malignant cells (Evan and Vousden 2001). Two fundamental different forms of cell death, necrosis and apoptosis, have been defined. Necrosis is usually considered to be an uncontrolled process that results in the disruption of the cell membrane and the progressive breakdown of cell structures in response to violent environmental changes such as severe hypoxia and extremes of temperature. This type of cell death is associated with

organelle swelling and early plasma membrane rupture (Farber and El-Mofty 1975); (Golstein and Kroemer 2007). The name “apoptosis” was first coined in a paper in 1972, to refer to cells undergoing cell death with defined morphological observations (Kerr, Wyllie et al. 1972; Kerr 2002). Apoptosis is an active process of cellular suicide that is a tightly regulated, energy-dependent process and has been conserved throughout evolution (Yuan 1996). Apoptotic cells undergo a typical series of morphological changes that are distinct from necrotic cell death. The cell membrane remains intact during the early stages, although subtle changes are observed, for example the exposure of phosphatidylserine to the external surface. Characteristic changes include cell shrinkage, membrane blebbing, nuclear chromatin condensation and DNA fragmentation (Kerr 2002; Danial and Korsmeyer 2004). The cell breaks down into cellular fragments, known as apoptotic bodies that are engulfed (*in vivo*) through phagocytosis (Savill and Fadok 2000). In cell culture apoptotic bodies lose the integrity of the plasma membrane during the later stages, and eventually undergo secondary necrosis (Vermeulen, Van Bockstaele et al. 2005).

Apoptosis plays a physiological role in the developmental morphogenesis of tissues in cellular homeostasis. It has been well defined in the nematode worm (*C. elegans*). The adult worm has 959 somatic cells, but during the developmental stages of its maturation the total number of cells reaches 1090. 131 of these cells become apoptotic, including 105 neurons (Sulston and Horvitz 1977). The developmental role of apoptosis has been highly conserved throughout evolution, for example the maturation of the lungs in foetuses and neonates (Scavo, Ertsey et al. 1998). Apoptosis occurs in adult organisms to maintain normal cellular homeostasis. This includes regulating a response to infectious agents (Shibata, Kyuwa et al. 1994) and eliminating cells that have acquired DNA damage (Schwarz, Bhardwaj et al. 1995). Increased levels of apoptosis lead to immunodeficiency, infertility and neurodegenerative diseases such

as Alzheimer's disease. Insufficient apoptosis can lead to pathologies such as cancer and autoimmunity (Strasser, O'Connor et al. 2000).

Two different pathways can initiate apoptosis and they are the extrinsic pathway mediated by death receptors and the intrinsic pathway mediated by mitochondria. The death receptor pathway (extrinsic) is activated by binding of ligands to death receptors such as Fas and other TNF receptor superfamily members (reviewed in (Danial and Korsmeyer 2004). Extrinsic activation of apoptosis can be induced by cytotoxic T lymphocytes and removes infected or transformed cells (Igney and Krammer 2002). The activation of the intrinsic pathway occurs at the mitochondrial membrane and proceeds via the release of cytochrome c and other apoptotic factors from the intermembrane space of mitochondria (Figure 1.2) (Martinou and Green 2001; Zamzami and Kroemer 2001).

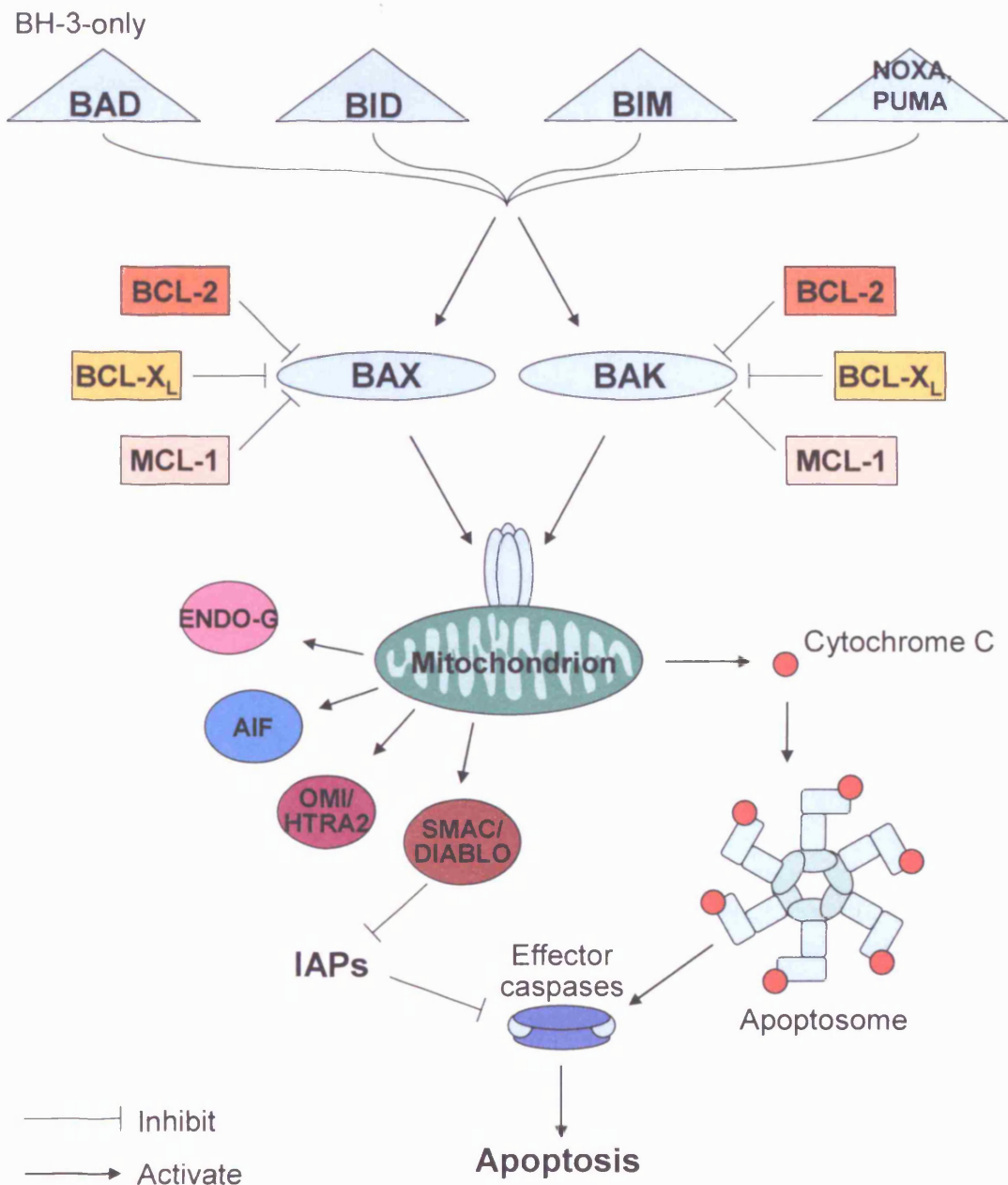


Figure 1.2: Intrinsic pathway of apoptosis

Activation of the BH3 only proteins (blue triangles) leads to the activation of Bax by direct activation or by the displacement of the Bcl2 protein from its complex with Bax. Bax undergoes a conformational change and is proposed to form a pore that leads to mitochondrial outer membrane permeabilisation (MOMP). MOMP leads to the release of intermembrane mitochondrial proteins that include cytochrome c and smac. Cytochrome-c, APAF1 and caspase 9 form a complex called the apoptosome that induces caspase 9 activation and leads to downstream caspase activation. Adapted from (Danial and Korsmeyer, 2004).

Intrinsic pathway of apoptosis

The intrinsic pathway initiates apoptosis and involves the participation of mitochondria in the release of caspase-activating proteins into the cytosol (Figure 1.2). Stimulating factors that cause the activation of the intrinsic pathway are DNA damage, heat shock, oxidative stress, cytotoxic drugs and cytokine withdrawal (Adrain and Martin 2001). The Bcl-2 family is a regulatory group of proteins that consist of both anti-apoptotic and pro-apoptotic members which play a key role in mediating the intrinsic pathway of apoptosis. The family is defined by four highly conserved regions (BH-1 - 4). The anti-apoptotic Bcl-2 subfamily contain BH-1 - 4 domains and operates by inhibition of the Bax/Bak proteins (Cory and Adams 2002). The pro-apoptotic Bax subfamily contains BH-1 – 3 which are activators of the downstream events of the intrinsic pathway. In the normal cell state, Bcl-2-like proteins are bound to the Bax subfamily and maintain their inactive state. The BH-3 only subfamily (Bad, Bim, Bmf, Puma and Noxa) consists of pro-apoptotic proteins that mediate cytotoxic signals and contain only the BH-3 domain (Cory and Adams 2002). Elevated levels of BH3-only proteins, due to activation (e.g. Bid, Bad, Bim and Bmf) or transcriptional upregulation (e.g. Puma, Noxa and Bim), initiate cell death by inactivation of pro-survival activity (Cory and Adams 2002). The BH-3 only proteins lead to the activation of Bax/Bak, by direct binding to Bax or displacement of Bcl-2-like proteins. The theory of direct binding involves BH-3 only proteins binding Bax/Bak and causing direct activation. This occurs following the displacement of Bax/Bak from the Bcl-2-like protein by Bad. Bim then binds to the freed Bax/Bak and activates the formation of the Bax/Bak polymer (Chen, Willis et al. 2005). The displacement theory suggests that BH3 only protein binds directly to the Bcl-2 protein, which displaces the inactive Bax/Bak. The pro-apoptotic function of Bax/Bak is activated once they are removed from Bcl-2 (Willis, Fletcher et al. 2007).

In healthy cells Bax is located within the cytosol (Hsu and Youle 1998). Following activation Bax is translocated to the mitochondrial membrane (Nechushtan, Smith et al. 1999). In response to cell death signals free Bax undergoes an allosteric conformational change allowing the formation of the oligomer by the exposure of the BH-3 domain. (Nechushtan, Smith et al. 1999; Suzuki, Youle et al. 2000). The conformational change also exposes two domains that are proposed to insert into the membrane and regulate the cell death machinery (Nechushtan, Smith et al. 1999). The hypothesis of Bax/Bak lipid pore formation is proposed to explain the molecular cause of mitochondrial outer membrane permeabilization (MOMP). MOMP causes the release of intermembrane proteins that include cytochrome c, Smac/Diablo, Endo-G, AIF and HtrA2 into the cytoplasm. Cytochrome c binds to the c-terminus of APAF1 (Zou, Henzel et al. 1997; Benedict, Hu et al. 2000), which in turn binds to dATP, exposing an oligomerisation surface and forms the apoptosome with caspase 9 (Benedict, Hu et al. 2000).

Apoptotic (intrinsic and extrinsic) signalling converges onto the activation of the cysteine aspartyl-specific proteases (caspases). Caspases are produced as inactive precursors, and are activated upon receipt of auto-proteolytic cleavage or cleavage by other caspases at aspartic acid residues (Thornberry, Rano et al. 1997). Initiator caspases such as caspase 9 are activated by the formation of the apoptosome. The inactive procaspase 9 is proposed to be self-activated by an induced proximity model (Shi 2002). This causes the 'caspase cascade' where the downstream effector caspases are activated by proteolysis. Effector caspases cause the cleavage at cysteine residues in a subset of cellular proteins. Smac/Diablo is released during apoptosis and binds the BIR2 domain of XIAP and allows caspase 3 activation (Chai, Du et al. 2000; Du, Fang et al. 2000). Plasma membrane changes are due to a caspase 3 dependent cleavage of gelsolin, which leads to actin reorganisation and cell rounding (Kothakota,

Azuma et al. 1997). Caspase-activated deoxyribonuclease inhibitor (ICAD) contains a cleavage site for caspase 3 which causes its deactivation during apoptosis. Following ICAD cleavage caspase-activated deoxyribonuclease (CAD) becomes translocated to the nucleus, where it causes intranucleosomal DNA cleavage (Sakahira, Enari et al. 1998). Caspase 3 has been shown to be essential for the nuclear changes associated with apoptosis, including the chromatin condensation following UV- or gamma irradiation (Woo, Hakem et al. 1998)

DNA damage induced apoptosis

Following the DNA damage insult, the cell type specific response can either be DNA repair, cell cycle arrest or apoptosis (Zhou and Elledge 2000; Norbury and Zivnotovsky 2004). Eukaryotic cells employ phosphoinositol-3-kinase-related proteins of the ataxia telangiectasia mutated/ataxia telangiectasia and Rad3 related (ATM/ATR) family to trigger a variety of DNA damage responses (Shiloh 2001). Models place the ATM/ATR kinases at or close to the sites of primary DNA damage with ATM responding to double stranded breaks and ATR specific to single stranded breaks. Downstream kinases (CHK1 and CHK2) are activated by direct phosphorylation by the ATM/ATR protein kinases (Ahn, Schwarz et al. 2000). CHK2 can phosphorylate p53 at Ser20, potentially blocking the MDM2-p53 interaction and modulating the DNA binding activity of p53 (Caspari 2000). ATM has been shown to be required for multisite phosphorylation of p53 (Caspari 2000). Levels of p53 rise when a cell has sustained DNA damage. This is achieved through post-translational modifications of the p53 polypeptide, with no dramatic induction of p53 mRNA levels being evident after DNA damage (Kastan, Onyekwere et al. 1991). The post-translational modifications of p53 increase protein levels by increasing the half-life of the protein. This causes an increased ability of p53 to bind DNA, mediating transcriptional activation (Maki and Howley 1997). Transcriptional activation of p53 can either initiate cell cycle arrest allowing time for DNA repair or initiate

removal of the damaged cells by triggering apoptosis. A key component of the DNA damage stress signal is the p53 pathway that can induce cell cycle arrest, senescence, differentiation and apoptosis (Vousden and Lu 2002). p53 initiates cell cycle arrest by stimulating transcription of p21. p21 is a cyclin dependent kinase inhibitor that inhibits the cyclin E/cdk2 and cyclin A/cdk2 kinases, preventing these kinases from promoting cell cycle progression. The triggering of apoptosis by p53 is achieved by directly activating transcription of Bax and the BH3-only proteins Noxa and PUMA (Nakano and Vousden 2001).

The intrinsic pathway of apoptosis is essential for the DNA damage-induced cell death. This has been revealed by using genetic disruption in mice targeting components of the intrinsic pathway (Davis 2000). For example the thymocytes from $Bax^{-/-}Bak^{-/-}$ animals displayed enhanced survival compared to littermate controls when exposed to gamma irradiation and etoposide treatment (Lindsten, Ross et al. 2000). This indicates that the activation of the intrinsic pathway is required for DNA damage induced cell death. The essential role of cytochrome c in DNA damage induced cell death was shown using mouse embryonic fibroblasts (MEF) that lacked the ability to produce cytochrome c. This revealed that loss of cytochrome c reduced caspase-3 activation following stimuli and that the knock out cells are resistant to the pro-apoptotic effects of UV irradiation (Li, Li et al. 2000). Apaf1, a component of the apoptosome, is required for mitochondrial pathways of apoptosis (Yoshida, Kong et al. 1998) and has been shown to be essential for DNA damage induced cell death. Caspase 9 is an initiator caspase of the intrinsic pathway and caspase 9^{-/-} ES cells were found to be resistant to a range of apoptotic stimuli including UV, gamma irradiation, etoposide and cisplatin (Hakem, Hakem et al. 1998). An effector caspase of the intrinsic pathway is caspase 3 and caspase 3^{-/-} ES cells are resistant to UV-irradiation (Woo, Hakem et al. 1998).

Cancer treatment by chemotherapy and γ irradiation has been proposed to kill cells by inducing apoptosis. Therefore modulation of the apoptotic pathway can directly influence therapy induced cell death. In cancer, cells can acquire resistance to apoptosis by the expression of anti-apoptotic proteins or by the downregulation of pro-apoptotic proteins. Examples of this include the increase in expression of the anti-apoptotic Bcl-2 and Bcl-XL proteins in cancer cells (Findley, Gu et al. 1997). Conversely, examples of downregulation or mutation of pro-apoptotic proteins leading to resistance to apoptosis include Bax, Apaf-1 and Caspase 8 (Rampino 1997; Teitz 2000; Soengas 2001). Alterations of the p53 pathway can also affect the sensitivity of tumour cells to apoptosis. Specific mutations in TP53 have been linked to primary resistance to doxorubicin treatment and early relapse in patients with breast cancer (Aas 1996). Tumours can be independent of survival signals because they have an upregulated PI3K/AKT pathway, which can enhance the insensitivity of tumour cells to induction of apoptosis. The resistance to apoptosis is an important clinical problem as patients who have a tumour relapse usually present with tumours that are more resistant to therapy than the primary tumour (Kelland 2000; Lowe and Lin 2000).

The MAP kinase pathways

Signalling pathways that are activated by DNA damaging stimuli include the JNK and p38 MAPKs pathways (Engelberg 2004). In mammalian systems, there appears to be six MAPK signalling pathways of which ERKs, JNK and p38 MAPKs subfamilies have been characterised in detail. The ERK signalling pathway is activated by mitogens while JNK and p38 pathways are activated by inflammatory cytokines such as TNF and by cellular stresses that include UV light, X-rays, osmotic shock, heat and withdrawal of growth factors (Ichijo 1999). Many of the JNK and p38 activating stimuli are pro-apoptotic but the biological

outcome of JNK and p38 is extremely varied and appears to be dependent on cellular context and type (Engelberg 2004)(Figure 1.3).

Mitogen activated protein kinases (MAPKs) are activated by a highly conserved mechanism that involves phosphorylation on both a threonine and a tyrosine residue (Ichijo 1999; Tibbles and Woodgett 1999; Bode and Dong 2003). The phosphorylation motif, Thr-Xaa-Tyr is located in the activation loop where the amino acid sequence (marked X) varies among different MAPK subfamilies. The MAP kinase signalling pathways involve a phosphorylation cascade. MAPKKK phosphorylates and thereby activates MAPKK; activated MAPKK in turn phosphorylates and activates MAPK (Figure1.3). Activated MAPKs then regulate the activities of transcription factors or further kinases by phosphorylation (Ichijo 1999; Tibbles and Woodgett 1999).

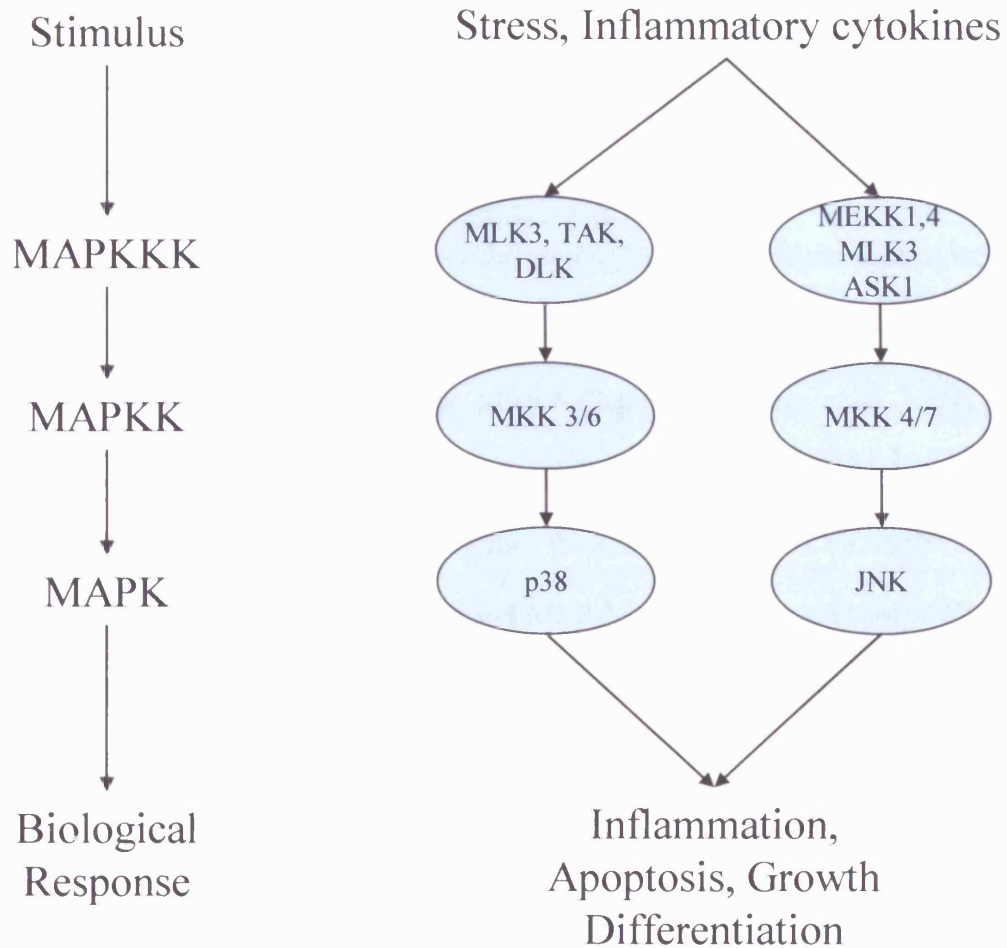


Figure 1.3: Stress response pathways

Following a range of stimuli including UV and TNF α treatment, the JNK and p38 MAPK pathways are activated. This occurs via a phosphorylation cascade where a MAPKKK phosphorylates and thus activates a MAPKK. The activated MAPKK then phosphorylates and activates the MAPK. The activation of p38 and JNK confers a range of responses depending on stimulus and cell type. This can lead to the induction of inflammation, apoptosis, growth or differentiation. Diagram adapted from (Tibbles & Woodgett, 1999)

The JNK subgroup contains the dual phosphorylation motif Thr-Pro-Tyr and is encoded by three genes. JNK1 and JNK2 are expressed ubiquitously while JNK3 is largely restricted to the brain, heart and testis (Davis 2000). Each JNK is expressed as a short form (46 kDa) and long form (54 kDa). JNKs have been shown to be involved in cell death by disruption of the JNK genes. JNK1 and JNK2 KO MEFS have reduced levels of UV induced cell death with reduced cytochrome c released from the mitochondria (Tournier, Hess et al. 2000). JNK3 disruption in mice causes resistance to the excitotoxic glutamate-receptor agonist kainic acid, which causes an absence of the excitotoxicity-induced apoptosis in the hippocampus (Yang, Kuan et al. 1997). JNKs are activated by MKK4 (Sanchez, Hughes et al. 1994; Derijard, Raingeaud et al. 1995) and MKK7 (Tournier, Whitmarsh et al. 1997). MKK4 and MKK7 phosphorylate the threonine and tyrosine within the activation loop TXY motif resulting in JNK activation. Knock out of both MKK4 and MKK7 is required to prevent JNK activation following UV light or anisomycin treatment (Tournier, Dong et al. 2001). MKKs are in turn phosphorylated at specific serine or threonine residues within their activation loop by MKKKs. A large group of MKKKs have been identified that activate the JNK pathway via MKK4 or MKK7. These include members of the MEKK group, the mixed lineage protein kinase group, the ASK group and TAK1 (Davis 2000). MAPK phosphatase 1 (MKP1) and MKP5 can act as negative regulators of JNK signalling (Zhang, Blattman et al. 2004; Wu, Roth et al. 2006). Reactive oxygen species (ROS) can inhibit MKP activity leading to prolonged JNK activation that promotes TNF-alpha induced cell death (Kamata, Honda et al. 2005). JNK has been identified to phosphorylate a variety of proteins including Itch, H2ax, Bmf and Bim which are proposed to induce apoptosis (Weston and Davis 2007). An aspect of JNK control is the organization of signalling complexes by scaffolding proteins. Scaffolding proteins generally have no catalytic function but encode docking sites for binding members of the MAPK module (Johnson and Nakamura 2007). It is proposed the scaffold protein and

specific MKKK provide the selectivity and spatio-temporal dynamics of MAPK activation by different stimuli. An example of a scaffold protein is JIPs (JNK Interacting Proteins) that bind to specific kinesins and the MLK group of MKKKs and appear to be important in cytoskeletal tracking of the JNK module in cells such as neurons (Morrison and Davis 2003).

Activated JNK can phosphorylate c-Jun on Ser-63 and Ser-73 which results in increased transcription activity (Pulverer, Kyriakis et al. 1991). c-Jun is a prototypical member of the Jun family of proteins that forms stable homo- or heterodimeric complexes with Fos, ATF and MAF family members. These complexes bind to AP-1 DNA recognition elements (Eferl and Wagner 2003). JNK can also activate other AP-1 proteins, including JunB, JunD and ATF2. Phosphorylation of c-Jun by JNK leads to inhibition of c-Jun ubiquitination and degradation (Musti, Treier et al. 1997). Thus JNK activation increases the half life of c-Jun and causes an accumulation of the c-Jun protein. JNK is proposed to be essential for AP-1 activation which is caused by stress and some cytokines (Yang, Tournier et al. 1997). Activation of c-Jun by JNK leads to an increase in expression of genes with AP-1 sites in their promoters. This initiates a positive feedback loop as a target of AP-1 transcription factor is the c-Jun gene. Genes that can be upregulated by c-Jun include Bim (Whitfield, Neame et al. 2001), EGFR (Zenz, Scheuch et al. 2003) and cyclin D1 (Bakiri, Lallemand et al. 2000) and c-Jun can repress the p53 promoter (Schreiber, Kolbus et al. 1999). Studies with c-Jun KO cells have shown that it is required for cell proliferation. c-Jun-deficient MEFs show proliferation defects and undergo premature senescence as a result of spontaneous DNA damage accumulation (Johnson, van Lingen et al. 1993; MacLaren, Black et al. 2004). As c-Jun deficient cells have proliferation defects the effect of JNK phosphorylation has been studied by the replacement of endogenous c-Jun with a mutant c-Jun allele with serines 63 and 73 mutated to alanines (termed JunAA). This study identifies c-Jun as the essential

substrate of JNK signalling during kainate-induced neuronal apoptosis leading to the conclusion that amino-terminal phosphorylation of c-Jun regulates stress-induced apoptosis (Behrens, Sibilio et al. 1999). Using the same method, the oncogenic transformation by Ras and Fos was found to be mediated by c-Jun amino terminal phosphorylation (Behrens, Jochum et al. 2000). AP-1 transcription factors have been linked to the induction of tumorigenesis for example c-FOS and c-Jun can transform cells in culture (Eferl and Wagner 2003). In summary, c-Jun has been linked to the regulation of stress induced apoptosis and to the induction of tumorigenesis.

The p38 subfamily of MAPKs contains four members that have been identified; p38 α , p38 β , p38 γ and p38 δ (Jiang, Gram et al. 1997; Zarubin and Han 2005). p38 γ and p38 δ are differentially expressed depending on tissue type while p38 α and p38 β are ubiquitously expressed. The p38 kinases have a Thr-Gly-Tyr (TGY) dual phosphorylation motif with the p38 genes sharing 60% identity (Jiang, Gram et al. 1997). To address the function of p38, knockout mice for p38 α and p38 β have been performed. p38 α knockout mice result in embryonic lethality due to a placental defect (Allen, Svensson et al. 2000; Mudgett, Ding et al. 2000). Deficiency in p38 β produced mice that were viable and had no deficiency in immune responses (Beardmore, Hinton et al. 2005). Conflicting data have been reported regarding the role of p38 α in stress induced apoptosis. Embryonic stem cells lacking p38 α showed no differences in cell death following staurosporin or adriamycin treatment (Allen, Svensson et al. 2000), while cardiomyocytes and fibroblasts lacking p38 α are more resistant to apoptosis induced by serum withdrawal and UV treatment (Porras, Zuluaga et al. 2004). The mechanism proposed was less Bax and Fas protein expression in the p38 α knockout cells and reduced cytochrome c release leading to a reduction in cell death (Porras, Zuluaga et al. 2004; De Chiara, Marcocci et al. 2006). A new study has clarified the role of p38 in cell

death, which identified p38 α as a sensor of ROS in tumorigenesis (Dolado, Swat et al. 2007). By using disruption methods it was determined that p38 α inhibits oncogene induced ROS accumulation by triggering apoptosis. The MAPKKs that have been identified to phosphorylate and activate p38 are MKK3 (Derijard, Raingeaud et al. 1995), MKK6 (Moriguchi, Toyoshima et al. 1996; Stein, Brady et al. 1996) and MKK4 (Derijard, Raingeaud et al. 1995). Using a mouse genetic model, TNF stimulated p38 activation was shown to be mediated by MKK3 and MKK6 (Brancho, Tanaka et al. 2003). Disruption of MKK3, MKK6 and siRNA mediated suppression of MKK4 prevented UV-mediated p38 activation (Brancho, Tanaka et al. 2003). There is a diverse range of MKKKs that participate in p38 activation, including TAK1, ASK1, DLK and MEKK4 (Zarubin and Han 2005). The activated p38 kinases can phosphorylate many transcription factors including ATF2, CHOP (Wang and Ron 1996), p53 (Huang, Ma et al. 1999) and MEF2C (Han, Jiang et al. 1997). In addition p38 can activate MAP kinase activated protein kinase 2 (MAPKAPK2), (Rouse, Cohen et al. 1994) MSK1 (Deak, Clifton et al. 1998) and Bcl2 (De Chiara, Marcocci et al. 2006).

Ste20 type kinases

Ste20 type kinases have been shown to function in signalling pathways that regulate cell cycle control, apoptosis, development, cell growth, cell stress, cell volume and ion transport (Dan, Watanabe et al. 2001; Strange, Denton et al. 2006). Many components of this class of kinases have been proposed to act as upstream components of the MAPK pathway. The ste20 type kinases are related to the budding yeast Ste20p and comprise about 30 kinases in mammals (Figure 1.6). The ste20 kinase group can be divided into germinal centre kinases (GCK) and p21 activated kinases (PAK) (figure 1.4). The Ste20p in yeast activates the MAP3K ste11p by phosphorylation to mediate the signal from the mating pheromone receptor to the MAPK

pathway (Wu, Whiteway et al. 1995; Drogen, O'Rourke et al. 2000). This pheromone response induces cellular changes required in mating, including cell cycle arrest (Wittenberg and La Valle 2003). This showed that Ste20p can act as a MAP4K raising the hypothesis that the mammalian homologues of ste20 also function as MAP4Ks. The ste20 type kinases are defined as possessing a signature sequence that is found in the kinase subdomain VIII (Sells, Knaus et al. 1997). The yeast Ste20p has been linked to the cell death that is induced by hydrogen peroxide and glucose (Ahn, Cheung et al. 2005; Du and Liang 2006). Ste20 kinase in *S. cerevisiae* translocates into the nucleus and is proposed to directly phosphorylate H2B at Ser-10 following hydrogen peroxide treatment. The H2B phosphorylation site mutants are resistant to the hydrogen peroxide induced cell death, suggesting that ste20 is vital in this process (Ahn, Cheung et al. 2005). *S. cerevisiae* ste20 mutants are resistant to glucose-induced cell death in the absence of other nutrients to support growth (Du and Liang 2006).

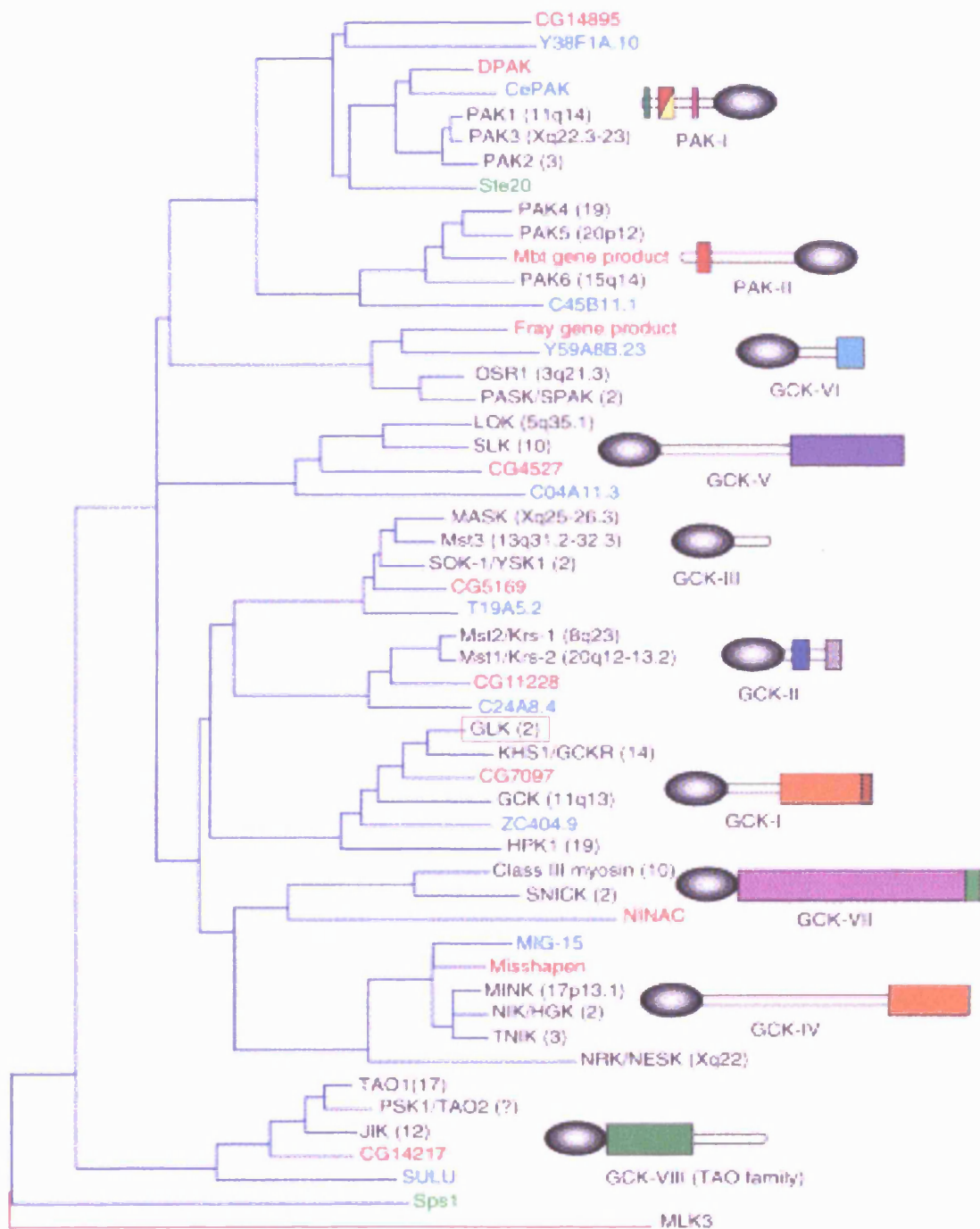


Figure 1.4: Ste20 kinase family

Phylogenetic tree of Ste20 kinase family. The ste20 type kinases are related to the budding yeast ste20p and comprise about 30 kinases in mammals separated into PAK and GCK subgroups. The GCK group is further divided into 7 GCK subgroups. An example of a group 1 GCK member is MAP4K3 (GLK) boxed red which is the focus of this project. Diagram from (Dan et al 2001)

Overexpression experiments using GCK group members can lead to either JNK and/or p38 activation (Kyriakis 1999). This evidence and the homology with yeast Ste20p led to the theory that GCK group 1 and group 7 are MAP4Ks (Dan, Watanabe et al. 2001). GCK group 1 comprise of HPK1 (MAP4K1), GCK (MAP4K2), GLK (MAP4K3) and GCKR (MAP4K5). The group 1 GCK subfamily have a conserved Citron like C-terminal domain and a Ste20 n-terminus kinase domain.

HPK1 is thought to activate the JNK pathway by direct phosphorylation of MEKK1 and MLK3 (Hu, Qiu et al. 1996; Kiefer, Tibbles et al. 1996). Furthermore HPK1 has been linked to induction of apoptosis in T cells with the identification of a caspase cleavage site (Schulze-Luehrmann, Santner-Nanan et al. 2002). HPK1 deficient mice have been characterised as more susceptible to experimental autoimmune encephalomyelitis. From this study HPK1 was found to negatively regulate T-cell receptor signalling and T cell-mediated immune responses (Shui, Boomer et al. 2007)

GCKR is activated by TNF signalling which leads to JNK activation (Shi, Leonardi et al. 1999). The TNF-mediated GCKR and JNK activation have been shown to be dependent on the TRAF2 lysine 63-linked polyubiquitin chain, via the E2 ligase Ubc13/Uev1 (Shi and Kehrl 2003). GCKR has been linked to the Bcr-abl oncogene and RAS to the activation of the stress activated kinases (Shi, Tuscano et al. 1999). GCKR deficient mice (MAP4K5 GCK1 group) have been reported with no phenotype and are viable (Shi, Huang et al. 2006). This study found that B-lymphocytes in Wnt3a-conditioned media have activated JNK and raised cytosolic beta-catenin levels. GCKR was required for Wnt-mediated JNK activation in B cells and removal of GCKR expression inhibits Wnt3a-induced phosphorylation of GSK3 β . This decreases the accumulation of cytosolic beta-catenin (Shi, Huang et al. 2006).

MAP4K3 was cloned in 1997 and was originally referred to as germinal centre-like kinase (GLK) (Deiner, Wang et al. 1997) (Figure 1.5). In overexpression studies it has been found to activate the JNK pathway with dominant negative studies suggesting MAP4K3 may function upstream of MEKK1 and MKK4 (Deiner, Wang et al. 1997). The study by Deiner et al showed that endogenous MAP4K3 could be activated by UV radiation and the proinflammatory cytokine TNF alpha (Deiner, Wang et al. 1997). MAP4K3 has been described as ubiquitously expressed (Deiner, Wang et al. 1997) by mRNA expression analysis. Quadruple overexpression studies using TRAF-2 + TANK + JNK + MAP4K3 (kinase dead) showed that MAP4K3 (kinase dead) acts as a dominant negative to TRAF2/TANK mediated activation of JNK. In another co-overexpression study using CD40+CD40L+JNK+MAP4K3 (kinase dead) the MAP4K3 (kinase dead) has a dominant negative effect on JNK activation (Chin, Shu et al. 1999). Endothelin A1 was found to bind to MAP4K3 in co-overexpression studies, which led to an increase in JNK activation (Ramjaun, Angers et al. 2001). MAP4K3 has recently been described as a nutrient sensitive regulator of the mTOR signalling pathway (Findlay, Yan et al. 2007). MAP4K3 in this study was found to be activated by amino acid addition and when suppressed conferred a decrease in cell size that is indicative of MAP4K3 regulating cell growth.

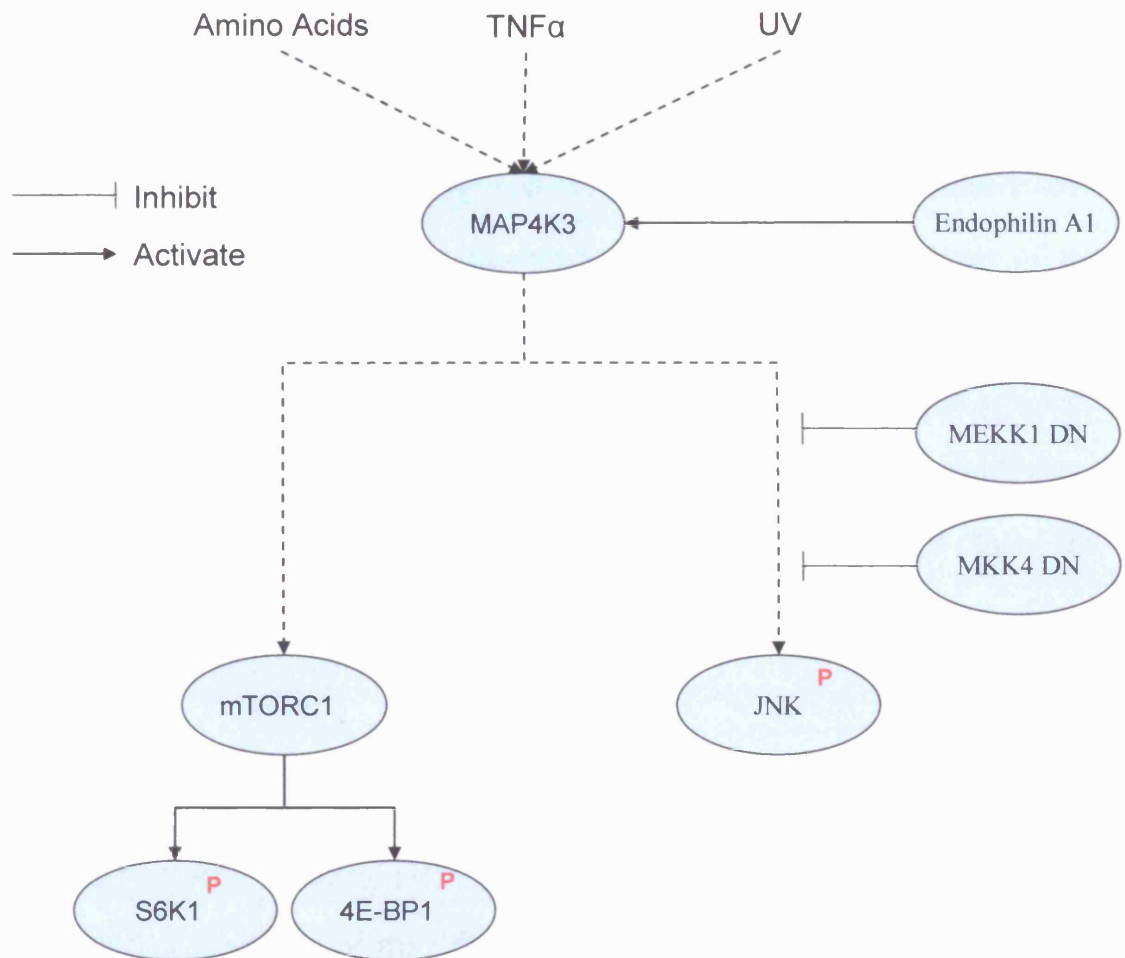


Figure 1.5: The involvement of MAP4K3 in the JNK and mTOR pathways

MAP4K3 has been identified as a protein kinase that is activated by TNF α , UV and by the addition of amino acids (Deiner, Wang et al. 1997)(Findlay, Yan et al. 2007). MAP4K3 has recently been proposed to induce the mTOR pathway leading to an increase in activity of S6K and an increase in the phosphorylation of 4E-BP1. The overexpression of MAP4K3 has been linked to an increase in JNK activity. Endophilin A1 has been described as a binding partner for MAP4K3 that binds to the proline rich region of MAP4K3 which leads to an increase in JNK phosphorylation induced by MAP4K3 overexpression (Ramjaun, Angers et al. 2001).

GCK activates the JNK pathway with endogenous GCK activated by polyinosine-polycytidine [poly(IC)], lipopolysaccharides (LPS), lipid A, interleukin-1 (IL-1), TNF- α and engagement of CD40. RNAi experiments indicate that GCK is required for the maximal activation of JNK by LPS, lipid A, and poly(IC) (Zhong and Kyriakis 2004). Endogenous GCK and MEKK1 have been shown to associate in vivo with GCK and TRAF2 activating MEKK1 in-vitro by inducing MEKK1 oligomerization and consequent autophosphorylation (Chadee, Yuasa et al. 2002). GCK is ubiquitinated and stabilized by inhibitors of the proteasome, indicating that GCK is subject to proteasomal turnover. GCK is constitutively active, and the kinase activity of GCK is required for GCK ubiquitination. Agonist activation of GCK involves the TRAF6-dependent transient stabilization of the GCK polypeptide rather than an increase in kinase activity suggesting a novel mode of regulation for GCK (Zhong and Kyriakis 2004).

Ubiquitin mediated proteasomal degradation

The ubiquitin proteolytic pathway plays an important role in a range of basic cellular processes including regulation of the cell cycle, modulation of the immune system and inflammatory responses, control of signal transduction pathways and differentiation (Ciechanover, Orian et al. 2000). Degradation of a protein via the ubiquitinated proteasome pathway involves two discrete steps; the protein is tagged with multiple ubiquitin molecules, followed by the degradation of the tagged protein by the 26S proteasome complex (Figure 1.6). Ubiquitin proteins are released and reused (Glickman and Ciechanover 2002).

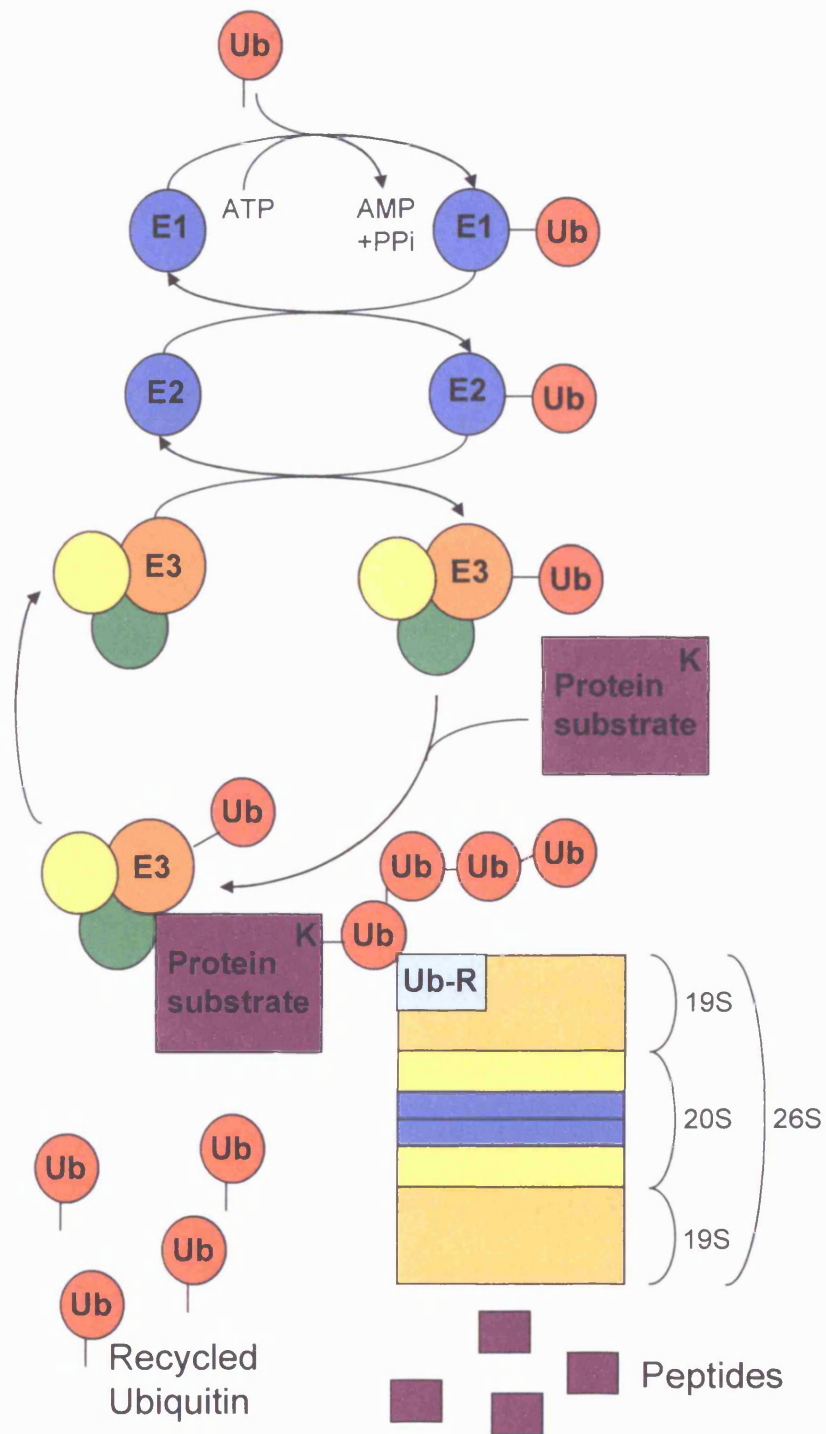


Figure 1.6 Ubiquitin proteasome proteolytic pathway

The protein to be degraded is tagged with multiple ubiquitin molecules by a process that involves E1, E2, E3 enzymes. The ubiquitinated protein is then degraded by the 26S proteasome complex with the recycling of the ubiquitin tag. Adapted from Ciechanover et al 2000

Ubiquitin is a highly conserved small regulatory protein that is uniformly expressed in eukaryotes (Pickart and Eddins 2004). Ubiquitin is a 76 amino acid protein of 8 kDa, identified in 1975 (Schlesinger, Goldstein et al. 1975). The conjugation of ubiquitin to substrates usually involves three enzymes, ubiquitin activating enzyme (E1), ubiquitin conjugating enzymes (E2) and ubiquitin protein ligase (E3) (Hershko, Heller et al. 1983). A hierarchical structure of the ubiquitin system has been proposed forming a pyramid structure. A single E1 interacts with several E2 and E2s interact with even more E3s. The E3s are found to interact with several different protein substrates via specific motifs. Specificity of the ubiquitin system substrates is determined by the recognition of a target protein by an E3 and by ancillary proteins such as molecular chaperones that act as recognition elements. The first event of the pathway is to activate the ubiquitin; this reaction is catalysed by the E1 enzyme via a two step reaction requiring ATP. This reaction generates a high energy E1 thiol ester-ubiquitin intermediate between the C-terminal carboxyl group of ubiquitin and the E1 cysteine residue (Hershko, Heller et al. 1983). One E2 enzyme transfers the activated ubiquitin to an additional high energy thiol ester intermediate of E2 to ubiquitin at the active site cysteine residue. The final step of the ubiquitination cascade requires the activity of one E3. E3s are capable of interaction with both E2 and substrate protein and as such they act as the substrate recognition modules of the system (Ciechanover, Orian et al. 2000). E3 enzymes can possess either one of two domains; The HECT (homologous to the E6-AP carboxyl terminus) domain or the RING finger domain. Transfer of ubiquitin can occur in two ways: directly from E2, catalysed by RING domain E3s or via an E3 enzyme, catalysed by HECT domain E3s. In the latter case, a covalent E3-ubiquitin intermediate is formed before transfer of ubiquitin to the substrate protein by E3 (Scheffner, Nuber et al. 1995). The ubiquitin is generally transferred to a lysine residue in the substrate to generate a covalent isopeptide bond or can be transferred to the N-terminus amino acid of a protein (Breitschopf, Bengal et al.

1998). There is no consensus as to the specificity of the internal Lys residues that are tagged by ubiquitin during proteasome degradation. In some cases distinct lysines are required; signal induced degradation of I κ B α involves two particular Lys residues, 21 and 22 (Scherer, Brockman et al. 1995). While in other cases there is little or no specificity; no single specific lysine residue is required for ubiquitination of c-Jun (Treier, Staszewski et al. 1994). In many cases, ubiquitin monomers are further added on to previously-conjugated ubiquitin to form a polyubiquitin chain (Chau, Tobias et al. 1989) with dogma suggesting a sequential addition model of the ubiquitin (Hochstrasser 2006). The Lys-48 of ubiquitin is normally utilised for these cross linking reactions (Chau, Tobias et al. 1989). If the chain is made up of at least four ubiquitin molecules, the tagged protein is efficiently degraded by the 26S-proteasome (Thrower, Hoffman et al. 2000).

The 26S proteasome, also known as the proteasome holoenzyme, is a 2.5 MDa multicatalytic protease that degrades polyubiquitinated proteins to small peptides. The structure of the 26S proteasome can be divided into two major subcomplexes; the 20S core particle contains the protease subunits and the 19S particle that regulates the function of the proteasome (Hoffman, Pratt et al. 1992; DeMartino G and Slaughter C 1999). The 20S core particle is a barrel shaped structure made up of four stacked heptagonal rings (Groll, Ditzel et al. 1997). The two inner rings contain the proteolytic active sites facing inward into the chamber. The 19S is comprised of at least 18 different subunits and can assemble at either end of the 20S and is proposed to form a lid and base substructure, which may specifically recognise ubiquitinated protein (Glickman, Rubin et al. 1998). The mechanism of how the proteasome recognizes ubiquitinated proteins has been partly described with the identification of an ubiquitin binding subunit called Rpn10/Mcb1 located in the 19S (van Nocker, Sadis et al. 1996). In most cases the proteasome cleaves protein substrates into small peptides, usually 3-22 amino acid

residues in length (Kisselev, Akopian et al. 1999). The ubiquitin molecules are cleaved off the protein by deubiquitinating enzymes (DUBs) (thiol proteases). There are at least five different structural classes of DUBs, and a wide range of substrate specificities and functions have been reported (Nijman, Luna-Vargas et al. 2005).

Aberrations in the ubiquitin proteasome system have been implicated in pathogenesis of diseases including certain malignancies, neurodegenerative disorders, and pathologies of the inflammatory immune response (Glickman and Ciechanover 2002). An example of this is the targeting of p53 for degradation by the human papillomavirus oncoprotein E6 in complex with the ubiquitin ligase E6-AP. This has been implicated in the pathogenesis of human uterine cervical carcinoma (Iwasaka, Oh-uchida et al. 1993; Scheffner, Huibregtse et al. 1993). The proteasome inhibitor, Bortezomib, has effective anti-tumour activity in cell culture and in animal models inducing apoptosis by increasing the expression level of cyclin-dependent kinase inhibitor, p21 (Adams, Palombella et al. 1999). Bortezomib is the first proteasome inhibitor to reach clinical use as a chemotherapy agent in the treatment of multiple myeloma (FDA 2003).

RNA interference mechanism

The discovery in 1998 that injecting double stranded (ds) RNA into *Caenorhabditis elegans* silences the cognate gene was a breakthrough that triggered the field of RNA interference (RNAi) (Fire, Xu et al. 1998). RNAi is considered a response to virus infection of eukaryotic cells as dsRNA is usually produced from the viral genes and RNAi occurs as an innate immune response (Tuschl and Borkhardt 2002; Zamore 2002). The finding that short RNA species were the effector molecules was first suggested in plants (Hamilton and Baulcombe 1999) and further evidence from *Drosophila melanogaster* extracts showed that dsRNAs are

cleaved into 22 nucleotide siRNA products (Zamore, Tuschl et al. 2000) and that chemically synthesised short interfering RNA (siRNA) caused the degradation of homologous RNA (Elbashir, Lendeckel et al. 2001).

The enzyme required for processing long dsRNA into siRNAs during the initiation step of RNAi is a ribonuclease enzyme termed Dicer (Bernstein, Caudy et al. 2001). The siRNA mediated target mRNA degradation is carried out by the RNA induced silencing complex (RISC) (Hammond, Bernstein et al. 2000). The RISC complex was identified from *Drosophila* S2 cells and was found to associate with siRNAs (Hammond, Bernstein et al. 2000). RISC targets single stranded complementary RNAs for degradation (Hammond, Bernstein et al. 2000). The duplex siRNA is unwound, leaving the antisense strand to guide RISC to its homologous target mRNA for endonucleolytic cleavage. The dsRNA processing and siRNA mediated target degradation is suggested to be a two step process (Bernstein, Caudy et al. 2001) (Figure 1.7).

The N-terminus of Dicer contains a RNA helicase domain, a PAZ domain (Piwi, Argonaute, Zwillig/pinhead), two catalytic RNase III domains and a c-terminal dsRNA binding domain (Cerutti, Mian et al. 2000). The RNase III family of nucleases specifically cleave double-stranded RNAs. siRNAs produced by the action of Dicer are 21-23 nucleotide siRNA duplexes with symmetric 3' overhangs of 2 nucleotides and have 5' phosphorylated end groups (Elbashir, Harborth et al. 2001).

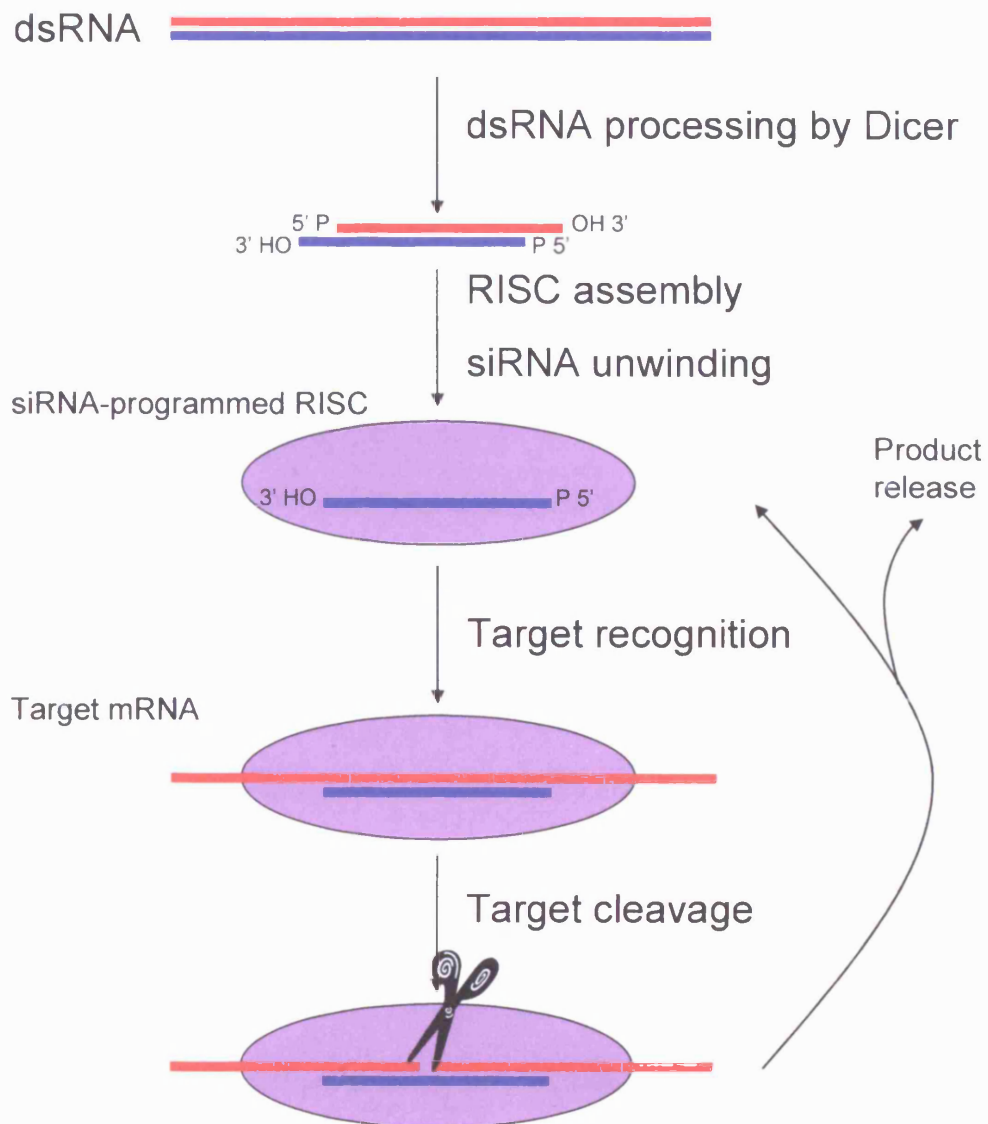


Figure 1.7 RNAi mechanism

dsRNA are processed by dicer into a 21 to 23 nucleotide siRNA duplex that contains a 2-nucleotide 3' overhang with 5' phosphate and 3' hydroxyl termini. The siRNA is unwound and incorporated into the RNA induced silencing complex (RISC). This RISC complex mediates the sequence specific degradation of the complementary mRNA. This degradation is catalysed by Ago2 that cleaves the mRNA. General pathway of RNAi adapted from (Sontheimer 2005)

The processed siRNAs still associated with Dicer are unwound by an unknown enzyme and one strand of the duplex is incorporated into the RISC. In *Drosophila*, the orientation of the heterodimer, consisting of Dicer-2 and dsRNA binding protein (R2D2), on the siRNA duplex determines which siRNA strand associates with the RISC protein argonaute 2 (Tomari, Matranga et al. 2004). The R2D2 binds the siRNA end with the greatest double-stranded character, thereby orienting the heterodimer on the siRNA duplex (Tomari, Matranga et al. 2004). The target mRNA is cleaved by RISC at a single site in the centre of the duplex region, between the guide siRNA and the complementary mRNA. This site is 10 nucleotides from the 5' end of the siRNA (Elbashir, Lendeckel et al. 2001) and cleavage severs the mRNA phosphodiester backbone. The RNA cleavage products are suggestive of RISC having an endonuclease activity (Martinez and Tuschl 2004). Argonaute 2, a component of the RISC complex, has been discovered to mediate the RNA cleavage and is considered the catalytic engine of mammalian RNAi (Liu, Carmell et al. 2004; Meister, Landthaler et al. 2004). The Argonaute protein x-ray structure reveals that a PIWI domain has a fold that is similar to that of Ribonuclease H (RNase H) (Song, Smith et al. 2004). This has led to the hypothesis that the PIWI domain contains the active site for the endonuclease activity of Ago2. The human dicer binds to Ago2 through interactions between the RNase III domain of dicer and the PIWI domain of Ago2 (Tahbaz, Kolb et al. 2004) and links the initiator and effector parts of RNAi.

Long dsRNA induces potent RNAi when introduced into worms, flies or plants by presenting various siRNA sequences to the target mRNA. Long dsRNA causes an interferon response in mammalian cells (Elbashir, Harborth et al. 2001). The dsRNA molecules of greater than 30 base pairs bind to and activate the protein kinase PKR and oligo-adenylate synthetase (Stark, Kerr et al. 1998). Activated oligo-adenylate synthetase activates RNASE L causing mRNA degradation in a sequence independent manner. PKR activation leads to phosphorylation of

the translation initiation factor eIF2 α leading to a global stop in translation. In 2001 the first evidence that 21 nucleotide siRNAs can mediate transient RNAi knockdown in mammalian cells was discovered by Tuschl and colleagues (Elbashir, Harborth et al. 2001).

The strategies for designing siRNAs to reduce expression of a gene have been described in detail (Dykxhoorn, Novina et al. 2003; Huppi, Martin et al. 2005; Yiu, Wong et al. 2005) with the siRNAs designed to load the antisense strand into the RISC complex termed functionally asymmetric. In fungi, plants and worms dsRNA are passed down generations by replication of the siRNA using a RNA-dependent RNA polymerase (RDRP) (Cogoni and Macino 1999; Dalmay, Hamilton et al. 2000; Sijen, Fleenor et al. 2001). In mammalian cells there is no indication of siRNA replication (Zamore 2002) and therefore vector based systems have been generated for stable knockdown (Sharp, Novina et al. 2003). Several groups have discovered that plasmids expressing short hairpin (sh) RNA from an RNA polymerase III promoter could be used to efficiently silence gene function (Brummelkamp, Bernards et al. 2002; Paddison, Caudy et al. 2002). An example of this stable suppression system is the pRetroSuper that was produced by Brummelkamp et al (Brummelkamp, Bernards et al. 2002; Brummelkamp, Bernards et al. 2002). The polymerase III H1 RNA promoter drives the expression of a short hairpin RNA transcript with the plasmid pSuper. The transcript is cleaved at the termination site making them resemble the ends of synthetic siRNAs that contain two 3' overhanging T or U nucleotides (Baer, Nilsen et al. 1990). The 19mer nucleotide sequence derived from the targeted gene is separated by a short hairpin from the reverse complement 19mer sequence. The resulting 19 base stem loop structure is suggested to be cleaved in the cell to produce the functional siRNA (Brummelkamp, Bernards et al. 2002). The pSuper cassette was cloned into a self inactivating pMSCV-puro retroviral plasmid to be able to perform stable suppression of

gene expression (Brummelkamp, Bernards et al. 2002). Inducible knockdown systems have also been generated to further explore the functions of genes (Ventura, Meissner et al. 2004).

High throughput genome wide RNAi screens have been performed by feeding worms collections of bacteria containing plasmids that express the long double stranded RNAs. These type of large scale screens have identified genes that regulate fat storage, (Ashrafi, Chang et al. 2003), affect worm development (Kamath, Fraser et al. 2003), and which serve to protect the genome against mutations (Pothof, van Haaften et al. 2003). siRNA has been utilised to perform loss of function genetic screens in mammalian cells. In order to perform loss of function analysis in mammalian cells, RNAi libraries have been produced by academic and commercial organisations (Dorsett and Tuschl 2004; Moffat and Sabatini 2006). A variety of mammalian RNAi screens have been performed and include a screen which uses a siRNA library targeting all the 650 kinases and a separate siRNA library containing 222 phosphatases to identify anti-apoptotic survival pathways (MacKeigan, Murphy et al. 2005). An example of a vector based screen was performed by Berns et al that identified five new modulators of p53-dependent proliferation arrest (Berns, Hijmans et al. 2004). At present the advantage of vector based screens over siRNA are that they can be delivered to non-transfectable primary cells and stable silencing can be generated for long term studies. The advantage of using siRNA based libraries is that they are less prone to non-specific effects due to greater control over the amount of transfected siRNA and high quality chemical synthesis production (Dorsett and Tuschl 2004). The generation of RNAi libraries has lead to the ability to perform large scale functional discovery in mammalian cells.

Aim

Defects in the apoptotic pathway can make cancer cells resistant to therapy, as both chemotherapy and irradiation act primarily by inducing apoptosis. Therefore the resistance to apoptosis constitutes an important clinical problem (Igney and Krammer 2002) and as such apoptosis will be investigated in my study.

The aim of this study was to identify novel regulators of DNA damage induced cell death by performing a genetic screen using a vector based RNAi library. The most promising candidate cell death regulator will then be further investigated to elucidate the mechanism of action. This will include gain of function analysis as well as the loss of function experiments to determine the signalling pathways that are affected.

Chapter 2: Materials and Methods**Materials**

All chemicals were from Sigma-Aldrich (Paisley, UK) unless otherwise stated.

Table 2.1- Primary antibodies

Antibody	Source	Company	ID No.	Dilution	Blocking	Mol. Wt (kDa)
(p)-ATF-2	Rabbit Polyclonal	Cell Signaling	9221	1:1000	5% BSA	70
Bax-NT	Rabbit Polyclonal	Upstate	06-499	1:1000	5% Milk	23
Bcl-2	Mouse Monoclonal	Pharmingen	65111a	1:1000	5% Milk	26
Bim (EL, L + S)	Rabbit Polyclonal	Calbiochem	202000	1:1000	5% Milk	25 (EL) 15 (L) 12 (S)
Bmf	Rabbit Polyclonal	Cell Signaling	4692	1:1000	5% BSA	18
(p)-ERK (2 + 1)	Rabbit Polyclonal	Cell Signaling	9101	1:1000	5% BSA	42 (2) 44 (1)
GFP	Mouse Monoclonal	Cancer Research UK	N/A	1:1000	5% Milk	Variab le
HA probe (Y11)	Rabbit Polyclonal	Santa Cruz	Sc-805	1:500	5% Milk	Variab le
(p)-JNK((1 + 2/3) (Thr183/Tyr185)	Rabbit Polyclonal	Cell Signaling	9251	1:1000	5% BSA	46 54
JNK-2/JNK-1	Mouse Monoclonal	Santa Cruz	Sc-7345	1:500	5% Milk	54 46
(p)-MAPKAPK2	Rabbit Polyclonal	Cell Signaling	3041	1:1000	5% BSA	47
(p)-MKK3/6 (Ser189/207)	Rabbit Polyclonal	Cell Signaling	9231	1:1000	5% BSA	40 (3) 41 (6)
MKK-4/SEK1 total	Rabbit Polyclonal	Cell Signaling	9152	1:1000	5% BSA	44
(p)-MKK4/SEK1 (Ser257/Thr261)	Rabbit Polyclonal	Cell Signaling	9156	1:1000	5% BSA	44

Table 2.1- Primary antibodies - continued

Antibody	Source	Company	ID No.	Dilution	Blocking	Mol. Wt (KDa)
MKK-7 total	Rabbit Polyclonal	Cell Signaling	4172	1:1000	5% BSA	48
(p)-MKK7 (Ser271/Thr275)	Rabbit Polyclonal	Cell Signaling	4171	1:1000	5% BSA	48
p21	Rabbit Polyclonal	Santa Cruz	Sc-758	1:5000	5% Milk	21
p38 total	Rabbit Polyclonal	Cell Signaling	9212	1:1000	5% BSA	43
(p)-p38 (Thr180/Tyr182)	Rabbit Polyclonal	Cell Signaling	9211	1:1000	5% BSA	44
p53	Mouse Monoclonal	Dako	DO-7	1:1000	5% milk	53
(p)-c-Jun (Ser63)	Rabbit Polyclonal	Cell Signaling	9261	1:1000	5% BSA	48
PUMA	Rabbit Polyclonal	Cell Signaling	4976	1:1000	5% BSA	16b 19a
(p)-S6K (Thr389)	Mouse Monoclonal	Cell Signaling	9206	1:1000	5% BSA	p85 p70
(p)-Stat-1 (Ser727)	Rabbit Polyclonal	Cell Signaling	9177	1:1000	5% BSA	91
Tubulin	Rabbit Polyclonal	Cell Signaling	2144	1:1000	5% BSA	53
Tubulin	Mouse Monoclonal	Sigma	T5168	1:2000	5% Milk	53

Table 2.2- Secondary antibodies conjugated to HRP

Antibody	Source	Company	ID No.	Dilution	Blocking
Anti-Mouse	Sheep	Amersham	NA931	1:2000	5% Milk
Anti-Rabbit	Donkey	Amersham	NA934	1:2000	5% Milk
Anti-Goat	Rabbit	Sigma	P0449	1:2000	5% Milk

Table 2.3- DNA Plasmids

Plasmid Name	Reference	Observation
pRS	(Brummelkamp, Bernards et al. 2002)	A retroviral vector derived from the murine Embryonic Stem Cell Virus (pMSCV) (Figure 2.1).
pRS K330	(Brummelkamp, Bernards et al. 2002; Berns, Hijmans et al. 2004)	First generation pRS RNAi library containing sequences for 330 genes with a three fold redundancy
pEGFP C-3 Bax	Justin Cross, CRUK	BAX cDNA cloned in frame into pEGFP C3 vector.
pRFP-C2 BclxL	Ingram Iaccarino, Institute of Genetics and Biophysics, Napoli, Italy	BclxL cDNA sequence was cloned using EcoRI/XhoI restriction sites into the pRFP-C2 vector.
pcDNA3.1/CT-GFP TOPO	Invitrogen; Catalogue number: K482001	A mammalian expression construct that expresses wild type GFP under the control of a CMV promoter (Figure 2.3).
pEGFP-N 1 vector	Clontech (Palo Alto, California); Catalogue #: 6086-1	A mammalian expression vector that encodes a red-shifted variant of wild-type GFP (EGFP) driven by the cytomegalovirus (CMV) promoter (Figure 2.4).
pBluescriptR IMAGE CLONE 5296205 (MAP4K3)	Geneservice, Cambridge, UK (Lennon, Auffray et al. 1996)	cDNA of MAP4K3 derived from human testis and cloned using Sall-XhoI/BamHI restriction sites into pBluescriptR plasmid (Figure 2.2)
pcDNA3.1-MAP4K3 CTGFP	see methods	Mammalian expression construct of MAP4K3 was prepared as a C-terminal cycle3GFP tagged protein. MAP4K3 cDNA from IMAGE CLONE 5296205 was amplified by PCR and cloned into pcDNA3.1/CT-GFP TOPO (Figure 2.3)
pcDNA3.1-MAP4K3 K45E-CTGFP	see methods	In order to create a kinase dead mutant of MAP4K3, site directed mutagenesis of the lysine 45 to glutamic acid 45 was performed on the MAP4K3 CTGFP plasmid (Figure 2.3)
pEGFP-N1 MAP4K3-EGFP tagged plasmids	see methods	To create deletion fragments of MAP4K3, MAP4K3 cDNA was cloned into pEGFP-N1 vector by the cohesive ends method. The MAP4K3 EGFP and mutant proteins were generated by subcloning PCR fragments into the Kpn1 and BamH1 sites of pEGFP N-1 (Figure 2.4)
pMT123 HA-Ubiquitin (x8)	Gift from Mario Rossi, MRC Toxicology (Treier, Staszewski et al. 1994)	pMT123 is a HA-tagged ubiquitin expression vector consisting of a CMV promoter that regulates the expression of eight ubiquitin repeats individually tagged with an influenza virus hemagglutinin (HA) epitope tag

Table 2.4- siRNA oligonucleotides

ID	Catalogue #	Sequence	Target
Scrambled	Ambion Silencer Negative Control #1	Sequence not specified.	Validated, non- targeting negative control
shRNA M4K3 #3	NCI	CCAATTATAATTAACCACA	Exon 34 of MAP4K3
MAP4K3 #4	Ambion silencer MAP4K3#1455	GGCACGGAAUGUUAACACUTT	Exon 1 and 2 of MAP4K3
MAP4K3 #5	Ambion silencer MAP4K3#1550	GGCGAGAUAAAGCUUUGGAUTT	Exon 3 and 4 of MAP4K3
MAP4K3 #6	Ambion silencer MAP4K3#1640	GGU AACACAAGAAAUUCATT	Exon 32 and 33 of MAP4K3
BclxL	Dharmacon siGenome duplex BCL2L2 # D-003458-03	CCUACAAGCUUCCAGAAUU	Exon 2 of BclxL

Methods

Cell culture

All cell culture plasticware was from Griner (Germany), unless otherwise stated. U2OS cells were cultured in DMEM (Gibco BRL, Paisley, UK) supplemented with 10% heat inactivated FCS (Invitrogen, Paisley, UK) and 100U/ml penicillin (Gibco BRL), 100µg/ml streptomycin (Gibco BRL). Cells were maintained at 37⁰C in 5% CO₂ atmosphere. HEK293 and Phoenix A packaging cells (Invitrogen) were cultured under the same conditions.

Retroviral expression

Phoenix A cells were grown on 150mm² culture plates to 60% confluence. The transfection cocktail was made up in an Eppendorf tube which contained 554µl serum free medium (DMEM), 16.6µl Fugene (Lipid-based transfection reagent, Roche, Switzerland) and 5.5µg of plasmid DNA (pRetrosuper or pRetroSuper K330). The culture medium was removed from the cells and 11ml of the complete media was added, followed by the transfection cocktail. Following transfection, Phoenix A cells were cultured at 37°C for 24 hours. Fresh media was added and the cells were grown at 32°C for 72 hours. The retroviral supernatants were harvested and placed through a 0.45µm filter. The supernatant was divided into 5ml aliquots and stored at -80°C.

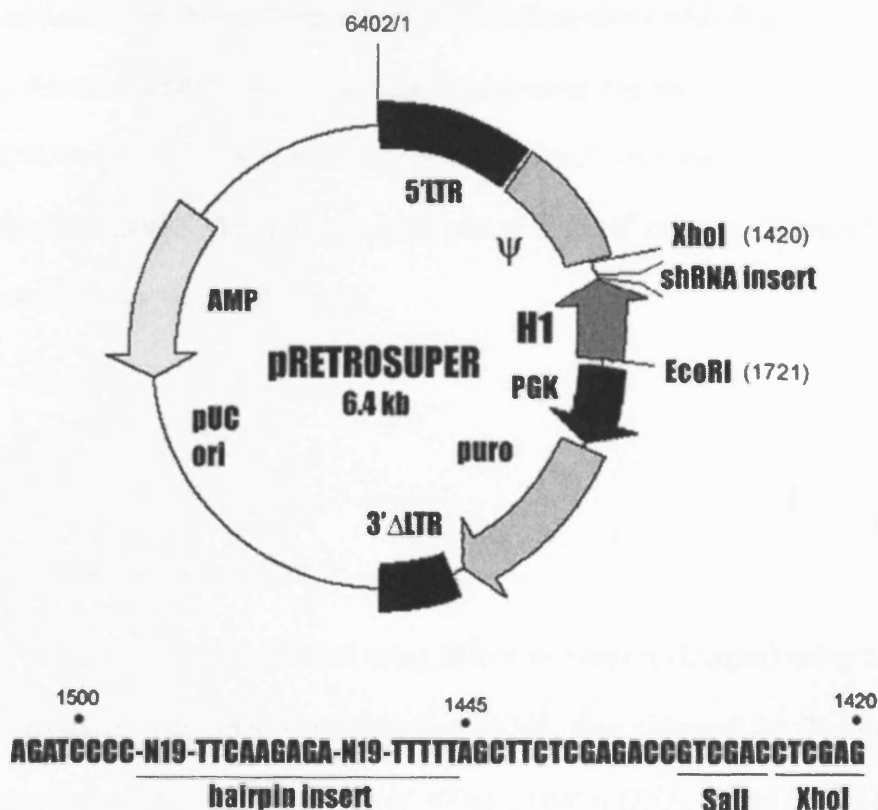


Figure 2.1 pRetrosuper library vector

The shRNA hairpin has been cloned in the RNAi library downstream of the histone H1 RNA promoter. pRetrosuper is a retroviral vector derived from the murine Embryonic Stem Cell virus (pMSCV). pRetrosuper has a deletion in the 3'LTR promoter elements. This deletion results in inactivation of the LTR mediated transcription upon retroviral integration. The small RNA transcript produced forms a hairpin structure with two T or U nucleotides at the 3' end. The hairpin transcript is processed in the cell into a 21 nucleotide siRNA. The first generation pRS RNAi library containing sequences for 330 genes with a three fold redundancy was used in this project. The 330 genes targeted by the K330 RNAi library are either kinases or proteins that could have a critical cellular function. Vector diagram adapted from <http://screeninc.nl>

Retroviral infection

U2OS cells were grown on 100mm² culture plates to 60% confluence. 5ml ecotropic retroviral supernatants (see above) were added to the culture along with 4µg/ml polybrene for 24 hours. Drug selection on U2OS cells was performed using 2µg/ml puromycin for 7 days in complete DMEM. Surviving cells were considered stable and were used in the RNAi screen. The U2OS PRS and U2OS K330 cell lines were plated at 2x10⁶ cells per 100mm² plate and cultured for 16 hours prior to UV treatment.

Transfections

U2OS plasmid DNA transfections

Transfection of U2OS cells was performed using Effectene reagent (Qiagen) using a modified manufacturer's protocol. The cells were seeded at 2x10⁵, then cultured for 24 hours in six well plates. Transfection cocktail consisting of 400ng plasmid DNA, 100µl buffer EC, 3.2µl enhancer and 2.5µl effectene was incubated for 20 minutes followed by the addition of 600µl of complete media. 1.6ml of fresh complete media was added to cells, followed by addition of the transfection cocktail. After 24 hours cell death counts were performed. For co-transfection experiments a 1:1 ratio of the plasmid DNA was used. To inhibit caspases, 50µM ZVAD-FMK (broad spectrum caspase inhibitor) (Bachem, Germany) was added to the appropriate wells at the time of transfection. For transfection in other types of dishes, quantities of reagents were proportionally adjusted.

Reverse transfection of U2OS cells with siRNAs

1.4µl of 50µM siRNA stock was distributed into Eppendorfs. Effectene transfection cocktail was made up using 100µl EC buffer, 3.2µl enhancer and 2.5µl effectene. This quantity was

added with each of the siRNA stock aliquots and incubated for 20 minutes followed by the addition of 600µl of complete media. 1.6ml of 1×10^5 /ml cells were added to the cocktail and mixed. This was then distributed onto a 96 well plate at 100µl per well and incubated for 48 hours. Quantities were proportionally changed for reverse transfection onto other types of dishes. These cells were then either treated with UV, cisplatin or addition of BrdU followed by the appropriate technique.

Nucleofection of U2OS cells

To achieve high transfection rate into U2OS cells, nucleofection was performed using the MAP4K3 EGFP plasmids. This was performed using the Amaxa nucleofector system according to the manufacturer's specification for U2OS cell line using kit V and program X-01. After 24 hours, these U2OS cells were used for protein lysates.

Transfection of HEK 293 cells

Transfection of 293 cells was performed using Effectene reagent using a modified manufacturer's protocol. Cells were seeded at 3×10^5 then cultured for 16 hours. A transfection cocktail was made up of 800ng plasmid DNA, 100µl buffer EC, 3.2µl enhancer and 10µl effectene. The transfection cocktail was incubated for 20 minutes, followed by the addition of 600µl of complete media. 1.6ml of fresh complete media was added to the cells, followed by the transfection cocktail. 48 hours post-transfection cells were untreated or UV treated and used for protein lysates.

Cell Treatments

UV treatment

The U2OS or 293 cells were washed with PBS and then treated in PBS with a UV-C dose between 5-150J/m² using Stratalinker UV Crosslinker (Stratagene). Cells were either used in cell survival assay or were collected after a given time-point and used for either DNA extraction, RNA extraction, protein lysates or prepared for FACS analysis.

Cisplatin treatment

Reverse transfection was performed on U2OS cells in 96 well plates (see above). A Cisplatin stock was made up in complete media to 1mM. This was shaken for 30 minutes then incubated at 37°C for a further 30 minutes. The cisplatin stock was diluted to a 5x stock for the concentration used (100µM). 48 hours post transfection 25µl was added to each of the wells without changing the cell culture media containing the siRNAs. The cells were cultured for a further 24 hours. These cells were used in the cell survival assay.

Proteasome inhibitor treatment

24 hours post 293 transfections; MG132 (Calbiochem, USA) was added to each well to make a final concentration of 1µM MG132. 24 hours after MG132 addition, cell lysis was performed on each well followed by Western blot analysis.

FACS Analysis

Cell death was assessed by propidium iodide (PI) staining (Molecular Probes, Paisley, UK). 24 hours after stimulation, both floating and attached cells were collected and resuspended in PBS. An aliquot was diluted in a PI solution (final concentration of 1 µg/ml), and viable (PI negative) and non-viable cells (PI positive) were counted using flow cytometry. In each assay 8,000 cells were collected by FACScan (Becton Dickinson, Oxford, UK) and analysed using the CellQuest program (Becton Dickinson).

Crystal violet assay

2x10⁵ U2OS cells plated in 100mm² dish were treated and used after 4 days for crystal violet staining as follows. U2OS cells were washed three times with PBS. Crystal violet stain (DNA stain) (0.5% w/v crystal violet in 40% ethanol) was applied to cells for 20 minutes. Crystal violet binds to DNA and yields intense purple staining of cell nuclei. Cells were rinsed thoroughly with distilled water 3 times. Stained colonies were counted, then solubilised in 40% ethanol and absorbance was measured at 600nm.

Cell fixation

U2OS cells were washed three times with phosphate buffered saline (PBS), then fixed in Accustain solution (10% formalin solution) for 20 minutes. Cells were washed 3 times with PBS. Nuclear staining was performed using Hoechst 33342 stain (Molecular Probes) at a concentration of 10 µg/ml in PBS for 10 minutes. Cells were washed 3 times and stored in PBS at 4^oC until analysis.

Cell Survival assay

Following fixation and Hoechst staining, cells were counted using the Cellomics Kinetiscan high throughput microscope (Cellomics, Pittsburgh, Pennsylvania, USA). Images of 20 fields per well were captured using a 10x objective and used for cell counts. Cellomics Cellscan algorithm was used to select viable cells. Cells were considered viable if the cell chromatin was uncondensed, and were distinguished morphologically from small bright nuclei with condensed chromatin in dead cells. The cell morphology algorithm was used in this assay with a threshold set on the Hoechst channel for total intensity per object to exclude nuclei with condensed chromatin. The cell number for each treatment condition was considered to be the number of viable cell nuclei and this was converted into percentage cell survival by comparing to the respective untreated control well.

BrdU proliferation assay

The assay was performed 48 hours post reverse transfection of U2OS cells with siRNA in a 96 well plate. BrdU Proliferation ELISA (Roche) was performed according to standard manufacturer's protocol. To each well 10µl BrdU labelling solution was added and the cells were re-incubated for 24 hours at 37°C. The medium was then removed by aspiration, then 200µl of FixDenat was added. After incubation at room temperature for 30 minutes the FixDenat was removed. 100µl of anti-BrdU-POD working solution was added to each well and incubated for 90 minutes at room temperature. The antibody conjugate was removed and the wells rinsed with 200µl of washing solution. The wash was repeated 3 times. 100µl per well of substrate solution was added and the plate was incubated for 20 minutes until the colour change was sufficient for photometric detection. The colour changes were measured by an ELISA reader (Tecan, Switzerland) at 370nm (reference wavelength was 492nm). For the

BrdU proliferation assay the siRNA MAP4K3 wells were compared to the scrambled siRNA well to determine the fold change in absorbance.

Immunocytochemistry

Following fixation with accustain, cells were blocked for 1 hour at room temperature. The blocking solution used was PBS with 1% BSA (v/v) and 0.1% saponin (v/v). The primary antibody was a BAX conformational specific antibody (clone 3, BD Biosciences), which was diluted to 1:250 with 1% BSA and 0.1% saponin. Cells were incubated overnight at 4^oC. The primary antibody was removed and the cells were washed once with blocking solution. Cells were then incubated with the secondary antibody goat anti-mouse conjugated with Alexa Fluor 488 (red) (Molecular Probes) at 1:500 in PBS with 1% BSA and 0.1% saponin for 1 hour at room temperature. The cells were washed with PBS 3 times. The cells were stained with Hoechst (as above), washed and then stored in PBS until analysis.

Microscopy and cell death counts

Fixed cells were analysed using a fluorescence light microscope. For the GFP expressing cells the analysis was performed using an Axiovert 40 CFL inverted microscope with an attached AxioCam monochrome digital camera. Cells were imaged at either 20x or 40x magnification under phase contrast and GFP filters. Images were captured and processed using Axiovision 4.3 software. 100-200 GFP positive cells were counted per transfection where Hoechst stain was used for analysis of nuclear morphology, in particular the condensation of chromatin.

Amplification of plasmid DNA

Competent *E. coli* bacteria (XL 10 Gold; Stratagene, La Jolla, California, USA) were transformed and plated according to manufacturer's protocol. Single colonies were then grown overnight for mini or maxi prep purification of DNA (Qiagen) according to manufacturer's protocols.

DNA sequencing

Sequencing reactions were performed using the BigDye Terminator v3.1 Cycle Sequencing kit (Perkin Elmer, Waltham, Massachusetts, USA) according to the manufacturer's protocol. The completed reactions were purified using the Qiagen DyeEx 2 spin kit as described in the manufacturer's instructions. Samples were sent for analysis on an Applied Biosystems 3730 sequencer.

Recovery of shRNA inserts from infected pRS K330 U2OS cells

7 days after UV treatment the Genomic DNA from pRS K330 U2OS cells was extracted using DNeasy spin columns (Qiagen) according to the manufacturer's protocol. PCR amplification of the shRNA inserts was performed with Expand Long Template PCR system (Roche) that uses a Taq DNA polymerase and Tgo DNA polymerase with proofreading activity. A PCR product containing the shRNA hairpin was amplified using pRS-fw primer and pRS-rev primer.

pRS-fw primer: 5'-CCCTTGAACCTCCTGTTTCGACC-3'

pRS-rev primer: 5'-GAGACGTGCTACTTCCATTTGTC-3'

The shRNA insert product was gel purified with Qiaquick Gel Extraction (Qiagen). The gel purified insert was then cloned into pCR4-TOPO using TOPO TA Cloning Kit (Invitrogen) and transformed into One Shot TOP10 E. coli (Invitrogen) according to the manufacturer's protocol. ShRNA inserts cloned into pCR4-TOPO were sequenced with Big Dye Terminator using H1 promoter sequencing primer.

H1 promoter sequencing primer: 5'-CGTGCGCCCTGGCAGGAAGATGG-3'

Generation of MAP4K3 expression plasmids

Generation of MAP4K3 CTGFP plasmid

Mammalian expression construct of MAP4K3 was prepared as a C-terminal cycle3GFP tagged protein (Figure 2.3). MAP4K3 cDNA from IMAGE CLONE 5296205 was amplified by PCR by use of the Expand Long Template PCR system using MAP4K3 For and MAP4K3 Rev primers.

For the following primers, the inserted Kozac sequences are in red and coding additions in green. A guanine base was added to MAP4K3 Rev 5' primer to code for alanine that keeps MAP4K3 in frame with GFP. The TGA stop codon from MAP4K3 cDNA was not included in the MAP4K3 Rev 5' primer.

MAP4K3 For 5'-GCCACCATGAACCCCGGCTTCGATTT-3'

MAP4K3 Rev 5'- GGTAAGTGTTCATGACCCGCCAG-3'

Following PCR amplification of MAP4K3 cDNA, the agarose gel extracted PCR product (Qiagen Gel extraction kit) was inserted in frame into pDNA3.1 TOPO CTGFP (Invitrogen). In brief, pDNA3.1 TOPO CTGFP kit is provided as a linearized vector with single 3'

thymidine (T) overhangs and topoisomerase covalently bound to the vector. Following ligation, bacterial transformation was performed. The DNA from selected clones was extracted from mini prep cultures and sequenced using T7 promoter primer and GFP reverse primer to confirm the DNA sequence was inserted at the correct site.

T7 promoter primer: 5'-TAATACGACTCACTATAGGG-3'

GFP reverse primer : 5'-GGGTAAGCTTCCGTATGTAGC-3'

Generation of MAP4K3 K45E CTGFP plasmid

A kinase dead MAP4K3 mutant was produced by site directed mutagenesis at the putative ATP binding domain of this kinase as previously published (Deiner, Wang et al. 1997). In order to create the kinase dead mutant of MAP4K3, site directed mutagenesis of the Lysine 45 to Glutamic acid 45 was performed using the quick-change site directed mutagenesis kit (Stratagene) using K45E for primer and K45E rev primer following the manufacturers protocol. To achieve the mutation the triplet in the MAP4K3 cDNA sequence corresponding to codon 133AAA135 was replaced with GAA, as shown in red on K45E primers.

K45E for primer:

5'-GGTGAATTAGCAATTGAAGTAATAAAATTGGAACCAGG-3'

K45E rev primer:

5'-CCTGGTTCCAATTTTATTACTTCAATTGCTGCTAATTCACCAG-3'.

Using the template pDNA3.1 MAP4K3 CTGFP, the oligonucleotides primers each complimentary to opposite strands of the vector were extended using PFU turbo DNA polymerase. Incorporation of the DNA primers generated the mutated plasmid. Following PCR the product was treated with DPN 1 which digested the parental DNA template and

selected for the mutated synthesised DNA. The mutated vector DNA was transformed into XL 10 gold chemically competent cells. The colonies were isolated and DNA mini preps generated. The DNA was sequenced using T7 promoter primer to identify correctly mutated DNA.

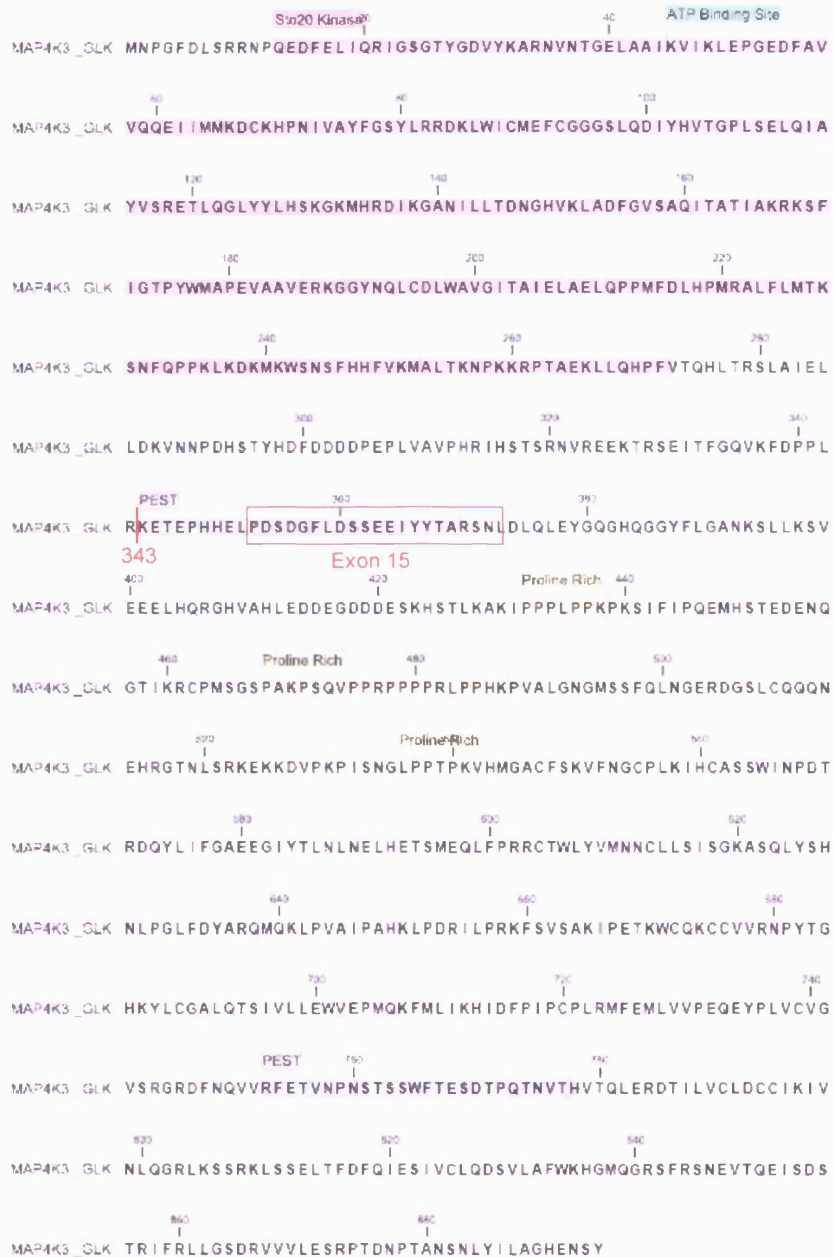


Figure 2.2 Amino acid sequence of MAP4K3

The amino acid sequence of MAP4K3 is shown above with annotations. The annotations shown are the kinase domain (pink), putative PEST domains (grey) and proline rich domains (yellow). The proline rich domain (PPRPPPPR) has been shown to bind to Endothelin A1. The MAP4K3 Image Clone 5296205 encodes an alternative splice variant consisting of a 874 amino acid protein with no exon 15 (marked by red box). The amino acid 343 is indicated in red as this is the site where deletion mutations were performed. A previous study generated a partial C-terminal deletion mutant by the removal of amino acids 362-844 (Deiner, Wang et al. 1997).

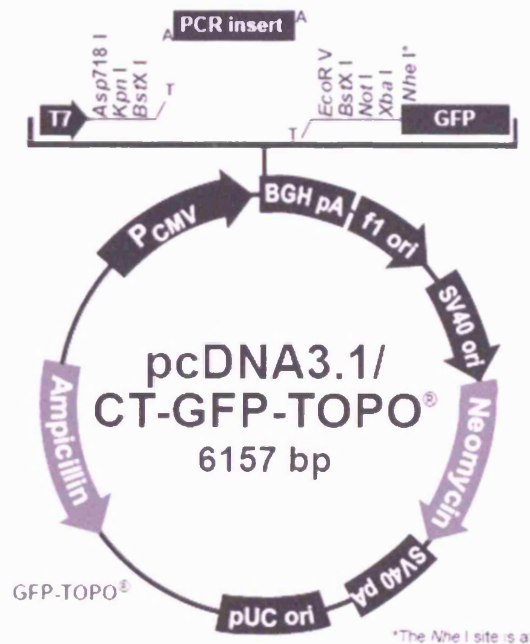
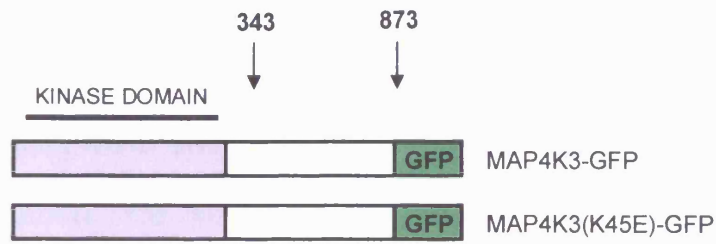


Figure 2.3 MAP4K3 fragments subcloned into pcDNA3.1/CT-GFP

pcDNA3.1/CT-GFP TOPO is a mammalian expression construct that expresses wild type GFP under the control of a CMV promoter. MAP4K3 cDNA from image clone 5296205 was amplified by PCR and cloned into the t-tailed pcDNA3.1/CT-GFP TOPO plasmid. Site directed mutagenesis at the putative ATP binding site was performed to generate a kinase dead mutant of MAP4K3 (K45E). Plasmid diagram adapted from www.invitrogen.com

Generation of MAP4K3 EGFP tagged plasmids

To investigate the fragment of MAP4K3 that can induce cell death, deletion fragments of MAP4K3 were cloned into pEGFP-N1 vector by the cohesive ends method (Figure 2.4). The PCR primers are designed to have a Kpn1 site on the forward primer and BamH1 cutting site on the reverse primer. The MAP4K3 EGFP and mutant proteins were generated by subcloning PCR fragments into the Kpn1 and BamH1 sites of pEGFP N-1. The pcDNA3.1 MAP4K3 GFP or pcDNA3.1 MAP4K3 K45E GFP plasmids were used in the PCR reaction using the Expand Long template system with the following primers as shown in table below.

Plamid ID	Forward Primer	Reverse Primer	Template
MAP4K3-EGFP	M4K3-EGFP-FL-St	M4K3-EGFP-FL-End	MAP4K3-CTGFP
MA4K3 K45E-EGFP	M4K3-EGFP-FL-St	M4K3-EGFP-FL-end	MAP4K3 K45E-CTGFP
MAP4K3 Δ 344-873-EGFP	M4K3-EGFP-FL-St	M4K3-Kin-rev	MAP4K3-CTGFP
MAP4K3 Δ 344-873(K45E)-EGFP	M4K3-EGFP-FL-St	M4K3-Kin-rev	MAP4K3-K45E-CTGFP
MAP4K3 Δ 1-343-EGFP	M4K3-CT-st	M4K3-EGFP-FL-End	MAP4K3-CTGFP

For the following primer sequences, the primer restriction sites are shown in blue, the inserted Kozac sequence in red and coding additions in green.

For M4K3-EGFP-FL-End primer; GC was added to MAP4K3 to encode for alanine in order to keep MAP4K3 in frame with EGFP and the stop codon from the MAP4K3 cDNA sequence was not included.

M4K3-EGFP-FL-St: TTTGGTACCGCCACCATGAACCCCGGCTTCGATTTG

M4K3-EGFP-FL-End: TTTGGATCCGGCGTAACTGTTTTTCATGACCCGC

For M4K3-Kin-rev; a guanine and cytosine base added to MAP4K3 to encode alanine that keeps MAP4K3 in frame with EGFP. The M4K3-CT-st; ATG start codon added and shown in green.

M4K3-Kin-rev: TTTGGATCCGCTCTTAAGGGTGGATCAAATTTC

M4K3-CT-st: CGGGGTACCGCCACCATGAAGGAGACAGAACCACA-TCATG

The PCR products were gel purified with Qiaquick Gel Extraction (Qiagen). Restriction digest performed on pEGFP-N1 plasmid and PCR amplified products, using Kpn1 and BamH1 followed by Qiaquick gel extraction. Ligation of purified DNA products in a ratio of 1:5 vector:insert performed using 1 ul T4 DNA ligase (New England Biosciences) in a total volume of 10µl for 20 minutes at 16⁰C . Following ligation, bacterial transformation was performed. The DNA from selected clones was extracted from mini prep cultures and sequenced using pEGFP-N For and pEGFP-N rev sequencing primer.

pEGFP-N For 5'-GAGTCTATATATAAGCAGAGCTG-'3

pEGFP-N rev 5'-CTGGTCGAGCTGGACGGCGACG-'3

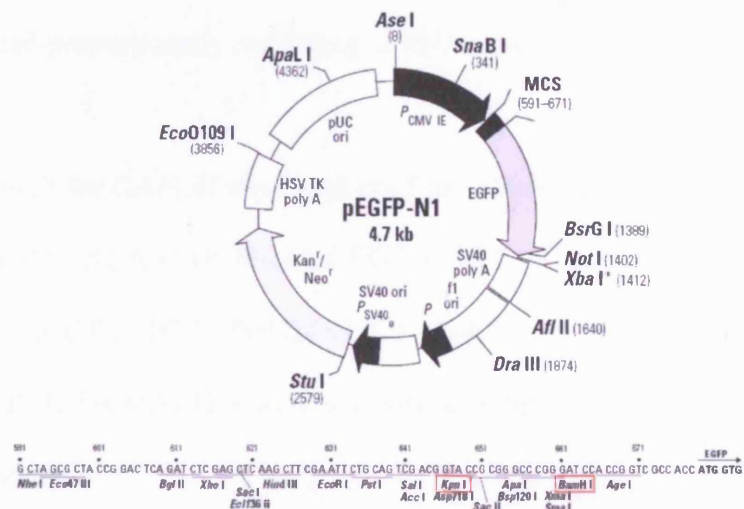
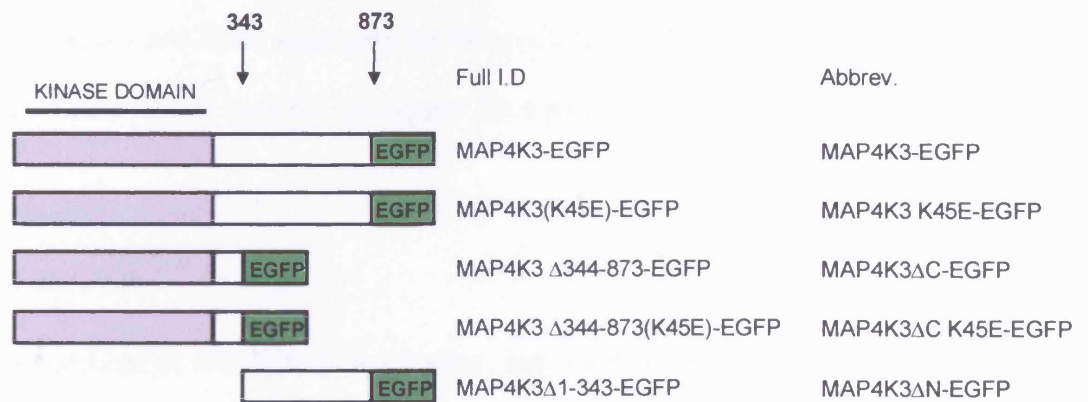


Figure 2.4 MAP4K3 fragments subcloned into pEGFP N-1 plasmid

MAP4K3 deletion mutants were generated by PCR amplification from the pcDNA3.1 MAP4K3 CT-GFP and cloned into the pEGFP-N1 vector by the cohesive ends method using Kpn1 and BamH1 restriction sites. pEGFP-N1 vector is a mammalian expression vector that encodes a red-shifted variant of wild-type GFP (EGFP) driven by the CMV promoter. Plasmid diagram adapted from www.clontech.com

RNA extraction

To isolate RNA from cell pellets the manufacturer's protocol was used for two kits; QIshredder (Qiagen) and RNA mini prep kit (Qiagen). QIshredder breakdown the genomic DNA and RNA miniprep is used for subsequent RNA purification.

Quantitative RT-PCR

To perform quantitative RT-PCR in a two-step, but one-tube reaction, from the extracted RNA, Qiagen Quantitect SYBR green RT-PCR kit was performed according to an adjusted manufacture's protocol on a Stratgene Mx4000. Total reaction volume was decreased to 30 μ l with regents reduced proportionally and 100ng of RNA used.

Primers for QRT-PCR for GAPDH were used at a final concentration of 1 μ M for each primer.

GAPDH-F: 5'- GGCTGAGAACGGGAAGCTTGTCAT-3'

GAPDH-R: 5'- CAGCCTTCTCCATGGTGGTGAAGA-3'

Primers for QRT-PCR for MAP4K3 were a quantitect primer mix (Qiagen, 10x stock) with the sequence unspecified.

The parameter CT (threshold cycle) for each reaction was determined with adaptive baseline algorithms using the Mx4000 Stratagene system software. The adaptive baseline algorithm calculates the baseline for each plot individually; thereby providing accurate Ct. A dissociation curve was generated for each reaction and was used to discriminate between specific and non-specific PCR products. The comparative Ct method was performed to determine relative expression changes in MAP4K3 mRNA levels (Pfaffl 2001). The normalization of expression of the gene GAPDH was performed to reduce the effect of differing total RNA input between samples. The sample of reference (Calibrator) for each

experiment was the respective scrambled siRNA control sample. Therefore the expression level of MAP4K3 in the calibrator is defined as 1.

Quantitative PCR

To perform quantitative PCR the SYBR green PCR mix (Qiagen) was used according to an adjusted manufacturer's protocol. SYBR green PCR was applied to human ovarian cancer gene expression cDNA panels (OriGene, Rockville, Maryland, USA) containing reverse transcribed DNA from 48 different patient RNA samples. A total of 30µl complete reaction mix plus the addition of 10x primer mix was added to each well on the 48 well plate. As in quantitative RT-PCR the CT was determined. Using the linearized pcDNA3.1 MAP4K4-CTGFP plasmid, a standard curve of copy number was generated in triplicate ranging from 1×10^4 to 1×10^8 copies of MAP4K3. The standard curve relates the initial quantity of the specific target to the Ct. The standard curve is then used to derive the initial template quantity in unknown wells based on their Ct values and this was calculated using the Stratagene software package

Protein lysates

Cells were washed with ice-cold PBS then lysed using ice-cold lysis buffer containing 0.5% Triton X-100 (BDH), 1x phosphatase inhibitor Cocktail Set II (Calbiochem, San Diego, California, USA) and 1x CLAP protease inhibitor cocktail. 1000x CLAP protease inhibitor cocktail containing 5mg/ml Chymostatin, 5mg/ml Leupeptin, 5mg/ml Antipain and 5mg/ml Pepstatin A in DMSO. Cell lysates were centrifuged at 12,000g for 5 min at 4⁰C. Protein concentrations in the lysates were determined using the Bradford assay (Biorad, Hemel Hempstead, Herts., UK). Whole cell lysates generated by the addition of 1x complete sample

buffer (Invitrogen), 4x stock with the addition of b- mercaptoethanol. Samples were heated to 95°C for 5 minutes.

Immunoprecipitation experiments

Immunoprecipitation (IP) designed to isolate cytosolic protein under non-denaturing conditions. The antibody beads were prepared using 50µl protein G sepharose coated beads (CRUK) and 2µg mouse monoclonal anti-GFP (CRUK) and placed in a 1.5ml Eppendorf tube. Triton X soluble fractions (see above) were added to the antibody coated beads for 1 hour at 4°C and kept in constant motion. Centrifugation of the tube to make a pellet of the beads and the clear supernatant was removed and transferred to a new Eppendorf. The beads were then washed using the lysis buffer, resuspended by vortexing, then centrifuged and the supernatant removed using G25 needle. This was repeated 3 times to remove any unbound cytosolic material. 50µl of 1x sample buffer was added and the sample heated to 95°C for 5 minutes to remove bound GFP. This IP sample was then used in Western blots.

Western blotting

Equal amounts of protein were separated using a range of 7.5% to 12.5% SDS-polyacrylamide gels electrophoresis (PAGE) with Tris-glycine running buffer using the BioRad protein II electrophoresis apparatus according to manufactures protocol. The SDS-PAGE gels were transferred onto methanol rinsed polyvinylidene difluoride (PVDF) membrane (Millipore, Billerica, Massachusetts, USA). The membrane was blocked with 5% non-fat dried milk in TBS-T buffer (20mM Tris-HCl, 500 mM NaCl and 0.01% Tween 20, pH 7.4) for 1 hour at room temperature and incubated overnight at 4°C with primary antibodies. After 3 washes with TBS-T buffer, the PVDF membranes were incubated with the

appropriate horseradish peroxidase-conjugated secondary antibodies for 1 hour at room temperature and rinsed a further 3 times in TBS-T for 15 minutes. To visualise the proteins ECL detection reagents (Amersham Bioscience, Bucks, UK) were used followed by exposure to X-ray film.

To strip the PVDF, the membrane was pre-washed in TBS-T, then incubated in the stripping buffer (25mM glycine-HCl, pH2, 1% SDS) for 30 minutes at room temperature, followed by 3x TBS-T 5 min wash steps and then proceeded as normal for primary antibody addition.

Chapter 3: Results

Chapter 3.1: An RNAi-based library screen to identify regulators of UV induced cell death

In order to identify putative suppressors of DNA damage a vector based RNAi library was used. This consisted of the first generation RNAi library (K330) produced at the Netherlands Cancer Institute. The library has since been further developed to include 7,914 human genes (NKi library) and has been used to identify genes involved in p53-dependent proliferation arrest (Berns, Hijmans et al. 2004). The K330 library encodes RNA hairpin (shRNA) molecules which, in theory, promote the siRNA mediated suppression of a subset of endogenous human kinases and other selected proteins that are involved in critical cellular survival processes. Loss of function analysis will be used to identify genes that when knocked down confer resistance to cell death. This loss of function genetic screening approach has been employed to perform a screen designed to identify novel regulators of DNA damage induced cell death.

A stable cell line expressing the K330 library was generated by retroviral transduction. To determine the optimal dose of UV for the screen, the levels of cell death had to be determined following treatment with different UV doses. The screen using the K330 library cell line was then performed and cells that survived DNA damage induced cell death isolated. Genomic DNA was isolated from the surviving cells and from this, the PCR amplified shRNA inserts were identified by sequencing. The candidate genes were identified by comparing the expression levels before and after UV treatment; in order to identify putative cell death regulators. The strongest candidate from the UV induced cell death screen was identified as

MAP4K3, as it was the most highly expressed following the enrichment cycle. MAP4K3 was therefore selected as a suitable candidate for further analysis.

Generation of a U2OS cell line expressing the K330 RNAi library

To generate a U2OS cell line that stably expresses the RNAi library, the retroviral production and infection procedure outlined in Figure 3.1.1 was performed. The cell line used for the production of retroviruses was the Phoenix A cells, which express the virus packaging proteins. The retroviral cassette in pRS (a replication-incompetent viral vector) requires packaging proteins expressed by the Phoenix A cell line. The Phoenix A cells were transfected with the empty vector control (pRS) or the K330 RNAi library plasmids. The retrovirus particles produced were harvested by the collection of the cell culture media, which was then used to infect U2OS cells. Puromycin selection was used to obtain a population of cells stably expressing the hairpin molecules. The U2OS K330 cell line was then used in the UV induced cell death regulator screen. The pRS control was used to determine the optimal UV dose to be used in the screen.

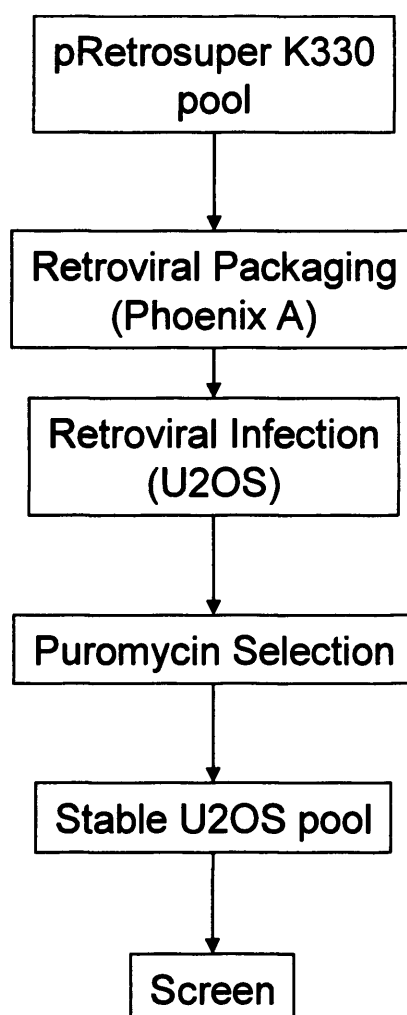


Figure 3.1.1 Diagram illustrating the strategy for the generation of a human cell line expressing a stable siRNA library.

The K330 RNAi library and vector control plasmids were transfected into a Phoenix A packaging cells and the retroviral supernatant was harvested after 4 days of incubation. The virus containing supernatant was used to infect U2OS cells and drug selection with puromycin was performed for 7 days. These cells were then considered to have stable expression of the shRNA encoding library and were used in the subsequent suppressor screen.

Establishment of UV assay conditions

To determine the dose of UV to use in the cell death regulator screen, preliminary experiments were performed with the U2OS pRS stable cell line. Cells were treated with UV at varying doses, incubated for 24 hours and the percentage of viable cells was determined using FACS analysis. Viable cells were defined as such because they were negative for PI, which is a membrane impermeant DNA stain. If the cells have lost their membrane integrity the stain is able to enter and bind DNA, which occurs in non-viable cells (Figure 3.1.2a). The numbers of viable cells were counted and 2×10^5 viable cells were returned to culture for a further 4 days. Crystal violet staining was used to stain the cells still attached to the culture plate, and was used to determine long term survival rates (Figure 3.1.2b and c). Quantitative analysis of the crystal violet staining was performed by solubilisation of the cells in ethanol and the absorption was measured at 600nm. The absorbance results were recorded and converted to percentage cell survival. The UV dose of 25 J/m^2 reduced viable cells to 77% after 24 hours and on the survival assay using the crystal violet staining showed 42% cell survival compared to the control; therefore this dose was considered to induce an insufficient amount of cell death for the UV screen. The UV dose of 50 J/m^2 and 100 J/m^2 resulted in cell survival rates of 44% and 36% respectively at 24 hours. In the long term survival assay, both 50 J/m^2 and 100 J/m^2 showed a reduction of cell survival to 9% and 7% respectively. At 100 J/m^2 there was significant cell death, but it was decided that this was too high a stringency with the number of long term surviving cells being too low. The dose of 50 J/m^2 was therefore chosen as the ideal dose in the cell death suppressor screens because it causes a significant amount of cell death, but also allowed long term survival of cells for further experiments to be performed.

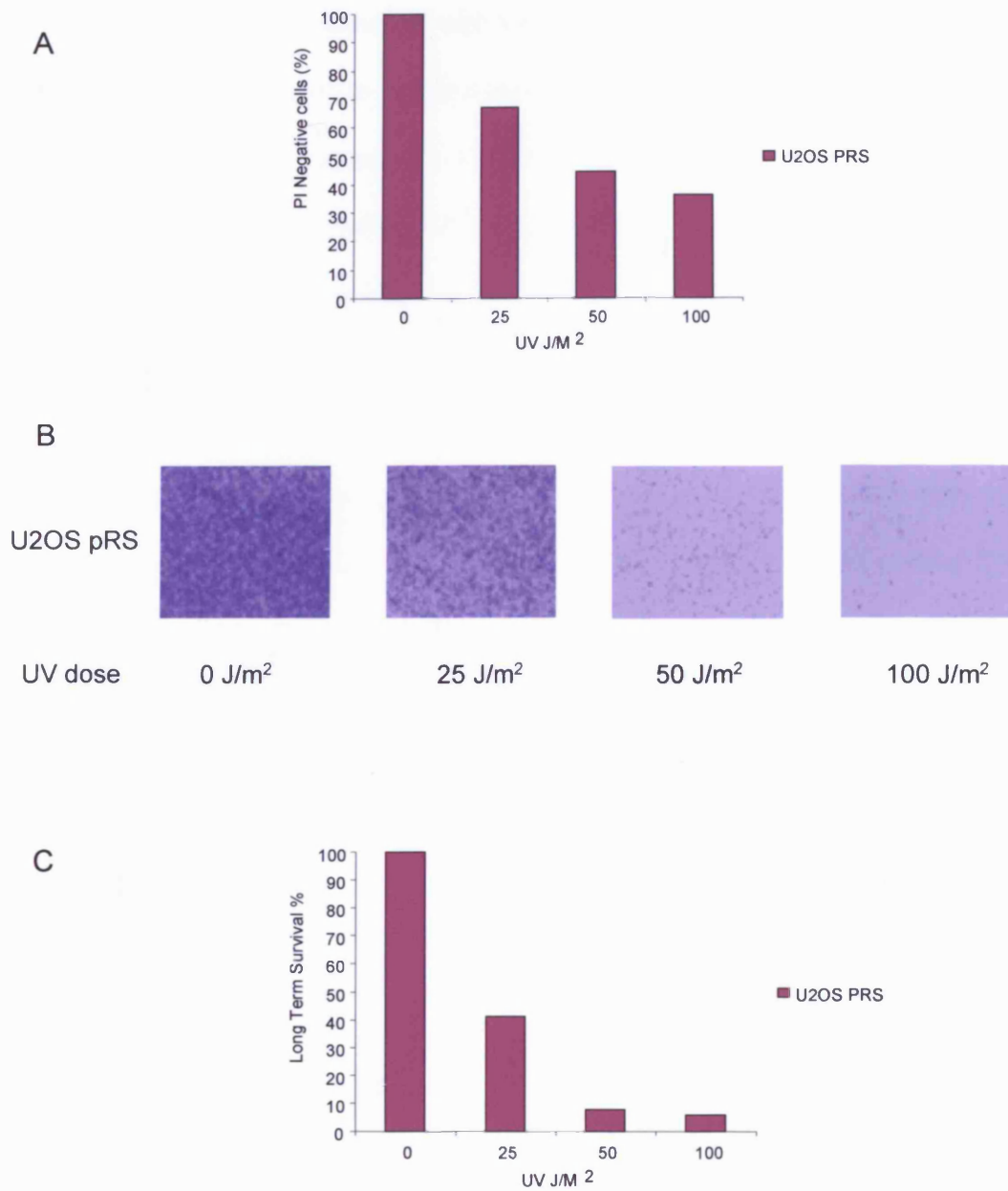


Figure 3.1.2 Establishment of UV assay conditions

U2OS pRS cells were exposed to UV-C irradiation at different doses (0-100J/m²). **A)** 24 hours following UV treatment, FACS analysis using propidium iodide was performed to determine the percentage of viable cells (PI negative). **B)** 2x10⁵ UV treated viable cells were plated onto 100mm² dishes and cultured for 4 days. Cells were then stained with crystal violet with representative image shown for each UV dose. **C)** To quantify the crystal violet staining, solubilisation of the cells on stained plates was performed and the absorbance was measured at 600nm. Relative cell survival was calculated by considering the untreated pRS control absorbance to be 100% long term cell survival.

Cell death suppressor screen

The cell death screen was performed with the stable U2OS K330 cell line (Figure 3.1.3). The UV dose of 50J/m^2 was used to induce a significant amount of cell death on the U2OS K330 cells. Treated cells were cultured for 4 days following which, the genomic DNA from the untreated U2OS K330 cells and the UV treated U2OS K330 cells was isolated. The surviving cells were considered to be enriched for the expression of candidate cell death suppressors. To identify the population of shRNAs expressed in the surviving K330 library cells, a region containing the shRNA hairpin sequence was amplified by PCR from the genomic DNA. The shRNA hairpin sequences were cloned into a sequencing vector and were then sequenced using the H1 promoter primer. The number of shRNA inserts sequenced was 254 in the untreated population and 97 following UV selection (Figure 3.1.4). From the identified 59mer targeting sequence the siRNA sequence was identified and matched to the corresponding target gene.

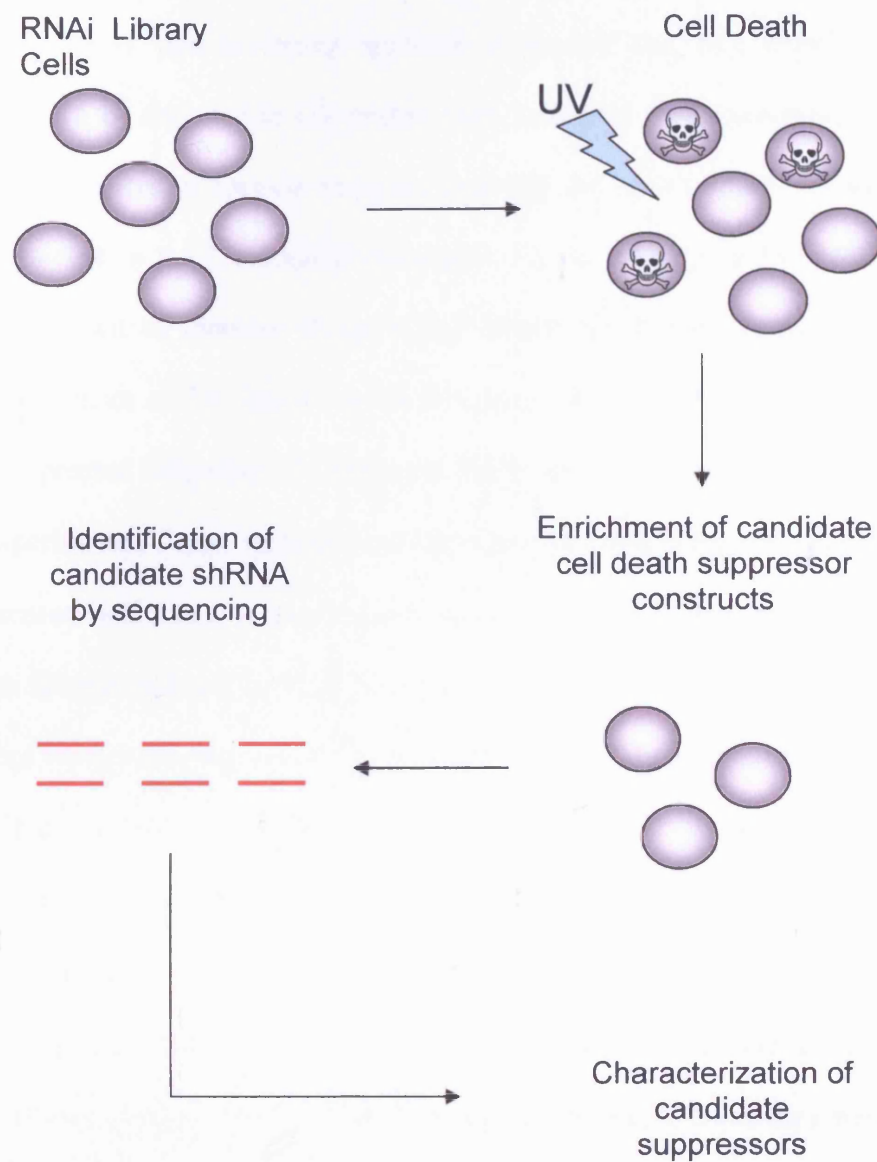


Figure 3.1.3 Schematic representation of the UV induced cell death suppressor RNAi library screen.

U2OS cells containing the RNAi library were treated with $50\text{J}/\text{m}^2$ UV radiation to induce cell death. Surviving cells were expanded and the genomic DNA was isolated. The targeted hairpins were PCR amplified and cloned into a sequencing vector. Sequencing was then performed using H1 promoter primer. Candidates were selected by comparing the sequences before and after treatment. The most abundant sequences were selected for further characterisation, as these were considered to be potential cell death regulators.

Identification of candidate modulators of UV induced cell death

The rationale behind this screening approach suggested that any putative cell death suppressors should be enriched in UV treated cells, compared to the untreated cells. Within the identified sequences, a specific sequence targeting the kinase MAP4K3 was the most abundantly detected in the UV treated population (Figure 3.1.4). The MAP4K3#3 shRNA sequence was shown to increase in the RNAi library population compared to untreated population by a factor of 2.6. Based on the fact that a MAP4K3 shRNA was the sequence most highly expressed following UV treatment, this kinase was chosen for follow up siRNA validation experiments. Targeting sequences that were identified in the UV treated population but not sequenced in the untreated population were considered to be enriched and were also considered to be potential cell death regulators. Of these, only targeting sequences that had been identified more than once in the UV treated population were deemed to be significant. This criterion selects Protein tyrosine kinase 2 beta (PTK2B) and CDC-like kinase 3 (CLK3) that were not sequenced before UV treatment but were respectively 3% and 2% of the population following UV treatment suggesting that they have been enriched in this screen (Table 3.1.5). The representation of the sequences targeting PKT2B and CLK3 within the untreated cells was unknown but was considered to be less than 0.4% as they were absent in the 254 sequences identified. In the untreated cells the MAP4K3#3 shRNA sequence was at 6% of the population and was therefore considered already enriched before UV treatment. This suggested that knockdown of MAP4K3 conferred an advantage to the cells causing the sequence to be enriched. MAD2L2 was enriched before UV treatment at 8.3% and following treatment was reduced to 1% of the population. This suggests that shRNA suppression of MAD2L2 might confer a proliferative advantage to cells where this transcript is suppressed and also might sensitise these cells to UV-induced cell death.

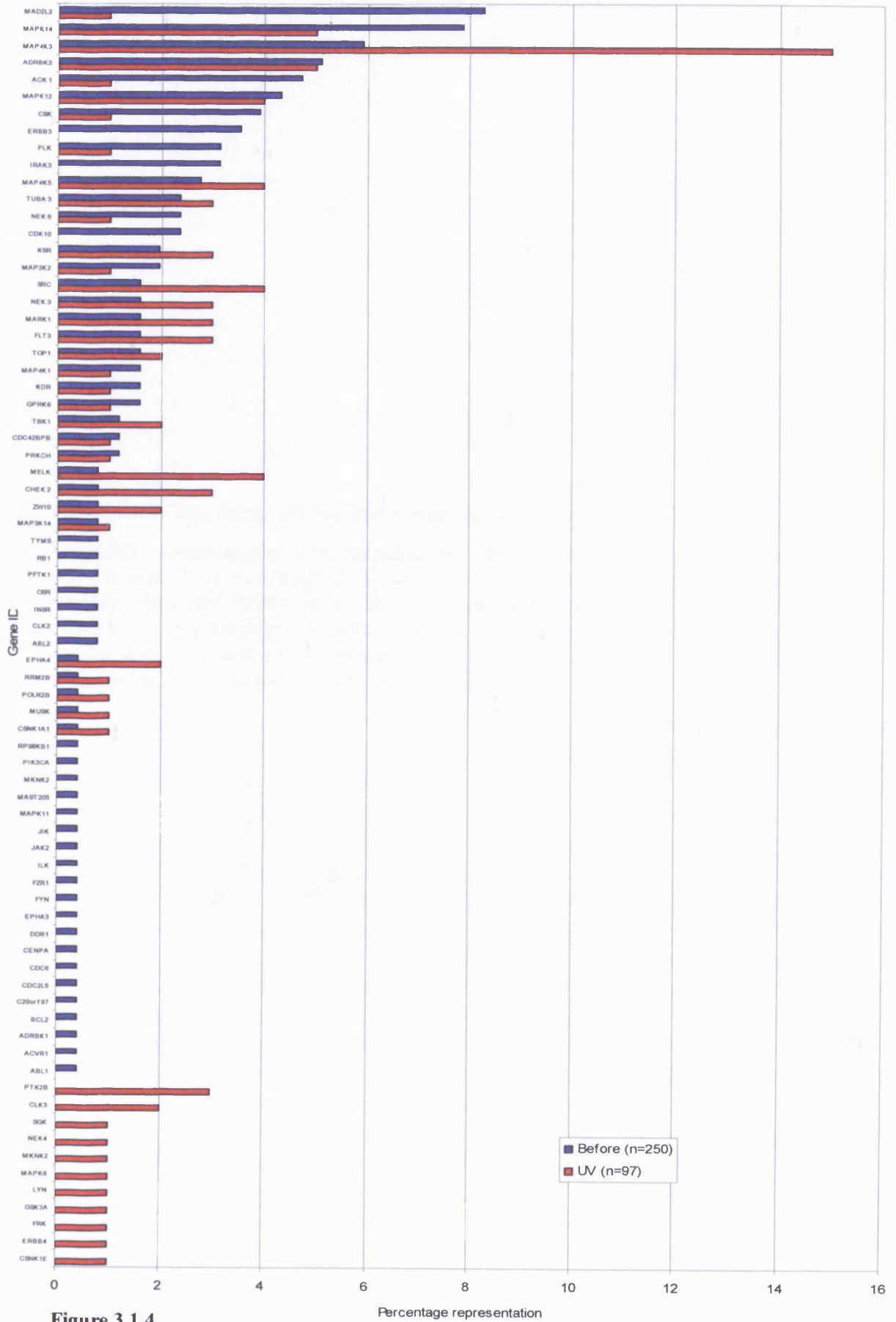


Figure 3.1.4

Figure 3.1.4: Population of identified hairpin sequences before and after UV treatment

The shRNA targeted genes were identified from the population of untreated U2OS K330 cell line and UV treated U2OS K330 cell line. Following UV treatment at 50J/m² or no treatment the U2OS K330 cell line was expanded and the genomic DNA was isolated. A region containing the shRNA targeting sequence was PCR amplified and sub-cloned into a transfer vector. Sequencing was then performed using the H1 promoter primer to identify the targeting 59mer sequence with the identified genes shown in the graph.

Name	shRNA Role	Described biological role	Control (%)	UV (%)
MAP4K3	Suppressor	Response to environmental stress (JNK pathway)	6	15.5
PTK2B	Suppressor	Involved in calcium induced regulation of ion channel and activation of MAPK pathways	<0.4	3
CLK3	Suppressor	Control of RNA splicing	<0.4	2
MAD2L2	Sensitizer	Inhibitor of the anaphase promoting complex Involved in DNA damage response (JNK pathway)	8.3	1

Table 3.1.5: Candidate cell death suppressors and cell death sensitizers identified by the UV-induced RNAi screen

Table shows the candidate cell death suppressors identified from the UV screen. They were selected as the sequences were enriched following UV treatment. MAP4K3 was the most abundant sequence while CLK3 and PTK2B were not identified in the control but following treatment represented 3% and 2% of the population respectively. MAD2L2 shRNA was considered to be a cell death sensitizer as following UV treatment the targeting sequence decreased by a factor of 8. MAD2L2 and MAP4K3 were enriched in the control population suggesting that they might confer a proliferative advantage to cells.

Chapter 3.2: The role of MAP4K3 in cell death and proliferation using gain & loss of function analysis

The Ste20 related kinase, MAP4K3 was identified as a putative cell death regulator using a suppressor screen. However, the screen strategy identified only one targeting sequence for MAP4K3 of the 3 independent sequences present in the library. The following experiments were performed to confirm if MAP4K3 is involved in DNA-damage induced cell death and to determine the role of this kinase in cell proliferation. In order to perform the validation experiments, three independent targeting sequences for MAP4K3 were employed in order to show the specificity of the knockdown. To confirm siRNA mediated suppression of MAP4K3 led to downregulation of this transcript, quantitative RT-PCR was performed. The hypothesis that suppression of MAP4K3 leads to a reduction in cell death following UV damage was tested using a cell survival assay following DNA damage. MAP4K3 was observed to be enriched in the untreated library cells suggesting MAP4K3 suppression confers an increase in proliferation. The contribution of MAP4K3 suppression to DNA synthesis was tested by determining the levels of BrdU incorporation into newly synthesised DNA. These experiments revealed that MAP4K3 suppression induces an increase in survival following DNA damage induced cell death and that MAP4K3 suppression induces an increase in DNA synthesis. This evidence supports the initial screen results and indicates that MAP4K3 is a regulator of UV induced cell death.

As results from loss-of-function analysis have linked MAP4K3 with regulation of cell death using siRNA mediated suppression, gain-of-function analyses were performed in order to further characterise the role of MAP4K3. The objective of such experiments was to determine if enhanced expression of MAP4K3 has an effect on cell death; such as directly inducing cell

death or sensitising cells to cell death stimuli. To determine this, MAP4K3 cDNA was tagged to GFP and overexpressed in U2OS cells. The amount of cell death was quantitated and further experiments were performed to characterise this cell death process. MAP4K3 truncation mutants were generated to investigate the requirement for different regions of MAP4K3 for cell death induction. This chapter shows that MAP4K3 induces cell death by the activation of Bax with the cell death dependent on caspase activity and on the mitochondrial pathway of apoptosis. The kinase activity is partially required to induce cell death with the kinase domain sufficient to induce cell death. In summary this chapter identifies MAP4K3 as a novel inducer of apoptosis.

Establishment of a system for the siRNA-mediated transient suppression of MAP4K3

To silence endogenous MAP4K3 in cultured cells, this kinase was targeted using 3 independent siRNA sequences by performing reverse transient transfection in U2OS cells. Total RNA was then isolated from these cells 48 hours post transfection and QRT-PCR analysis of the MAP4K3 transcript was performed. This revealed that the three MAP4K3 targeting siRNAs used in this project induced at least 75% downregulation of the MAP4K3 messenger RNA when compared to the scrambled control (Figure 3.2.1A). This shows the system for transient MAP4K3 knockdown is effective and experiments can be performed to investigate the role of MAP4K3 in UV induced cell death.

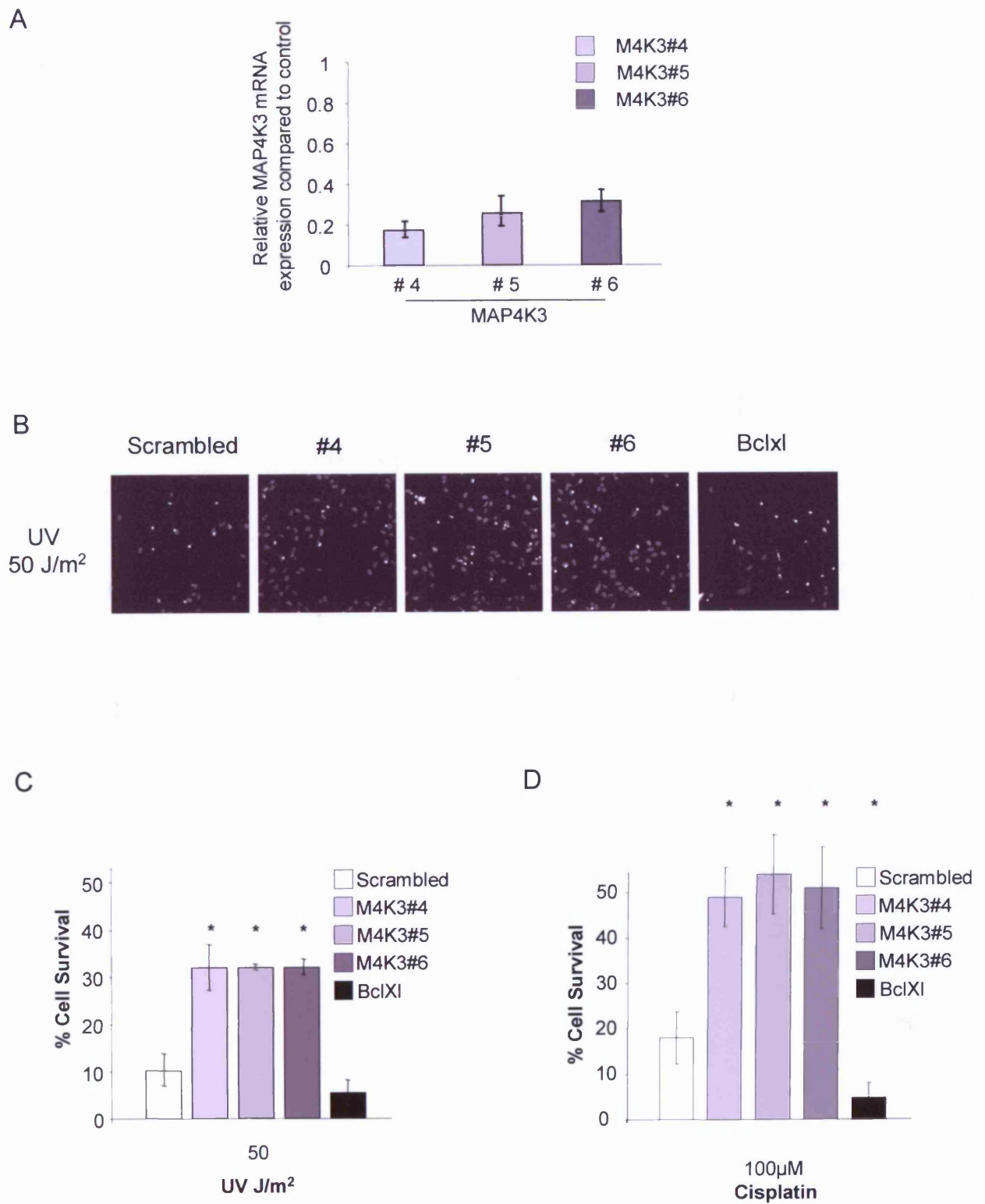


Figure 3.2.1: siRNA mediated suppression of MAP4K3 protects from DNA damage induced cell death.

Figure 3.2.1: siRNA mediated suppression of MAP4K3 protects from DNA damage induced cell death.

Reverse transfection of U2OS using siRNAs was performed and the cells were cultured for 48 hours. **A)** The RNA was extracted and real time PCR performed to determine relative levels of MAP4K3 mRNA. The loading control mRNA used was GAPDH, with the average relative expression of MAP4K3 compared to the scrambled siRNA control. The errors bars shown are the standard deviation of the mean from one representative experiment. **B)** The transfected cells were treated with 50J/m² UV and fixed and stained with Hoechst after 24 hours. Representative fields for each siRNA are shown of Hoechst staining. **C)** To quantify the cell survival following UV treatment, a viable cell count was performed. Cellomics microscope captured 20 fields per well and an algorithm was used to identify viable cells by the state of their nuclear morphology. These cell counts were converted into percentage by comparison to the respective untreated siRNA. Data shown is the mean from three independent experiments with error bars being the standard deviation of the mean. Data were analyzed by two-sample T-Test and * indicates $P < 0.05$; a statistically significant difference compared to the scrambled siRNA control cells. **D)** To determine if MAP4K3 suppression protects from cisplatin induced cell death, the cell survival assay was performed as in C using 100 μ M cisplatin. Data shown is the mean from three independent experiments performed in triplicate with error bars as the standard deviation of the mean. Data were analyzed by two-sample T-Test and * indicates $P < 0.05$; a statistically significant difference compared to the scrambled siRNA control cells

siRNA mediated suppression of MAP4K3 protects from DNA damage induced cell death

To confirm that suppression of MAP4K3 results in enhanced cell survival, U2OS cells were transiently transfected with siRNA targeting MAP4K3 and treated with 50J/m² UV. 24 hours post UV treatment U2OS cells exhibited shrinkage and membrane blebbing, characteristic of cells undergoing apoptosis with the majority of the cells detached from the plate. These cells were fixed and the nuclei were stained. The BclxL siRNA transfection was performed as a positive control for the experiments as suppression of BclxL is known to sensitise cells to apoptosis. Representative images in Figure 3.2.1B suggest that suppression of MAP4K3 confers an enhanced survival compared to cells transfected with scrambled siRNA. To quantify the number of attached viable cells, an automated microscopy system was used (Cellomics Kinetiscan) and the number of viable cells determined using an algorithm as described in the material and methods section. The resulting cell counts excluded cells that contained nuclei with condensed chromatin (apoptotic) and for each siRNA the counts were normalised to its untreated control value. The resulting number was converted to percentage and termed cell survival with the average of three independent experiments shown in figure 3.2.1C. A cell survival rate of 10% was obtained using the scrambled siRNA control following UV treatment of 50J/m². Three independent siRNA sequences were used in this study to ensure consistency of MAP4K3 suppression on cell survival and rule out possible off target artefacts. The average cell survival for each sequence was 33% (Figure 3.2.1C). This is an increase of 23% cell survival when compared to the scrambled control and is statistically significant difference (t-test, p<0.05). This lead to the conclusion that siRNA mediated suppression of MAP4K3 results in a significant increase in cell survival following UV induced cell death.

In order to test if MAP4K3 is a more general mediator of DNA-damage induced cell death, a second DNA damaging agent, cisplatin, was used. Cells were transfected with siRNAs targeting MAP4K3, treated with cisplatin and cell survival was determined. The cell survival assay was performed as in the UV experiment with the percentage cell survival calculated from 3 independent experiments that were performed in triplicate (Figure 3.2.1D). This analysis revealed that cisplatin treatment resulted in 24% cell survival in cells transfected with scrambled siRNA control. In comparison siRNA mediated suppression of BclxL resulted in 5% cell survival, a significant decrease when compared to control siRNA thus confirming the efficiency of the transfection assay. siRNA mediated suppression of MAP4K3 conferred an increase of cell survival from scrambled control level of 24% to 49%, 54%, 51% for the MAP4K3#4, #5 and #6 siRNAs respectively. These changes are statistically significant (t-test $p < 0.05$) and show that siRNA mediated suppression of MAP4K3 confers enhanced resistance to DNA damage-induced apoptosis triggered by cisplatin (Figure 3.2.1D)

MAP4K3 triggers caspase dependent cell death

To further characterise the role of MAP4K3 in cell death, overexpression experiments were performed to determine if increased levels of this kinase are sufficient to induce cell death. This was performed by expressing MAP4K3 as a GFP fusion in U2OS cells and by the generation of a kinase dead MAP4K3 mutant. The level of apoptosis in GFP positive cells was determined by scoring the percentage of green fluorescent cells with condensed chromatin. This method revealed that MAP4K3 induced significantly more cell death (65%) compared to a GFP control of transfection (8%) (Figure 3.2.2). The kinase-dead mutant of MAP4K3-(K45E)-GFP induced 28% cell death which is a significant reduction compared to the MAP4K3-GFP but significantly higher than the GFP control. This data suggests that MAP4K3 lacking the kinase activity is still able to induce cell death. Ectopically expressed

MAP4K3-(K45E)-GFP is localised to the cytosol in viable U2OS cells, with a small percentage (3%) displaying a distinct punctate localisation. These experiments reveal that MAP4K3 is a potent inducer of cell death, with the kinase activity required for the maximal induction of cell death.

Given that overexpression of MAP4K3 resulted in condensation of chromatin, a characteristic of caspase dependent apoptotic cell death, the involvement of caspases was studied. To test if MAP4K3-induced cell death is caspase-dependent; zVAD-fmk, a broad-spectrum caspase inhibitor, was used. As a positive control caspase 8 tagged to EGFP a known inducer of apoptotic cell death was used. The zVAD-fmk inhibitor was used at 50 μ M; at this concentration it was able to inhibit chromatin condensation induced by Caspase 8 expression. To inhibit caspases 50 μ M zVAD was added during transfection with MAP4K3 plasmid DNA. This reduced the cell death to 7% compared to MAP4K3 alone at 65%. This shows that MAP4K3 induced cell death is dependent on caspase activity.

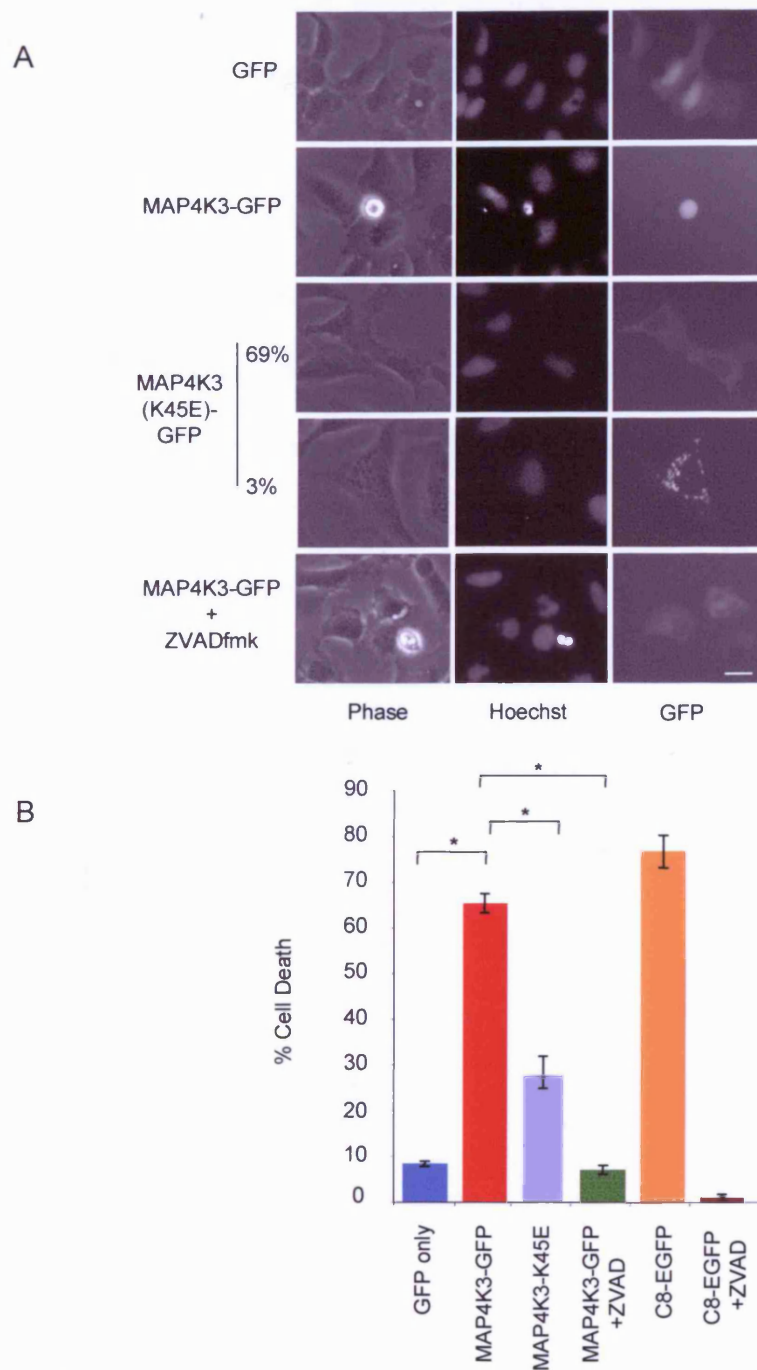


Figure 3.2.2: Overexpression of MAP4K3 induces caspase dependent cell death

Overexpression of GFP tagged MAP4K3 mutants by transient transfection of U2OS was followed by fixation and Hoechst staining. **A)** Representative images using phase contrast (whole cell), Hoechst (nuclei) and GFP (overexpressed protein). Scale bar represents 10 μ m. **B)** The levels of apoptosis in GFP positive cells was determined by scoring the percentage of green fluorescent cells with condensed chromatin. 50 μ M zVAD-fmk was used in appropriate transfections to inhibit caspase activity. Counts are the mean from 200 cells per transfection from three independent experiments. Statistical significance calculated using t-test with * indicates $P < 0.05$.

The MAP4K3 Δ 343-874 deletion mutant is sufficient to induce cell death

In order to test if the kinase domain of MAP4K3 was sufficient to induce cell death, truncation mutants were fused to GFP and ectopically expressed in U2OS cells. The cell death was scored as described previously. This study showed that MAP4K3 Δ C induced significantly more cell death (72%) compared to an EGFP control of transfection (12%) (Figure 3.2.3). The MAP4K3 Δ C K45E (MAP4K3 Δ 343-874(K45E)-EGFP) only induced 5% cell death, indicating that MAP4K3 Δ C K45E does not induce cell death. Therefore the cell death induced by overexpression of MAP4K3 Δ C is dependent on its kinase activity. The C-terminal regulatory domain of MAP4K3 (MAP4K3 Δ 1-343-EGFP) induced 8% cell death when overexpressed in U2OS cells, which is not a significant difference compared to the EGFP control and suggests that the kinase domain is required for induction of cell death. In summary MAP4K3 Δ C is sufficient to induce high levels of cell death and the kinase activity is required for this cell death.

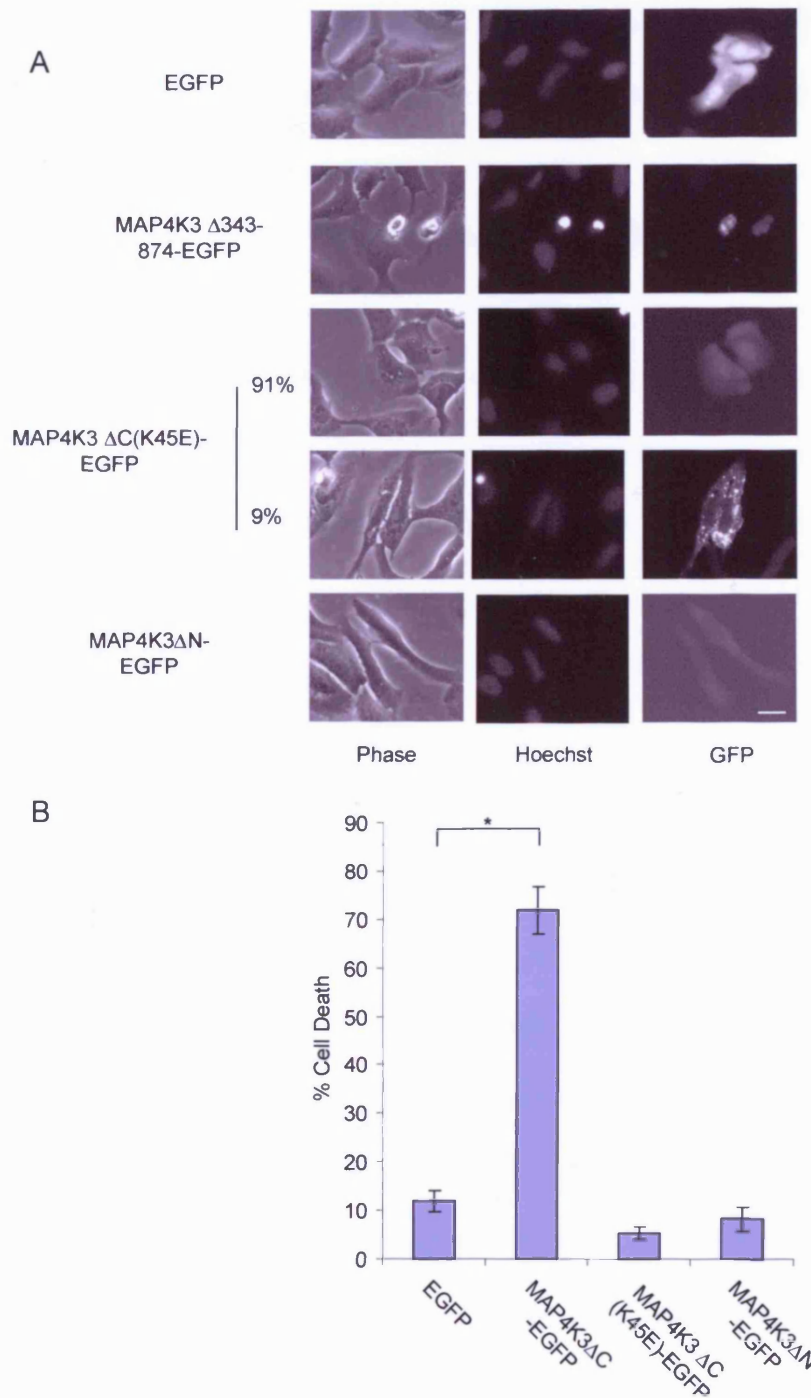


Figure 3.2.3: MAP4K3 kinase domain is sufficient to induce cell death

Overexpression of EGFP tagged MAP4K3 mutants by transient transfection of U2OS was followed by fixation and Hoechst staining. **A)** Representative images using phase contrast (whole cell), Hoechst (nuclei) and GFP (overexpressed protein). Scale bar represents 10 μ m. **B)** The levels of apoptosis in EGFP positive cells was determined by scoring the percentage of green fluorescent cells with condensed chromatin. Counts are the mean from 100 cells per transfection from three independent experiments. Statistical significance calculated using t-test with * indicating $P < 0.05$ compared to the EGFP transfection.

MAP4K3 modulates mitochondria-dependent apoptotic cell death

The results presented so far indicate that MAP4K3 induced cell death is caspase dependent. Bax, a proapoptotic member of the Bcl-2 family, normally resides in the cytosol and translocates to mitochondria in response to a variety of apoptotic stimuli (Hsu, Wolter et al. 1997; Wolter, Hsu et al. 1997). In mitochondria, Bax exerts a proapoptotic action by disrupting mitochondrial membrane potential, leading to release of cytochrome c (Jurgensmeier, Xie et al. 1998; Reed, Jurgensmeier et al. 1998). As well as the change in localisation, Bax undergoes a conformational change allowing the formation of an oligomer (Nechushtan, Smith et al. 1999; Suzuki, Youle et al. 2000). To investigate if MAP4K3-induced cell death activates the mitochondria dependent pathway of apoptosis the effects of overexpression of MAP4K3 on the conformation state of Bax were investigated. U2OS cells were transfected with MAP4K3-GFP in the presence of zVAD-fmk to block the execution stage of apoptosis. These cells were further processed for immunofluorescence using a Bax conformationally specific antibody. In a previous study the anti-Bax Clone 3 used in this project behaved as a conformation-specific antibody that recognized an epitope that is normally concealed and is only exposed during apoptosis (Dewson, Snowden et al. 2003). The levels of Bax activation in GFP positive cells was determined by scoring the percentage of green fluorescent cells with Bax staining in a conformationally active state. The Bax positive U2OS cells showed clustering of Bax which is indicative of Bax activation at the mitochondria. MAP4K3 positive cells display 69% active Bax, with the GFP control displaying 14% and MAP4K3 K45E having 12% active Bax (Figure 3.2.4). Using this experimental system I have been able to determine that MAP4K3 overexpression induces a Bax conformational change and therefore is likely to modulate apoptotic cell death by promoting mitochondrial dependent apoptosis.

As MAP4K3 induces a conformational change in Bax, the next question to address is if this cell death is dependent on the intrinsic pathway of apoptosis. As Bax-induced caspase activation and apoptosis via cytochrome c release from mitochondria is inhibited by Bcl-xL (Finucane, Bossy-Wetzel et al. 1999), investigated in this project. By performing simultaneous overexpression of MAP4K3-GFP and BclxL-RFP into U2OS cells, chromatin cell death counts of GFP and RFP positive cells were performed (Figure 3.2.5). As a positive control for BclxL-RFP suppression of cell death, a co-transfection with Bax-EGFP was performed that resulted in a reduction in cell death from 72% to 19%. The control of RFP and GFP transfected cells had a background cell death of 11% with MAP4K3 GFP and RFP positive cells inducing 70% cell death. The MAP4K3-GFP and BclxL-RFP positive cells had a cell death of 31% which is a significant reduction in the cell death. This data indicates that BclxL overexpression significantly reduces the cell death induced by MAP4K3 overexpression.

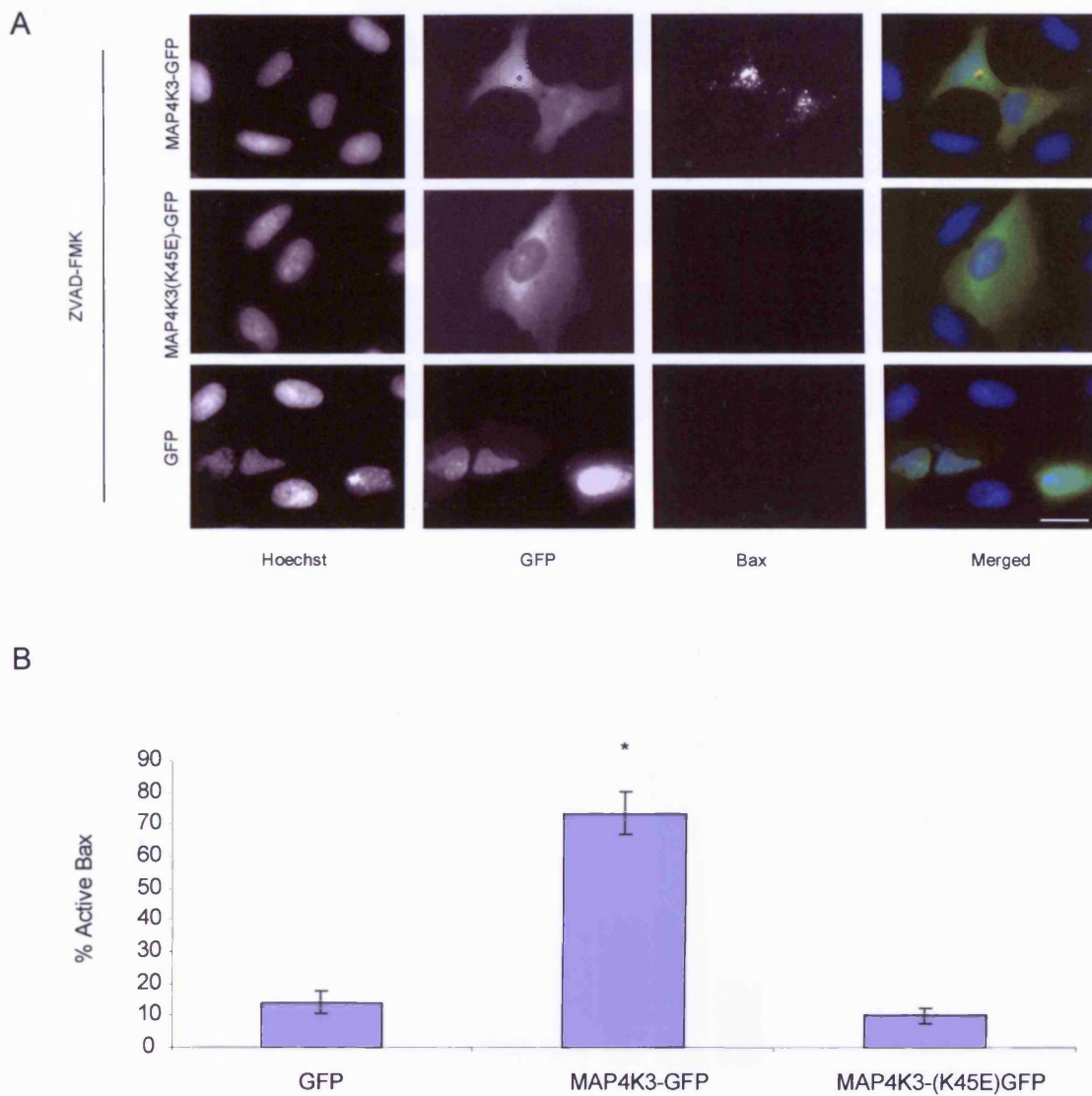


Figure 3.2.4: MAP4K3 induces Bax conformational change

Overexpression of EGFP tagged MAP4K3 mutants by transient transfection of U2OS was followed by fixation, Hoechst staining and immunostaining using a conformational specific Bax antibody. **A)** Representative images of Bax (red), Hoechst (nuclei) and GFP (overexpressed protein). Scale bar represents 10 μ m with false colour added in the Merge column. **B)** The levels of active Bax were determined by counting the percentage of GFP positive cells with Bax staining. Counts are the mean from 100 cells per transfection from three independent experiments. Statistical significance was calculated using t-test with * $P < 0.05$ compared to the GFP transfection.

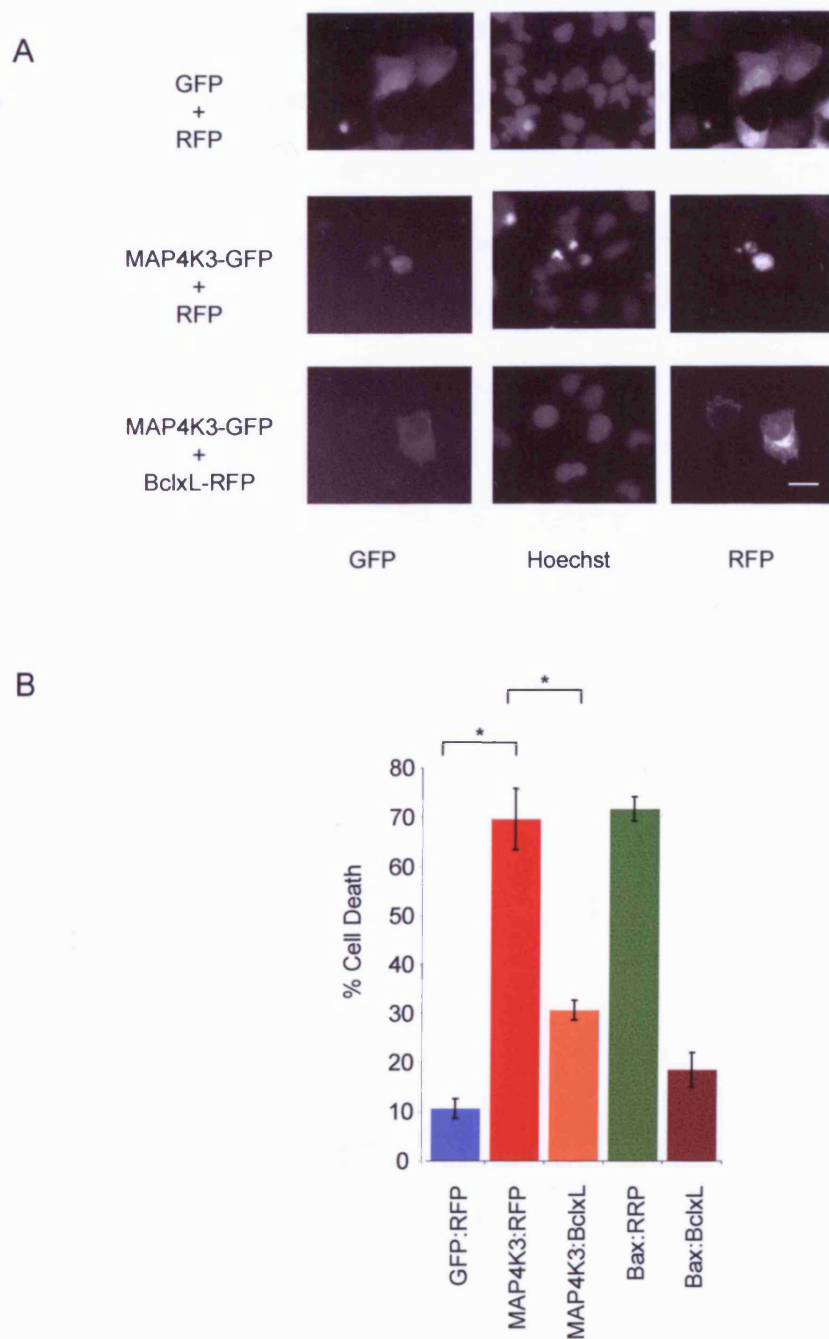


Figure 3.2.5: MAP4K3 induced cell death is suppressed by BclxL overexpression

Overexpression of EGFP and RFP tagged proteins by transient transfection of U2OS was followed by fixation and Hoechst staining. **A)** Representative images using Hoechst (nuclei), RFP (Bcl-xL) and GFP (overexpressed protein). Scale bar represents 10 μ m. **B)** The levels of apoptosis in double positive cells was determined by scoring the percentage of green fluorescent and red fluorescent cells with condensed chromatin. Counts are of 100 cells per transfection from three independent experiments. Statistical significance was calculated using t-test with * indicating $P < 0.05$ compared to either the control or MAP4K3

Suppression of MAP4K3 enhances cell proliferation

The results of the screen suggest that a MAP4K3 shRNA was enriched before treatment suggesting that downregulation of this transcript might confer a proliferative advantage to cells. To determine the role of MAP4K3 in cell proliferation, transient suppression of MAP4K3 was performed using 3 independent siRNAs followed by quantification of DNA synthesis using a BrdU ELISA assay (Figure 3.2.6). This revealed that siRNA mediated suppression of MAP4K3 using 3 independent targeting siRNAs, resulted in a significant increase in DNA synthesis compared to the scrambled control (three independent experiments performed in triplicate, t-test $p < 0.05$). This significant increase of BrdU incorporation in MAP4K3 knockdown cells suggests that DNA synthesis is enhanced upon suppression of this kinase. Thus cells lacking normal levels of MAP4K3 might have a proliferative advantage when compared to control cells.

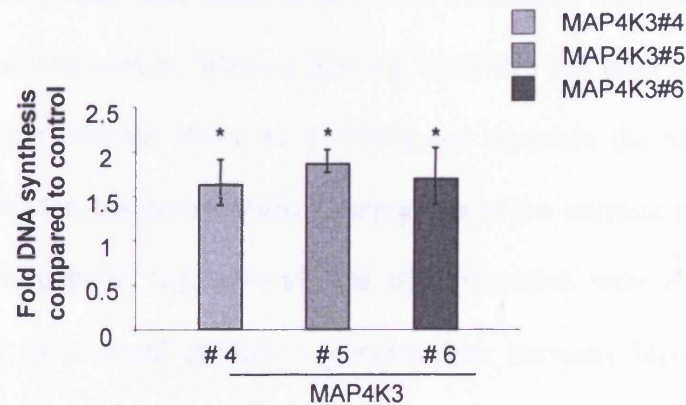


Figure 3.2.6 siRNA mediated suppression of MAP4K3 induces an increase in DNA synthesis

Transient suppression of MAP4K3 mediated by siRNA in U2OS was performed, followed by cell culture for 48 hours. BrdU proliferation ELISA was performed to investigate if MAP4K3 can modulate cell proliferation. Data shown is the mean from three independent experiments performed in triplicate. The absorbance from ELISA has been normalised to the scrambled control for each experiment. Error bars shown are standard deviation. Statistical significance calculated using t-test with * indicates $P < 0.05$ compared to the scrambled control.

Chapter 3.3: Analysis of MAP4K3 dependent signal transduction pathways

To characterise downstream signalling components that are activated by MAP4K3, transient overexpression experiments were performed in 293 cells. These experiments could identify signalling pathways that are involved in the activation of the intrinsic pathway of cell death by MAP4K3. Whole cell lysates were prepared from cells transfected with different MAP4K3 expressing plasmids and analysed by Western blotting. MAP4K3 has been previously found to induce JNK activation (Deiner, Wang et al. 1997) and therefore the MAPK pathways provided a starting point for this investigation. Components of the intrinsic pathway such as BH3 only proteins and apoptotic regulators such as p53 expression were also investigated. This was investigated as it could provide a possible link between MAP4K3 and Bax activation.

The data from chapter 3.2 using siRNA mediated suppression of MAP4K3 and the previous work with the endogenous protein (Deiner, Wang et al. 1997) has linked MAP4K3 to a role following UV treatment. Therefore overexpression studies were performed to determine if the expression levels of MAP4K3-GFP are affected by UV treatment and if MAP4K3-GFP leads to more JNK phosphorylation following UV treatment. Loss of function analyses of MAP4K3, using both siRNA mediated suppression and an ectopically expressed MAP4K3 kinase dead mutant, were used to investigate the role of MAP4K3 on the phosphorylation of JNK following UV treatment. The results from this section reveal that ectopic expression of MAP4K3 lead to an induction of the JNK and p38 pathways in 293 and U2OS cells. This activation is dependent on the kinase activity with the kinase domain sufficient to induce the phosphorylation cascade. The kinase dead MAP4K3 and siRNA mediated suppression of

MAP4K3 did not affect JNK or p38 phosphorylation following UV treatment and MAP4K3-EGFP levels were not altered following UV treatment.

Overexpression of MAP4K3 results in enhanced phosphorylation of JNK and p38

To investigate downstream components of MAP4K3 signalling, transient transfections were performed in 293 cells with various MAP4K3 EGFP expression plasmids followed by Western blot analysis. Anti-GFP immunoblots revealed that all the MAP4K3 fusion proteins were observed at the predicted molecular weight (Figure 3.3.1). This also revealed that the levels of the MAP4K3 fragments vary, with the two fragments missing the C-terminus being expressed at a higher level compared to the full length protein. This suggests that the C-terminus region of the kinase could be involved in protein stability (see Chapter 3.4). The MAP4K3 kinase dead protein was detected at a lower level compared to the wild type protein suggesting that the kinase activity might affect the stability of MAP4K3.

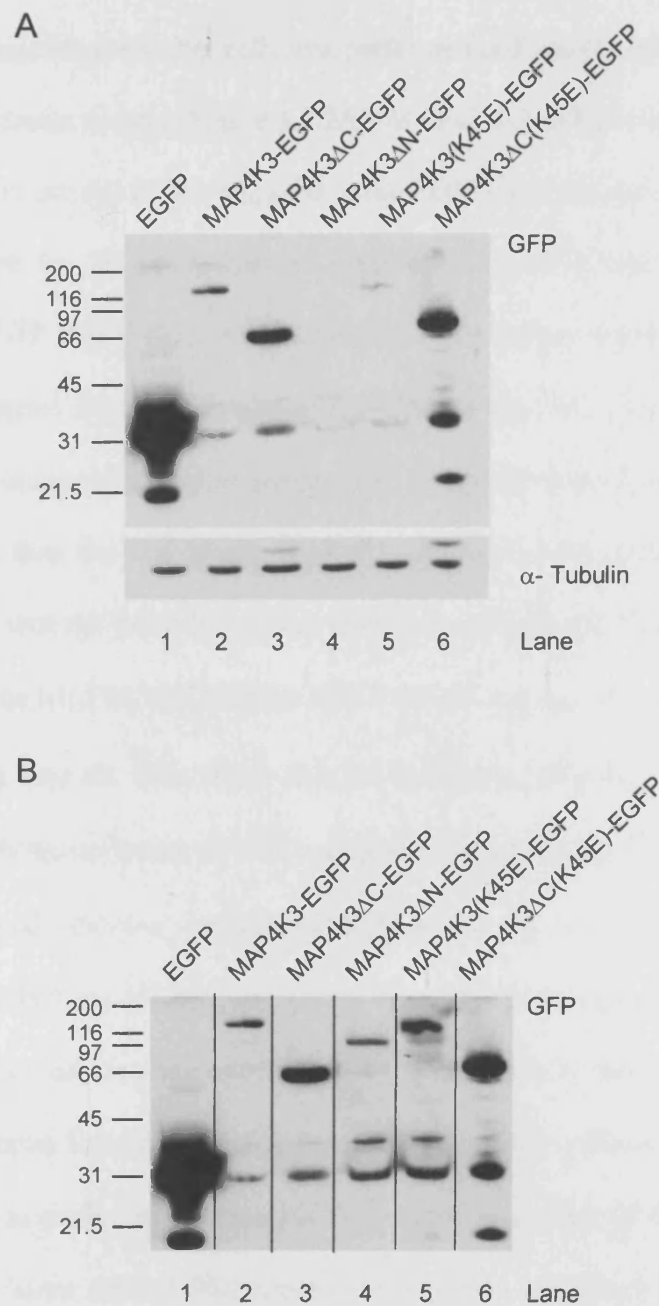


Figure 3.3.1: Confirmation of expression of MAP4K3 EGFP tagged protein fragments

Transient transfection of MAP4K3 EGFP tagged expression plasmids into 293 cells. Thereafter, whole cell extracts were prepared and subjected to immunoblot analysis. **A)** Western blot analysis using anti-GFP antibody to confirm size and expression of EGFP tagged proteins. **B)** To show clearly all the GFP bands from the same immunoblot, different exposure times were merged as shown by dividing lines.

To investigate how MAP4K3 affects different signal transduction pathways, transient overexpression of this kinase in 293 cells was performed and phospho-specific antibodies were used against downstream targets (Figure 3.3.2A). MAP4K3-EGFP increased the levels of (p)-p38 and (p)-JNK but not (p)-ERK compared to the EGFP vector control (Figure 3.3.2A, lane 2 compared to lane 1). This induction of (p)-p38 and (p)-JNK was not observed in the MAP4K3 K45E EGFP lane (Figure 3.3.2A, lane 5). This result reveals that the kinase activity of MAP4K3 is required for the induction of (p)-p38 and (p)-JNK. The MAP4K3 Δ C-EGFP protein induces an increase in (p)-p38 and (p)-JNK compared to the EGFP control and causes a higher induction than the full length MAP4K3 (Figure 3.3.2A, lane 3 compared to lane 1&2). This reveals that the MAP4K3 kinase domain is sufficient to induce the JNK and p38 phosphorylation. The MAP4K3 Δ C (K45E)-EGFP did not induce phosphorylation of JNK and p38 (Figure 3.3.2A lane 6). This shows that the C-terminal deletion mutant (MAP4K3 Δ C) ability to induce phosphorylation of JNK and p38 is dependent on its kinase activity. The MAP4K3 N-terminal deletion mutant (MAP4K3 Δ N) did not induce an increase in phosphorylation of JNK or p38 (Figure 3.3.2A lane 4). This reveals that the active kinase domain is required to induce phosphorylation of JNK and p38 in this overexpression model. As MAP4K3 has been linked to the regulation of the mTOR pathway, a phospho-specific antibody was used to probe for induction of S6K. This result showed that MAP4K3 did not alter the phosphorylation state of S6K under normal growth conditions in 293 cells, but does induce the phosphorylation of JNK and p38 (Figure 3.3.2A, lane 2 compared to lane 1).

As MAP4K3 overexpression has been shown in this thesis to induce the phosphorylation of JNK and p38, the upstream kinases of these two signalling pathways have been investigated. To investigate the MAPKKs upstream of JNK and p38, that MAP4K3 could activate, phosphorylation specific antibodies against MKK3/6, MKK4 and MKK7 were used to probe

whole cell lysates derived from 293 cells (Figure 3.3.2B). The phosphorylation of MKK3 and MKK6 following MAP4K3 overexpression was investigated by using phospho-specific antibodies against both MKK3 and MKK6. This revealed that MAP4K3 Δ C overexpression induces phosphorylation of MKK3/6 (Figure 3.3.2B, lane 3 compared to lane 1). This phosphorylation is dependent on the kinase activity of MAP4K3 Δ C as the MAP4K3 Δ C K45E mutant does not induce the MKK3/6 phosphorylation (Figure 3.3.2B, lane 6 compared to lane 3). To further define the kinase signal cascade following MAP4K3 overexpression the two upstream kinases of JNK, MKK7 and MKK4 were probed using phosphorylation specific antibodies. This showed that MAP4K3 Δ C induces phosphorylation of MKK7 and MKK4 (Figure 3.3.2B, lane 3 compared to lane 1). This increase in phosphorylation of MKK7 and MKK4 was found to be dependent on the kinase activity as the MAP4K3 Δ C K45E mutant does not induce MKK4 or MKK7 phosphorylation (Figure 3.3.2B, lane 6 compared to lane 3). The remaining MAP4K3 fragments that included MAP4K3 GFP, MAP4K3 (K45E)-GFP and MAP4K3 Δ 1-343-EGFP did not induce detectable increases in phosphorylation of the MKKs. In summary the expression of MAP4K3 Δ C induces the phosphorylation of MKK3/6, MKK4 and MKK7.

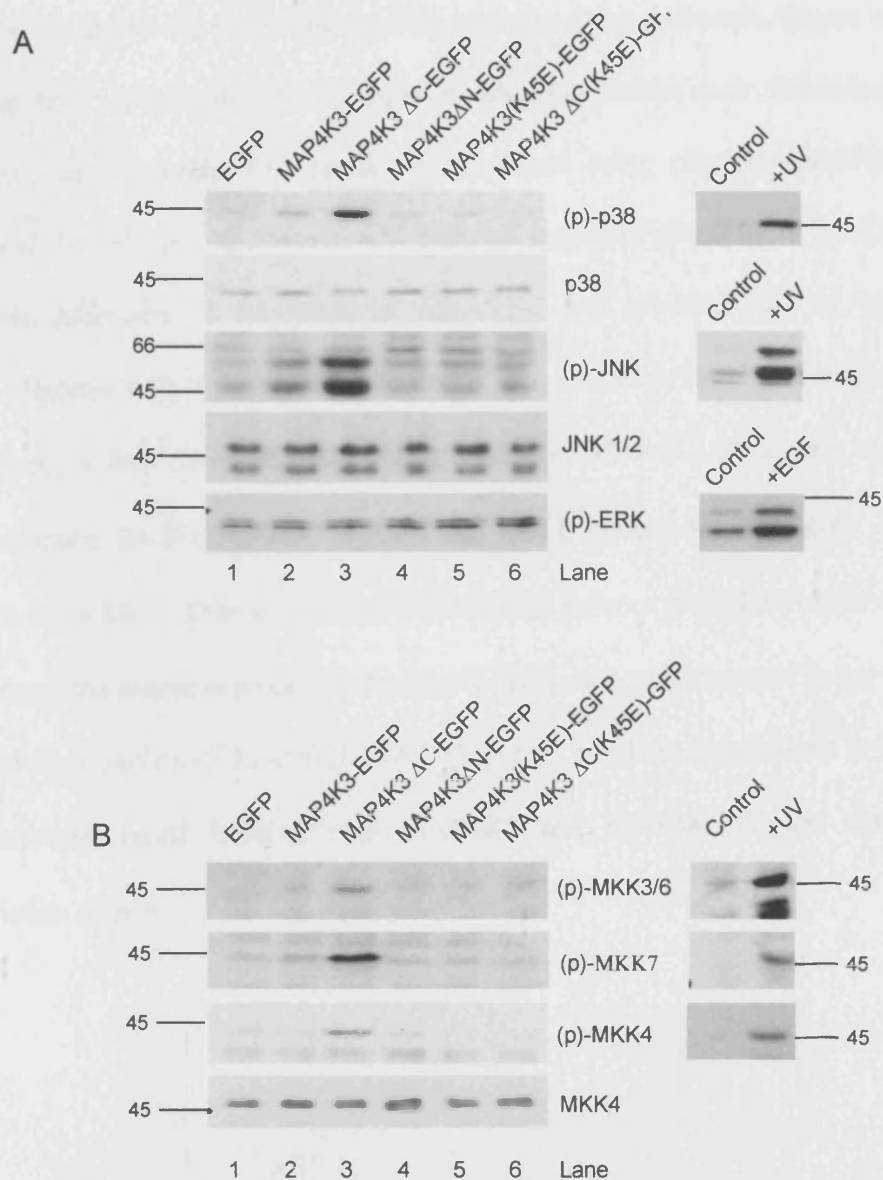


Figure 3.3.2: MAP4K3 induces JNK and p38 phosphorylation

A) Phospho-specific antibodies were used to examine S6K, ERK, JNK and p38 phosphorylation levels in whole cell lysates from 293 cells following transfection with MAP4K3 EGFP expression plasmids. As loading control total p38 and total JNK were probed. For positive control lane, 293 cells were treated with 100 J/m² UV irradiation and 1 hour after treatment the cells were harvested with whole cell lysates generated. For the (p)-ERK positive control blot, 293 cells were treated with 10 ng/ml epidermal growth factor (EGF) and 20 minutes after treatment the cells were harvested with whole cell lysates generated. **B)** The cell lysates from A) were probed using phospho-specific antibodies against MKK3/6, MKK4 and MKK7. As loading control total MKK4 was probed.

In this thesis I have revealed that overexpression of MAP4K3 induces the phosphorylation of JNK and p38. To define the involvement of the two signalling pathways, targets of these two kinases have been investigated for changes in phosphorylation state following MAP4K3 overexpression in 293 cells. The lysates were probed using phospho-specific antibodies against ATF-2, MAPKAK2 and Stat-1, which are all targets of p38 (Figure 3.3.3). There was no detectable difference in the levels of (p)-ATF-2 and (p)-MAPAK2 in the MAP4K3 expression plasmids cells (Figure 3.3.3, lanes 2&3 compared to lane 1). Using the anti-(p)-Stat-1 antibody, it was observed that overexpression of MAP4K3 Δ C causes an increase of (p)-Stat1 compared to MAP4K3 Δ C (K45E) and EGFP control lanes (Figure 3.3.3, lane 3 compared to lanes 6&1). This reveals that MAP4K3 Δ C induces phosphorylation of Stat-1 that is dependent on the kinase activity. No detectable difference was observed in (p)-Stat-1 levels following overexpression of MAP4K3-EGFP (Figure 3.3.3, lane 2 compared to lane 1). This is an unexpected result because both MAP4K3 and MAP4K3 Δ C are able to induce phosphorylation of p38.

A

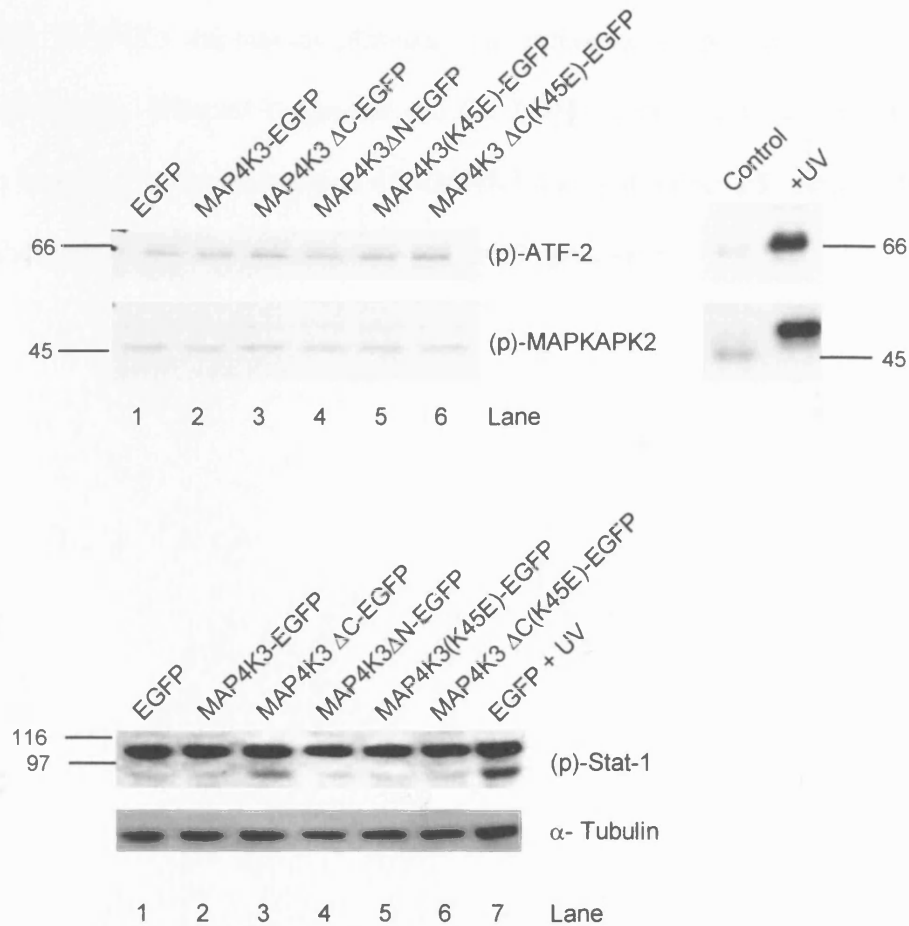


Figure 3.3.3: MAP4K3 induces phosphorylation of Stat-1

Phospho-specific antibodies were used to examine ATF-2, MAPKAPK2 and Stat-1 phosphorylation levels in whole cell lysates from 293 cells, following transfection with MAP4K3 EGFP expression plasmids. For positive control lane, 293 cells were treated with 100 J/m^2 UV irradiation and 1 hour after treatment the cells were harvested with whole cell lysates generated. For (p)-Stat-1 immunoblot, an additional lane is included where EGFP transfected 293 have been treated with 100 J/m^2 UV irradiation and harvested 1 hour after treatment.

The overexpression of MAP4K3 can lead to the induction of cell death. Two key mediators of cell death, p21 and p53, have been studied by the investigation of the protein expression levels. The protein expression levels of p21 and p53 were investigated following MAP4K3 overexpression in 293 cells using Western blot analysis. In the transient transfection of 293 cells with the MAP4K3 expression plasmids, no difference in p21 and p53 levels was observed between the different fragments and the EGFP control (Figure 3.3.4, lanes 2&3 compared to lane 1). The overexpression of MAP4K3 does not induce p53 or p21 expression, suggesting that MAP4K3 does not affect the p21 or p53 pathways.

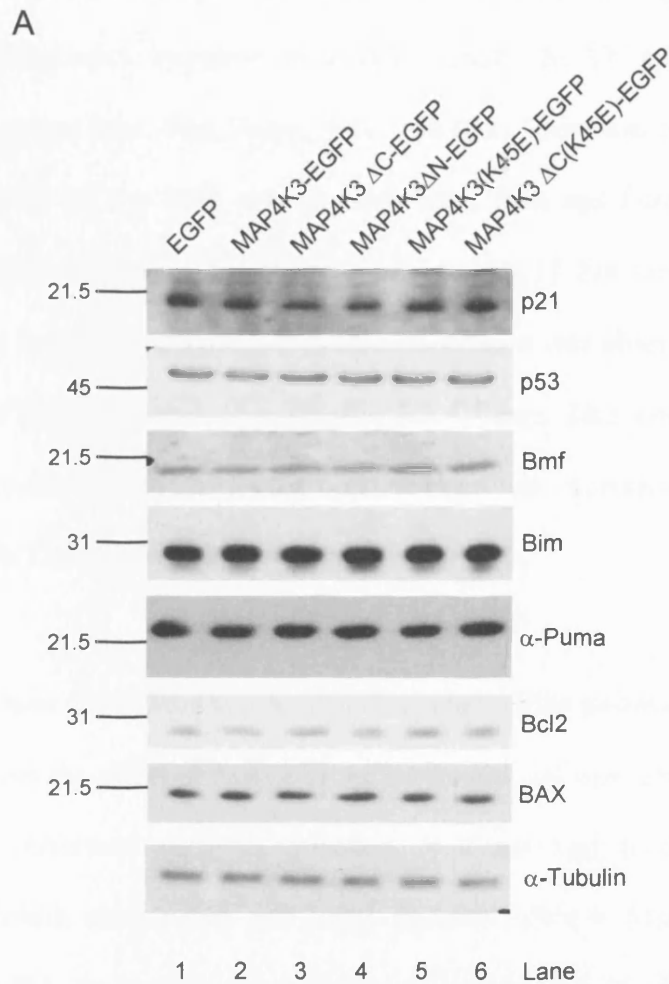


Figure 3.3.4: MAP4K3 does not affect expression levels of proteins involved in cell death

A) Antibodies were used to examine p21, p53, Bmf, Bim, Puma, Bcl2 and Bax protein levels in 293 cells following transfection with MAP4K3 EGFP expression plasmids. Whole cell lysates were used and the loading control was Tubulin as shown.

From the results in section 3.2, I have determined that MAP4K3 can induce a conformational change in Bax. The activation of Bax can be affected by the Bcl-2 family of proteins. To investigate if MAP4K3 overexpression in 293 cells affects the expression levels of pro-apoptotic and anti-apoptotic members of the Bcl-2 family, the 293 cells lysates were probed with antibodies against Bmf, Bim, Puma, Bcl-2 and Bax. There was no detectable difference in expression levels for the BH3 only proteins Bmf, Bim and Puma following MAP4K3 overexpression (Figure 3.3.4, lanes 2&3 compared to lane 1). For the pro-apoptotic Bax and the anti-apoptotic Bcl-2, no difference in protein expression was observed by western blotting compared to the EGFP control lane (Figure 3.3.4, lanes 2&3 compared to lane 1). In summary, the immunoblots revealed no difference in protein expression of Bcl-2 like proteins following MAP4K3 overexpression.

In this section, I have determined that MAP4K3 can induce the p38 and JNK pathways in 293 cells. To investigate the effect of MAP4K3 on a different cell line, transient transfection into U2OS cells was performed using nucleofection to achieve high levels of transfection. The anti-GFP immunoblot reveals that full length MAP4K3-EGFP, MAP4K3-K45E-GFP and MAP4K3 Δ N-EGFP had very low expression levels, with it not being possible to reproducibly detect these three EGFP tagged proteins. These lanes have remained in the Western blots of overexpression in U2OS cells, but any observed results are unreliable given the low expression of the MAP4K3 EGFP tagged proteins (Figure 3.3.5, lanes 2, 4 and 5). For the Western blots shown in Figure 3.3.5 the results from only the EGFP control, MAP4K3 Δ C and MAP4K3 Δ C(K45E) will be described. These immunoblots reveal that MAP4K3 Δ C induces phosphorylation of p38 and JNK that is dependent on the kinase activity of MAP4K3 Δ C (Figure 3.3.5, lane 3 compared to lanes 1 and 6). A substrate of JNK is the transcription factor c-Jun. To determine if MAP4K3 Δ C is able to induce phosphorylation of c-Jun, a phospho-

specific antibody against c-Jun was used in the immunoblots. This revealed that MAP4K3 Δ C is able to induce an increase in p-c-Jun that is dependent on the kinase activity of MAP4K3 Δ C. In summary, this shows that in the U2OS cells, where the overexpression of MAP4K3 Δ C is sufficient to induce apoptosis, the induction of the p38 and JNK pathways occurs and this is dependent on the kinase activity of MAP4K3 Δ C.

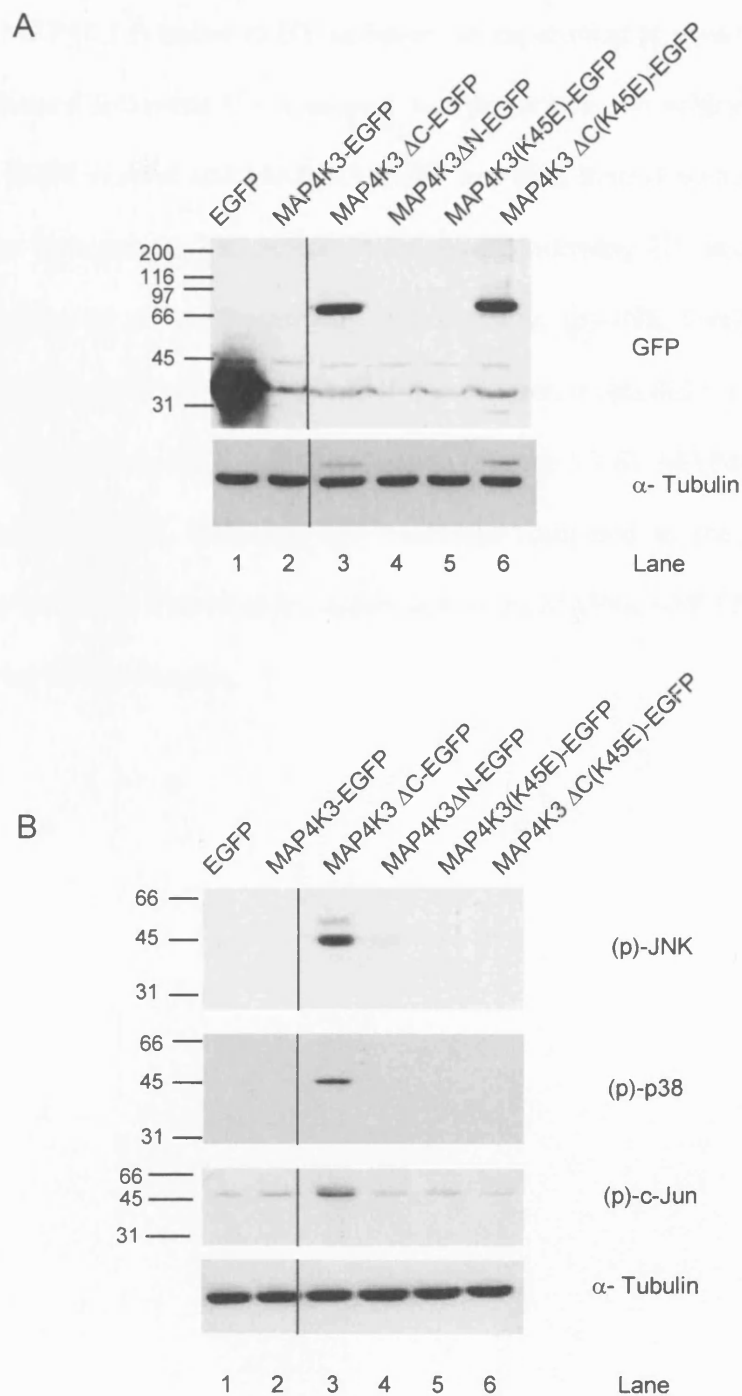


Figure 3.3.5: MAP4K3ΔC induces p38 and JNK phosphorylation in U2OS cell line

Nucleofection of MAP4K3 EGFP expression plasmids into U2OS cells followed by whole cell lysis and Western blot analysis. The line on the Westerns signifies removal of two lanes
A) Anti-GFP antibody was used to examine expression level of overexpressed protein. **B)** Phospho-specific antibodies were used to examine JNK, p38 and c-Jun phosphorylation. The loading control is Tubulin as shown.

UV treatment has no effect on MAP4K3-EGFP expression levels

As activation of MAP4K3 is linked to UV radiation, an experiment to investigate if MAP4K3 protein level increased following UV treatment was performed. To achieve this, cells were transfected with EGFP control and MAP4K3-EGFP and then treated with UV irradiation of 150 J/m². Lysates were prepared at different time points following UV and MAP4K3 levels were measured using an anti-GFP antibody. Additionally, (p)-JNK levels were measured using the phospho-JNK antibody. MAP4K3-EGFP expression levels did not change following UV treatment in 293 cells in the 8 hour time-course (Figure 3.3.6). MAP4K3-EGFP did not alter the induction of p-JNK following UV treatment compared to the respective EGFP control lanes (Figure 3.3.6). Therefore the expression of the MAP4K3-EGFP was not found to be altered following UV irradiation.

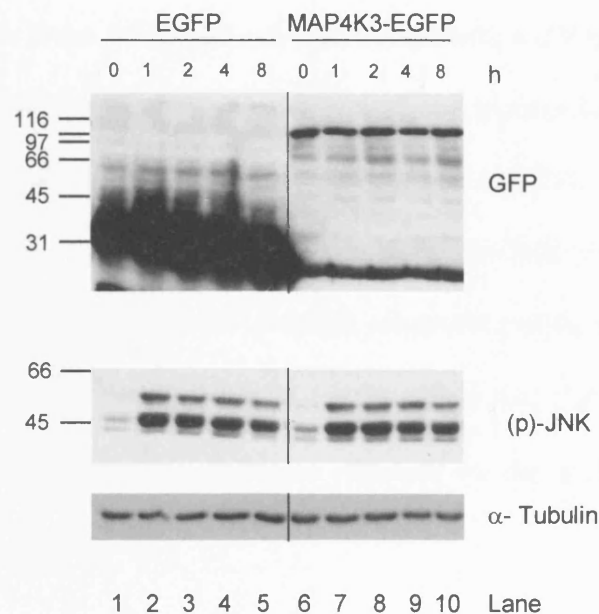


Figure 3.3.6: UV treatment has no effect on MAP4K3-EGFP expression

The transient transfection of expression plasmids for EGFP and MAP4K3-EGFP were performed in 293 cells. 24 hours post transfection the cells were treated with 150 J/m^2 UV irradiation and a 8 hour time-course performed. Whole cell lysates were generated and probed with phospho-specific antibody to JNK and an antibody against GFP. As loading control an anti-Tubulin antibody was used. The line on the immunoblot signifies removal of two lanes

siRNA mediated suppression of MAP4K3 or MAP4K3 K45E overexpression does not effect UV-induced phosphorylation of JNK and p38

To investigate if a kinase inactive form of MAP4K3 can act as a dominant negative on UV induced signal transduction pathways the ectopic expression of MAP4K3 expression plasmids was performed. These 293 cells were then treated with a UV dose of 100 J/m^2 and at the 1 hour time point, whole cell lysates were generated and immunoblots performed (Figure 3.3.7). As the overexpression of MAP4K3 can affect the p38 and JNK pathway, the levels of (p)-JNK or (p)-p38 were determined. No difference in (p)-JNK or (p)-p38 levels was observed between the different MAP4K3 expression constructs and the EGFP control plasmid (Figure 3.3.7, lanes 1 to 5). Therefore these results reveal that the MAP4K3-K45E and MAP4K3(K45E) Δ C do not act as a dominant negative on the p38 and JNK pathways following a UV dose of 100 J/m^2 .

As suppression of MAP4K3 leads to an increase in cell survival during DNA damage-induced cell death the possible signal transduction pathways that could be affected by MAP4K3 suppression were investigated. As MAP4K3 can induce the p38 and JNK pathways in overexpression experiments, the effect of MAP4K3 suppression on the JNK and p38 pathways was investigated after UV treatment. To achieve this, a time course was performed using a dose of 50 J/m^2 UV on U2OS cells with siRNA mediated suppression of MAP4K3 (Figure 3.3.8). 75% of the cell pellet was used to make whole cell lysates and 25% of the cell pellet was used for RNA extraction. MAP4K3 knockdown was confirmed by real-time PCR of MAP4K3 showing at least 70% suppression of MAP4K3 mRNA across the time points of the experiment compared to the scrambled control (Figure 3.3.8A). From the western blot analysis there was no effect on the (p)-JNK and (p)-p38 induction following UV treatment between the scrambled control and MAP4K3 suppression lanes (Figure 3.3.8B, lanes 8-12

compared to lane 2-6). In summary the suppression of MAP4K3 was not found to alter the phosphorylation of JNK and p38 following UV treatment.

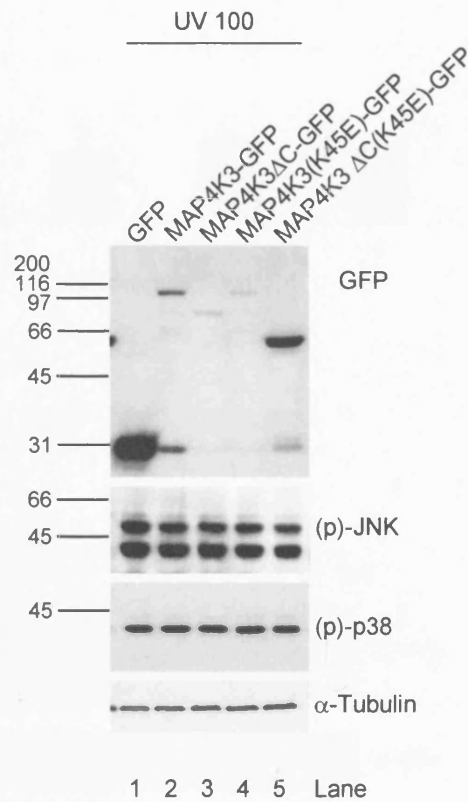


Figure 3.3.7: MAP4K3 K45E does not act as a dominant negative on UV induced stress response pathways

The transient transfection of MAP4K3-EGFP expression plasmids were performed in 293 cells. 24 hours post transfection the cells were treated with 100 J/m² UV irradiation and 1 hour after treatment the cells were harvested with whole cell lysates generated. The lysates were probed with phospho-specific antibody against JNK and p38. As a loading control Tubulin was probed and an antibody against GFP was also used.

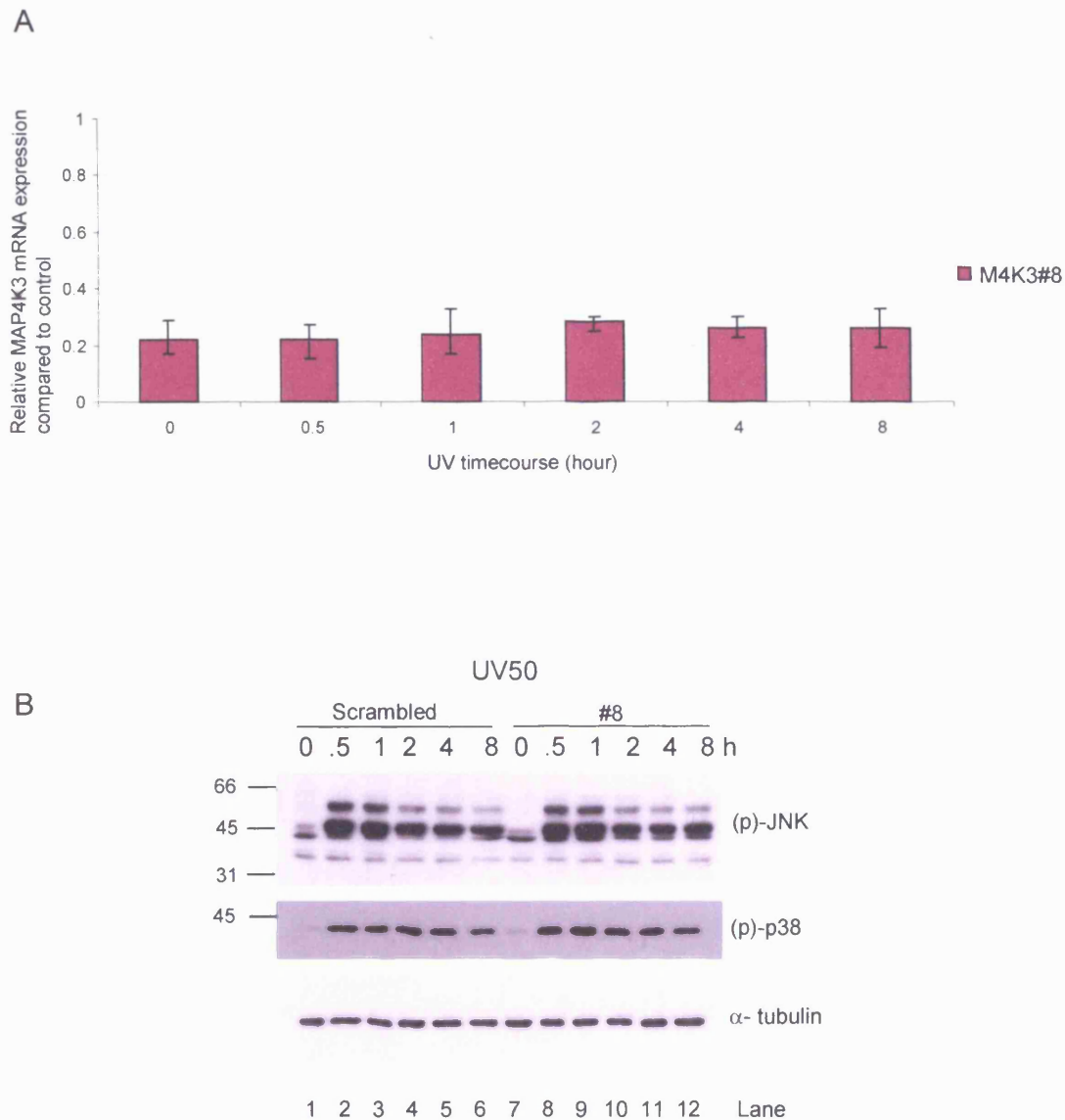


Figure 3.3.8: siRNA mediated MAP4K3 knockdown has no effect on UV induced stress response pathways

Reverse transfection of U2OS using siRNAs was performed and the cells cultured for 48 hours. The cells were treated with 50 J/m² and a time-course performed before generation of either whole cell lysates or mRNA samples. **A)** The RNA was extracted at the appropriate time-point and real time PCR was performed to determine relative levels of MAP4K3 mRNA. The loading mRNA used was GAPDH with the average relative expression of MAP4K3 compared to scrambled control siRNA plotted from one representative experiment. The errors bars shown are the standard deviation of the mean. **B)** The whole cell lysates were probed with phospho-specific antibody against JNK and p38. As loading control Tubulin was probed for.

Chapter 3.4: Proteasomal regulation of MAP4K3

Differential expression levels between the MAP4K3-EGFP and MAP4K3 mutant proteins were observed in overexpression studies suggesting different kinetics of expression or degradation (chapter 3.3). MAP4K3 is a member of the GCK-I family of protein kinases with GCK, the prototypical GCK-1 kinase being known to be degraded in a proteasome-dependent manner (Zhong and Kyriakis 2004). In order to address the stability of over-expressed MAP4K3, I determined the levels of expression of the different MAP4K3 truncation mutants by western blot analysis. Using this system, and a proteasome inhibitor, I determined that MAP4K3 levels are controlled post-translationally through proteasomal-dependent degradation. Furthermore by co-transfecting MAP4K3 and ubiquitin, it was determined that MAP4K3 is ubiquitin tagged. This was performed by immunoprecipitating MAP4K3 and Western blotting for the presence of HA tagged ubiquitin. The results from this chapter show that overexpressed MAP4K3 is degraded by the ubiquitin dependent proteasome pathway. These results show for the first time that MAP4K3 could be controlled by the ubiquitin proteasome pathway.

Proteasomal regulation of MAP4K3

The results shown in chapter 3.3 indicate that MAP4K3 expression fragments have different levels of expression which in combination with MAP4K3 containing PEST domains, raised the hypothesis that MAP4K3 levels could be regulated by the proteasome pathway of degradation. To investigate if MAP4K3 is degraded by the proteasome, MG132 was used to inhibit the 26S proteasome complex. The transient transfection of various MAP4K3 EGFP expression plasmids into 293 cells was followed by 1 μ M MG132 treatment for 24 hours. The

anti-GFP immunoblot revealed that the full length MAP4K3 and all the fusion proteins of MAP4K3 were stabilised by inhibition of the proteasome (Figure 3.4.1). The full length MAP4K3-EGFP protein is stabilised by the addition of MG132 compared to the untreated MAP4K3-EGFP (Figure 3.4.1, lane 3 compared to lane 4). There was also observed an increase of possible degradation products in the MG132 treated lane of MAP4K3-EGFP compared to the untreated MAP4K3-EGFP lane. This suggests that full length MAP4K3 could be degraded by the proteasome. The MAP4K3-K45E-EGFP protein is increased by the addition of MG132 suggesting that the kinase activity is not required for proteasome mediated degradation (Figure 3.4.1, lane 10 compared to lane 9). An additional observation was that the MAP4K3-K45E-EGFP protein is expressed at a lower level than MAP4K3-EGFP protein suggesting the kinase activity affects the stability of MAP4K3 (Figure 3.4.1, lane 9 compared to lane 3). To address if a region of MAP4K3 is essential for the proteasome degradation, the truncation mutants were included in the proteasome inhibitor experiments. The MAP4K3 Δ N protein is expressed at a lower level than the full length MAP4K3 (Figure 3.4.1, lane 7 compared to lane 3). MAP4K3 Δ N protein level is stabilised following proteasome inhibition with the observed increase in the expression of the full length MAP4K3 Δ N band (Figure 3.4.1, lane 8 compared to lane 7). This suggests that the C-terminus of MAP4K3 contains regions that induce proteasome degradation. Both MAP4K3 Δ C and MAP4K3 Δ C(K45E) protein are expressed at a higher level than MAP4K3 suggesting a role for the deleted C-terminus of MAP4K3 in stability (Figure 3.4.1, lane 5 & 11 compared to lane 3). Following proteasome inhibition the full length MAP4K3 Δ C protein is not increased but a larger molecular weight form of MAP4K3 Δ C is stabilised by inhibition of the proteasome (Figure 3.4.1, lane 6 compared to lane 5). This reveals that even though the removal of the C-terminus results in a more highly expressed protein, the C-terminus is not essential for proteasome degradation. The results using MAP4K3 Δ C(K45E) expression plasmid reveal that the full

length mutant protein is not stabilised but a larger and smaller molecular weight form are stabilised by proteasome inhibition (Figure 3.4.1, lane 12 compared to lane 11). There is also an observed increase in possible degradation products in the proteasome treated lane. In summary, the MAP4K3 expression plasmids reveal that ectopically expressed MAP4K3 is stabilised by inhibition of the proteasome.

A

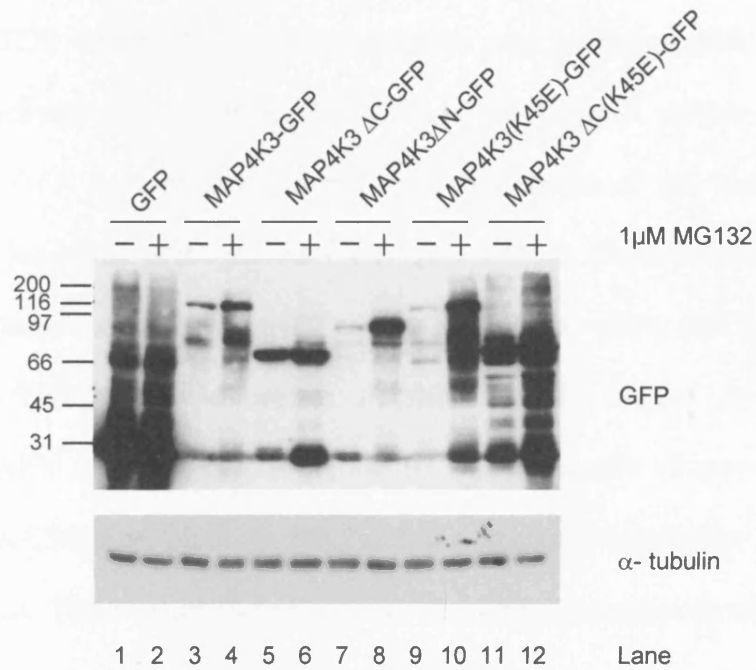


Figure 3.4.1: Proteasome inhibition stabilises MAP4K3-EGFP

The transient transfection of MAP4K3-EGFP expression plasmids were performed in 293 cells. 24 hours after transfection of 293 cells with MAP4K3 EGFP expression plasmids the cells were treated with 1 μ M MG132 and incubated for a further 24 hours. Whole cell lysates were generated and were probed with an antibody against GFP and Tubulin as loading control.

In ubiquitin mediated proteasome degradation the ubiquitin protein is covalently bound to a lysine residue on the targeted protein (Glickman and Ciechanover 2002). To determine if MAP4K3 is poly-ubiquitinated, co-overexpression experiments were performed. In these experiments, HA-ubiquitin and MAP4K3-EGFP were co-expressed in 293 cells. Following transfection and MG132 treatment, immunoprecipitation was performed with an anti-GFP antibody under non-denaturing conditions. The input of the Triton-X soluble fraction was western blotted for GFP showing the presence and stabilisation of the MAP4K3-EGFP fragments following inhibition of the proteasome (Figure 3.4.2A). This shows that following inhibition of the proteasome, the same trend as was seen in the whole cell lysates is also observed in the Triton-X soluble protein fraction. The IP lysates for GFP were immunoblotted for GFP and this confirmed the IP was successful (Figure 3.4.2B). To determine if the HA-Ubiquitin binds to MAP4K3 the immunoprecipitation lysates were immunoblotted for HA. This western blot showed the characteristic smears for all the MG132 treated MAP4K3 expression plasmid lanes (Figure 3.4.2C). These smears are indicative of ubiquitination and were not observed in the EGFP control lane. This suggests that neither the C-terminus nor the N-terminus of MAP4K3 were essential for ubiquitination. In summary, these experiments reveal that HA-ubiquitin co-immunoprecipitates with MAP4K3 which suggests that the MAP4K3 complex that is immunoprecipitated is ubiquitinated.

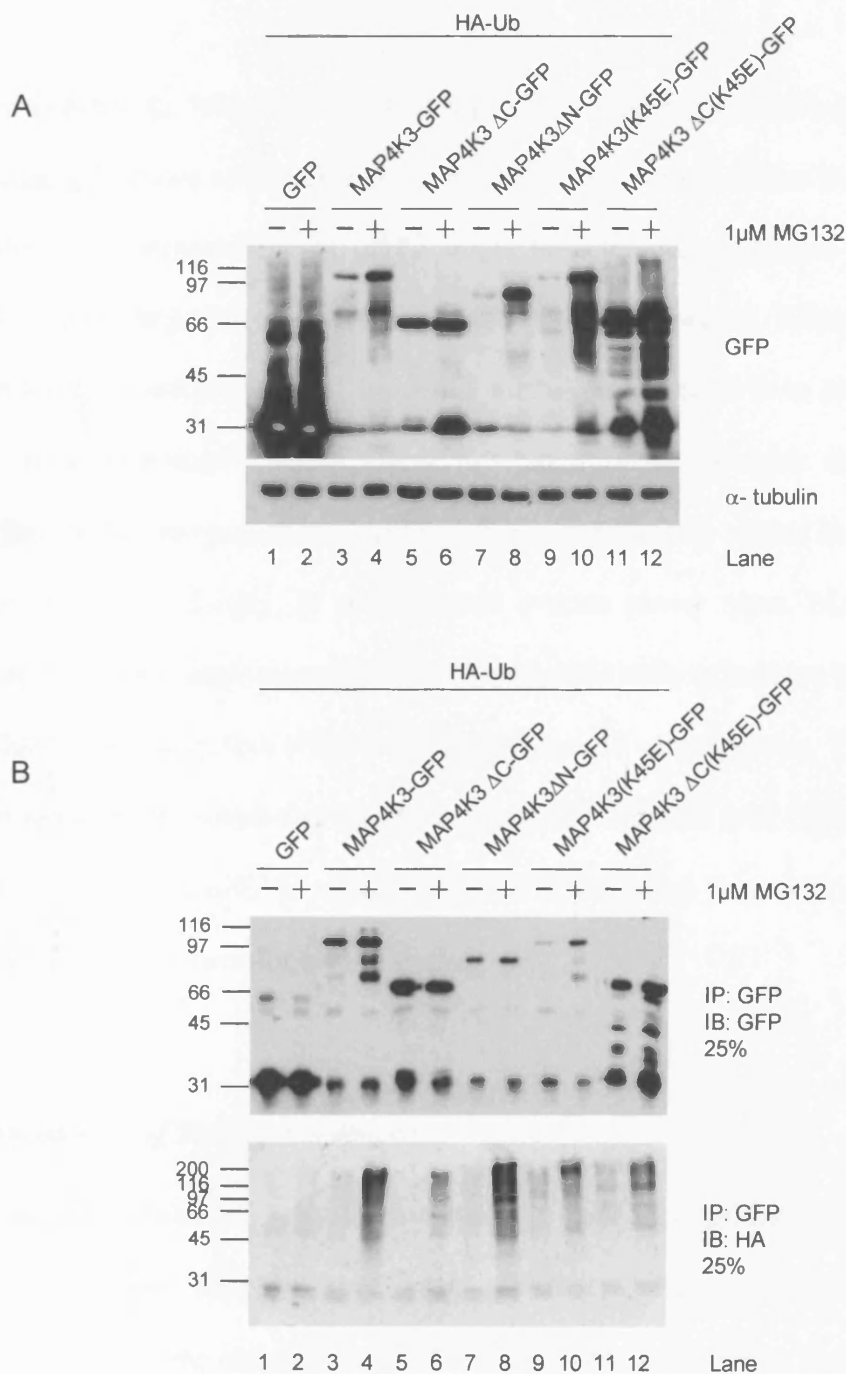


Figure 3.4.2: MAP4K3 IP Complex is poly-ubiquitinated

Co-transfection of 293 cells with MAP4K3 EGFP expression plasmids and HA:Ub expression plasmid in a 1:1 ratio. Following incubation for 24 hours the MG132 at a final concentration of 1 μM was added. The cells were incubated for a further 24 hours followed by immunoprecipitation for GFP in non-denaturing conditions. **A)** Input for the IP was probed using antibodies against GFP and Tubulin. **B)** The IP for GFP samples were immunoblotted using a anti-GFP antibody and anti-HA antibody.

Chapter 3.5: Analysis of MAP4K3 levels in normal and tumour tissues

Results shown so far indicate that loss of MAP4K3 results in increased cell survival following DNA damage induced cell death and that MAP4K3 suppression results in an increase in DNA synthesis. This suggests that MAP4K3 might be a tumour suppressor gene and therefore certain tumours might have reduced levels of MAP4K3 expression. Bioinformatic searches as well as experimental analysis of MAP4K3 mRNA levels have been performed comparing cancer tissue to normal controls. Using two bioinformatics analysis of microarray data, I found that the transcriptional level of MAP4K3 is significantly altered in a number of human tumours. More specifically, in two different ovarian cancer types, MAP4K3 mRNA was shown to be significantly downregulated. This *in-silico* analysis lead me to attempt to confirm a possible link between loss of MAP4K3 expression and tumorigenesis. The experiments with the ovarian cancer samples revealed that contrary to what was expected, the levels of MAP4K3 were increased. In summary this analysis failed to reveal any conclusive link between MAP4K3 expression and ovarian cancer.

In-silico analysis of MAP4K3 in cancer

To investigate if MAP4K3 is mutated in cancer, I searched a catalogue of somatic mutations (COSMIC) (Sanger). This database contains 14 different primary tumour types from a total of 210 patients. Only one mutation for MAP4K3 has been reported that leads to a single amino acid substitution of S669T (missense). This was from one patient out of 37 lung cancer patients (Davies, Hunter et al. 2005) and was considered to be a “passenger” mutation that is not causally involved in oncogenesis. The follow up study recently published showed that MAP4K3 was not, in terms of somatic mutations, a driver of cancer (Greenman, Stephens et al. 2007) as the statistically defined probability of a driver mutation was zero.

To investigate if there is a change in MAP4K3 in tumour development, an analysis on the levels of MAP4K3 transcript in normal tissues compared to tumour derived tissues was performed using both Oncomine and Gene Logic datasets. The Genelogic datasets comprises affymetrix data representing 3,600 normal and 1,701 neoplastic human tissue samples. The Oncomine database contains DNA microarray studies of 264 independent data sets, totalling more than 18,000 microarray experiments, which span 35 cancer types with differential expression analysis for cancer versus normal tissue totalling 66 data sets (Rhodes, Kalyana-Sundaram et al. 2007).

I performed a bioinformatics search of the Gene Logic dataset. Gene expression analysis of statistically significant changes in MAP4K3 expression ($p < 0.05$) are shown and this data is summarised in table format with sample number in brackets for each study (Figure 3.5.1A). From the Gene Logic dataset comparing normal tissue to cancer tissue, MAP4K3 mRNA expression was found to be significantly downregulated in 8 comparisons and upregulated in three studies. Therefore this search revealed that expression levels for MAP4K3 in a variety of tumour types can be marginally up- or downregulated. Two studies from the Gene Logic dataset show downregulation of MAP4K3 in ovarian cancer samples. Experimental analysis was performed to confirm the microarray data using real time PCR. In this analysis, samples were obtained from OriGene representing human ovarian cancer tissue samples.

The Oncomine expression dataset consisting of 66 microarray studies, was searched for significant differences in MAP4K3 expression in cancer samples versus normal samples ($p < 0.05$). The fold difference was calculated by using the medians provided (Figure 3.5.1B). From the 66 data sets MAP4K3 mRNA expression was found to be significantly

downregulated in two studies and upregulated in three studies. The expression of MAP4K3 from the data set shows up- and downregulation of the mRNA compared to the control tissue. This analysis fails to reveal any conclusive association between MAP4K3 downregulation and tumor progression.

A	Control	Experiment	Fold change
	Kidney (80)	Renal Cell Carcinoma, clear cell type (44)	-1.54
	Ovary (89)	Adenocarcinoma, clear cell type (6)	-1.59
	Ovary (89)	Adenocarcinoma, papillary serous type (33)	-1.41
	Stomach (52)	Adenocarcinoma, excluding signet ring cell type (29)	-1.63
	Stomach (52)	Adenocarcinoma, signet ring cell type (9)	-1.47
	Endometrium (23)	Adenocarcinoma, endometrioid type (49)	-1.43
	Skin (60)	Malignant Melanoma (7)	-1.45
	Breast (69)	Infiltrating lobular carcinoma (17)	-1.22
	Adrenal (13)	Adrenal cortical adenoma (3)	1.78
	Prostate, Benign (33)	Adenocarcinoma (88)	1.24
	Colon (173)	Adenoma (18)	1.24

B	Control	Experiment	Fold change
	Benign Lymphoid (31)	Diffuse Large B-Cell lymphoma (63)	-4.9
	Normal Testis (6)	Adult Male Germ Cell Tumor, Seminoma (91)	-1.86
	Normal Testis (3)	Testicular Cancer (27)	3.3
	Normal Bone Marrow (22)	Smoldering Multiple Myeloma (12)	1.84
	Normal Brain From Epilepsy Patient (23)	Glioblastoma Multiforme (77)	1.4

Figure 3.5.1 : Gene expression analysis of MAP4K3 in normal tissues versus tumours

A) Bioinformatics search of the Gene Logic expression database (Affymetrix HG-U133 data) representing 3,600 normal and 1,701 neoplastic human tissue samples was performed. Gene expression analysis of statistically significant changes in MAP4K3 expression ($p < 0.05$) are shown. This data is summarised in table format with sample number in brackets for each study. **B)** The Oncomine expression database was searched for significant differences in MAP4K3 expression in cancer samples versus normal samples ($p < 0.05$). The fold difference was calculated by using the medians provided.

Experimental analysis of MAP4K3 levels in normal and tumour tissues

To determine the expression levels of MAP4K3 in cancer tissue compared to normal tissue a panel of cDNAs derived from mRNA reverse transcribed from ovarian cancer was obtained, as well as appropriate normal tissue controls. The TissueScan real-time panels provide certified tumour and normal samples prepared as pre-normalized cDNA and ready for real-time PCR. The cDNA panel contains 48 unique samples per panel comprising of 7 normal and 41 ovarian cancer samples covering all four progression stages (Figure 3.5.2A). Origene has performed RT-PCR and normalised the cDNA content for each sample against β actin expression. SYBR green QPCR analysis of MAP4K3 expression from the ovarian TissueScan™ Real-Time PCR plate (origene) was performed with two independent repeats. The ovarian tumour samples showed significant upregulation of MAP4K3 mRNA compared to the control samples (Figure 3.5.2B). To investigate if MAP4K3 mRNA increases in ovarian tumour progression the ovarian cancer samples were separated into grades and the box and whisker plot is shown in Figure 3.5.2C. As there were only three samples for ovarian grade I and IV these were added to grade II and grade III respectively. This separation of the data showed no significant difference between the grade I+II samples compared to the grade III+IV samples. This analysis suggests that MAP4K3 levels have not increased following tumour progression from grade I+II to III+IV.

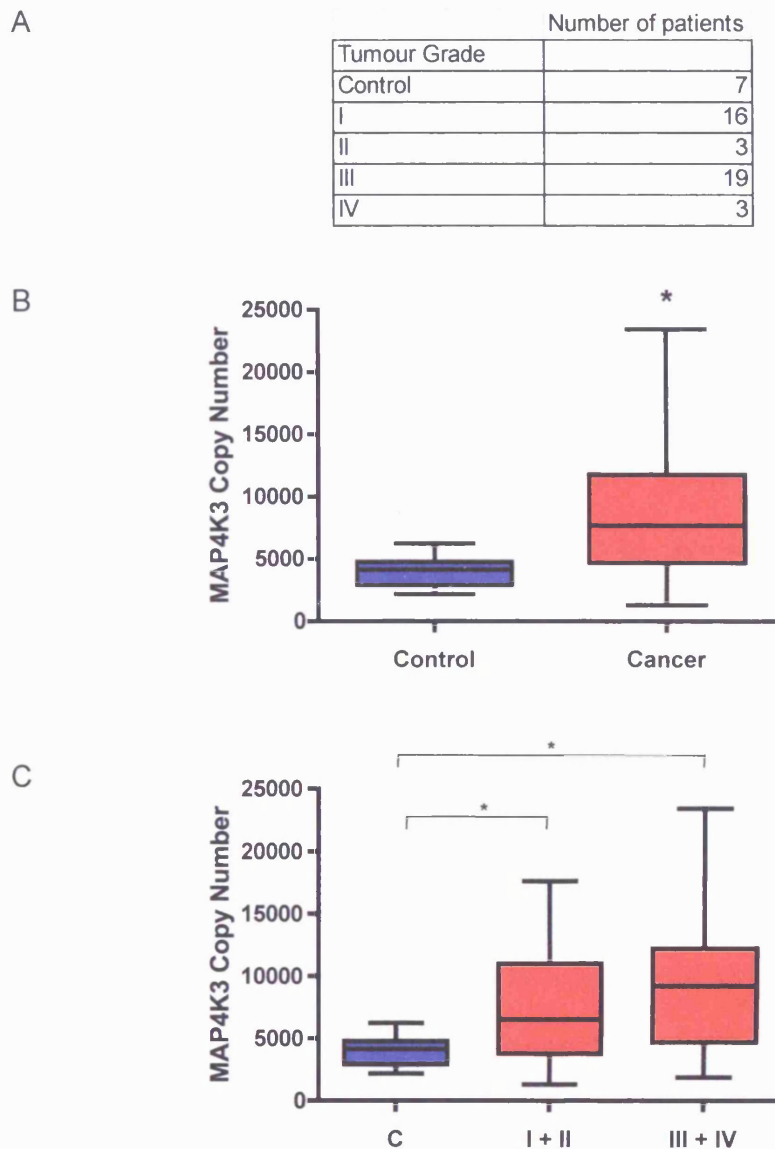


Figure 3.5.2: Comparison of MAP4K3 mRNA levels in control vs ovarian cancer samples

A) Table to summarize the different grades of ovarian tumour contained in the human ovarian cancer gene expression cDNA panel. B) QRT-PCR analysis of MAP4K3 performed on ovarian tissue cDNA panel with MAP4K3 mRNA expression converted into MAP4K3 copy number. To generate the MAP4K3 copy number, a standard curve using the linearized pDNA3.1 MAP4K3 GFP plasmid was generated. The data is presented as a box and whisker blot of the distribution of MAP4K3 expression in control tissue and the ovarian cancer samples. Two independent repeats were performed and statistical significance was calculated using t-test with * indicating $P < 0.05$ compared to control samples. C) The QRT-PCR analysis of MAP4K3 performed on ovarian tissue cDNA panel is presented as a box and whisker blot comparing control tissue to different grades of ovarian cancer. Statistical significance was calculated using t-test with * indicating $P < 0.05$ compared to control samples. The difference between I+II and III+IV is not statistically significant using the t-test.

Discussion

An RNAi-based library screen to identify regulators of UV induced cell death

The objective of this project was to employ an RNAi based screening approach to identify novel regulators of cell death. RNAi technology has recently been shown to be an efficient method of knocking down gene expression in order to gain insights into gene function. At present, functional information is only available for approximately 15% of human genes (Brummelkamp and Bernards 2003). RNAi libraries have been used in large scale screens to identify components of cellular processes, for example, as a screen for the bypass of p53-dependent proliferation arrest (Berns, Hijmans et al. 2004). The vector-based RNAi library employed in our screen was made available from NCI/CRUK and it was easily adapted to perform a small scale genetic screen for regulators of cell death. The decision to perform a screen for cell death modulators was made because resistance to cell death is a hallmark of cancer (Hanahan and Weinberg 2000). DNA damage-induced apoptosis was chosen for this study because loss of the mitochondria-dependent apoptotic pathway results in significant contribution to the resistance of cancer cells to cytotoxic therapies that induce DNA damage (Lowe, Ruley et al. 1993). UV irradiation was selected as damaging agent in the screen for its DNA-damage inducing properties. Following UV treatment the apoptosis that occurs has been found to be dependent on the mitochondrial pathway of apoptosis (Davis 2000). The U2OS cell line was chosen as U2OS are p53 wild-type cells that readily undergo apoptosis following UV and cisplatin treatments (Allan and Fried 1999; Al-Mohanna, Manogaran et al. 2004).

To identify the shRNAs present in the control and UV-treated cells, genomic DNA derived from pooled cells was isolated. This has clear practical advantages over the single colony genomic isolation method (Berns, Hijmans et al. 2004), as more sequences can be identified and compared to the untreated cells. The disadvantage compared to the single colony method

is that the sequences were pooled together and more than one targeting sequence could have been present in a single cell clone. An alternative method of identification of the sequences is by employing a barcode microarray sequencing method (Brummelkamp, Fabius et al. 2006). However this methodology was not available in our laboratory, but would have given a more thorough read-out of the population of shRNA inserts present in the cells, as opposed to the small sample of sequences identified in this project.

The candidate genes, identified in the screening approach deployed in this thesis, were selected using non-biased criteria. My results suggest that MAP4K3, PKT2B and CLK3 are putative cell death suppressors while MAD2L2 was considered a putative cell death sensitizer. MAP4K3 was considered the strongest candidate as a shRNA targeting MAP4K3 was the most highly expressed following UV treatment. Secondary validation on MAP4K3 was performed with three independent targeting sequences to show knockdown specificity as only one out of the three targeting sequences had been identified from the original screen. MAD2L2 (MAD2B, hRev7) could have been used as a positive control for the proliferative advantage as literature shows it is involved in the inhibition of the anaphase promoting complex (Chen and Fang 2001). Since performing the screen, new published data has shown that siRNA depletion of MAD2L2 sensitises nasopharyngeal carcinoma cells to cisplatin induced cell death (Cheung, Chun et al. 2006). Another recent study showed MAD2L2 to be involved in DNA damage response by promoting the phosphorylation of ELK1 by JNK. Additionally, MAD2L2 is also involved in permitting DNA damage bypass during replication (Zhang, Yang et al. 2007). PKT2B (PYK2, RAFTK) has been widely studied and has an expression pattern primarily in neuronal and hematopoietic tissues (Lev, Moreno et al. 1995). PKT2B has been linked to variety of processes including to the recruitment of Src-family kinases and the activation of ERKs. PKT2B can be activated by stimuli that increase

intracellular calcium levels in cells and it is also activated in response to stress signals such as UV and TNF α , thereby inducing JNK activation (Avraham, Park et al. 2000). Overexpression of PKT2B was found to induce apoptotic cell death in fibroblasts and epithelial cells (Xiong and Parsons 1997). PKT2B^{-/-} mice are viable and fertile with this study proposing that PKT2B has a role in cell migration and macrophage function (Okigaki, Davis et al. 2003). CLK3 is proposed to be involved in pre-mRNA splicing (Duncan, Stojdl et al. 1998) with no link to DNA damage response. Taken together, this evidence demonstrates the viability of my screen approach. From the results of the screen and the data recently published by others, these candidate genes could have been pursued but the decision was taken to concentrate on the most robust candidate identified in my UV screen. Therefore the MAD2L2, PKT2B and CLK3 genes have not been characterised further in this project.

The RNAi screen identified in both the untreated and treated populations pRS vectors that contained the H1 promoter but no 59-mer insert (data not shown). A revised version of the NKi library has been generated (Bernards, Brummelkamp et al. 2006). The new NKi library is composed of a revised vector termed pRSC (pRetroSuper chloramphenicol) containing a chloramphenicol bacterial selection marker in close proximity to the hairpin cassette. This marker serves to prevent recombination of the pRSC during bacterial culturing used for high-throughput plasmid DNA isolation and prevents loss of integrity to the RNAi library. This information regarding the integrity of the library raises the possibility that there were more MAP4K3 and MAD2L2 targeting shRNA plasmids in the library before retroviral production. This evidence shows that it is vital that validation of the potential pro-survival advantage of MAP4K3 suppression is assayed using a marker of proliferation.

As only a small sample of the population was identified by sequencing, statistical analysis is difficult. For example if the untreated cells showed a uniform distribution of shRNA inserts, the number of sequences needed to identify all 990 shRNA sequences would have been 2970 (~3 times the size of library) (Nolan Lab Group 2007). Given that the distribution of inserts was likely not to have been uniform; in reality the number would have been much higher. An inherent problem of the identification method used was that sequencing thousands of inserts was not considered to be practical or economical. An improvement to the screening approach would have been to perform an independent repeat or to do further enrichment rounds. Enrichment cycles refer to subcloning the hairpin cassette back into the pRS vector and repeating the screen with this new library. This would have lead to further enrichment of potential cell death regulators. Nevertheless this screening approach revealed a *bona fide* cell death modulator. As the kinase MAP4K3 was identified as being highly enriched following the initial cycle it was then selected and validated in further experiments using gain and loss of function analysis.

The role of MAP4K3 in cell death and proliferation using gain & loss of function analysis

MAP4K3 was identified as a candidate cell death regulator using the RNAi based UV screen described in this thesis. As only one targeting shRNA for MAP4K3 was detected and given that the screen was performed in a pool format, further experiments were needed to validate the specificity of knockdown. Using three independent siRNA sequences, transient experiments were performed to confirm the screen results. The objectives of such experiments were to determine if MAP4K3 suppression was involved in resistance to multiple DNA damaging agents. Experiments were also performed to investigate if MAP4K3 suppression conferred a proliferative advantage to cultured cells.

MAP4K3 has been termed a putative cell death regulator, based on the evidence obtained from the RNAi screen. The screen was performed in a pooled population with cells surviving if their shRNAs confer a selective advantage. The selective pressure used in the screen was UV-induced cell death. To quantify the survival following the DNA damage, a cell survival assay was performed. This showed that suppression of MAP4K3 conferred an increase in cell survival following UV-induced cell death. To define further the pro-survival phenotype of MAP4K3 suppression, another cell survival assay was performed using a different DNA damage-inducing agent. Cisplatin was used to determine if MAP4K3 regulation of survival following UV treatment is specific to UV induced cell death or if it is a general response to DNA damage-induced cell death. Nucleotide excision repair (NER) is essential for the genomic repair of UV-induced pyrimidine dimers or bulky, helix-distorting chemical adducts caused by compounds such as cisplatin (McKay, Becerril et al. 2001). UV and cisplatin cause DNA damage that is removed by the NER machinery and as such, could be considered as inducing a similar DNA damage-repair response. Suppression of MAP4K3 conferred an

increase in cell survival following cisplatin treatment. As both UV and cisplatin induce apoptosis, the increase in cell survival for MAP4K3 suppression could be due to a decrease in cell death, but as apoptosis was not directly measured, other factors such as defects in cell cycle arrest could also be involved.

Suppression of MAP4K3 increases cell survival following DNA damage which raises the hypothesis that MAP4K3 is involved in the regulation of apoptosis. To complement the findings of the loss of function analysis, experiments were performed to investigate if gain of function of MAP4K3 can lead to an induction of cell death. This was addressed by overexpression of MAP4K3 and the quantification of apoptosis. Further studies were performed with truncation mutants to determine the function of the different domains present in MAP4K3. The cell death that was observed was characterised to determine if the process of classical apoptosis was occurring and if the intrinsic pathway of apoptosis was activated.

A well described characteristic of apoptotic cell death is nuclear chromatin condensation (Danial and Korsmeyer 2004). Therefore analysis of nuclear morphology was used to determine if MAP4K3 can induce apoptosis. The overexpression of MAP4K3 was determined to induce cell death with the characteristic nuclear morphology of apoptotic cell death. Furthermore, to determine if the cell death was caspase dependent, a caspase inhibitor was used. The caspase inhibitor suppressed cell death, suggesting that MAP4K3-dependent cell death requires caspase activity. Taken in combination, the requirement of caspase activity and the chromatin condensation morphology strongly suggests that the type of cell death induced by MAP4K3 is classical apoptosis. This is the first data demonstrating that MAP4K3 is a robust inducer of apoptosis.

To determine the importance of the domains of MAP4K3 in the induction of cell death, deletion mutants and kinase dead proteins were generated and assayed for their ability to induce cell death. These studies revealed that for the full length MAP4K3 protein, the kinase activity is required for the maximal induction of cell death. Deletion mutants were generated of which MAP4K3 Δ C truncation mutant encodes a 343 amino acid protein that is similar to a C-terminal deletion mutant of MAP4K3 that has been previously described and shown to produce an active protein kinase (Deiner, Wang et al. 1997). This revealed that the MAP4K3 Δ C mutant with the active kinase domain is sufficient to induce cell death, which was comparable to the high level of cell death induced by full length MAP4K3. MAP4K3 Δ C mutant encodes the kinase domain and a region of 70 amino acids with low complexity. This 70 amino acid region could be considered unlikely to have a role in induction of cell death, as the kinase activity of MAP4K3 Δ C is required for the induction of cell death. The MAP4K3 Δ N mutant did not induce cell death, which adds to the evidence that the kinase domain and activity is important in inducing cell death. As MAP4K3 Δ C K45E and MAP4K3 Δ N do not induce cell death, the explanation of why the MAP4K3 K45E induced a low level of cell death is not clear. It is possible that the full length MAP4K3 K45E might bind to another protein or to endogenous MAP4K3 leading to the induction of cell death. To add to this hypothesis, the removal of the C-terminal regulatory domain in MAP4K3 Δ C K45E mutant means that it is missing the proline rich regions which could be involved in binding with other proteins and therefore no cell death was induced. From the data it is clear that the kinase activity is important in the ability of MAP4K3 to induce cell death as shown by the kinase dead proteins that either abolish or reduce the amount of cell death and by the fact that the kinase domain alone is sufficient to induce cell death.

Effector caspases can be activated during apoptosis by two different pathways. They are the mitochondrial mediated pathway and the receptor mediated pathway. The binding of ligands such as Fas ligand to Fas death receptor can lead to the activation of the receptor mediated pathway of apoptosis (Danial and Korsmeyer 2004). The intrinsic pathway of apoptosis is activated by mitochondrial release of apoptotic proteins secondary to genomic stress (Martinou and Green 2001; Zamzami and Kroemer 2001). The apoptosis induced by DNA damage has been found to be dependent on the mitochondrial pathway of apoptosis (Davis 2000). In this thesis I have linked the suppression of MAP4K3 to the resistance of DNA damage induced apoptosis. Therefore as MAP4K3 overexpression induces cell death, the involvement of the intrinsic pathway of apoptosis in MAP4K3 induced cell death has been studied. During the early stages of apoptosis, Bax translocates from the cytosol to mitochondria (Hsu, Wolter et al. 1997; Wolter, Hsu et al. 1997) where it participates in mitochondrial disruption and the release of cytochrome c (Jurgensmeier, Xie et al. 1998; Reed, Jurgensmeier et al. 1998). As well as the change in localisation, Bax undergoes a conformational change allowing the formation of the oligomer leading to the proposed formation a Bax/Bak lipid pore (Nechushtan, Smith et al. 1999; Suzuki, Youle et al. 2000). As Bax can activate the mitochondrial pathway of apoptosis, the conformational state of Bax in MAP4K3 overexpressing cells was addressed. The expression of MAP4K3 induced a conformational change in Bax and induced Bax clustering, which indicated that MAP4K3 overexpression leads to Bax activation. In this context, MAP4K3 K45E mutant did not induce Bax clustering suggesting that Bax activation by MAP4K3 is dependent on its kinase activity. The overexpression of the MAP4K3 K45E mutant induces 28% cell death, but this mutant does not induce Bax clustering. This raises the possibility that MAP4K3 K45E mutant is able to activate a cell death signalling pathways other than a Bax-dependent pathway.

To investigate if the cell death induced by MAP4K3 is dependent on the intrinsic pathway of apoptosis, a co-overexpression study was performed using BclxL. BclxL is an anti-apoptotic protein that blocks the mitochondrial cytochrome c release (Kluck, Bossy-Wetzell et al. 1997). These studies showed that BclxL co-overexpression reduced MAP4K3 dependent cell death. The cell death induced by MAP4K3 was not completely rescued by BclxL co-overexpression. As the positive control of co-overexpression of Bax with BclxL did not rescue all the cells, the remaining cell death could be considered to be due to inefficiencies in the experimental setup. This evidence suggests, at least in part, the induction of cell death induced by MAP4K3 is dependent on the intrinsic pathway of apoptosis. The two pieces of evidence showing the activation of Bax and rescue by BclxL suggest that MAP4K3 acts upstream of the mitochondrial pathway to induce apoptosis.

MAP4K3 cDNA used in this thesis is an alternative splice variant with exon 15 missing which results in the partial removal of one of the two PEST domains. This alternative splice variant was first described by others (Ramjaun, Angers et al. 2001) from a rat brain cDNA expression library screen and the human cDNA has been cloned from human testis by the I.M.A.G.E consortium (Lennon, Auffray et al. 1996). The MAP4K3 isoform used in this project is not thought to alter the signalling components that MAP4K3 can interact with as it is still able to activate the JNK pathway as shown in a previous study.(Ramjaun, Angers et al. 2001). The relevance of the three isoforms derived from EST analysis (Ensembl) is unknown in terms of functional differences and expression levels.

This thesis has shown that gain of function of MAP4K3 leads to induction of cell death with the loss of function leading to an increase in cell survival following DNA damage induced cell death. This is the first reported link between MAP4K3 and the regulation of cell death

and as such I will describe other GCK family kinases that have been linked to cell death. Of the GCK-I subfamily, HPK-1 has been linked with the induction of apoptosis in T cells (Schulze-Luehrmann, Santner-Nanan et al. 2002). Overexpression of HPK1 in CD4(+) T cells results in an increase in spontaneous and TCR/CD3-mediated apoptosis with an accompanying increase in Fas ligand expression (Schulze-Luehrmann, Santner-Nanan et al. 2002). Other members of the GCK superfamily have been linked to the induction of apoptosis including Mst1, Mst3, MASK, PSK2 and SLK (Dan, Watanabe et al. 2001; Dan, Ong et al. 2002; Hao, Takano et al. 2006; Zihni, Mitsopoulos et al. 2006). The yeast homologue of the Ste20 group of kinase has been linked to the process of hydrogen peroxide-induced apoptosis in *S. cerevisiae* by the proposed Ste20 kinase phosphorylation of histone H2B at serine 10 (Ahn, Cheung et al. 2005). Therefore the identification of MAP4K3 as a cell death regulator is not unexpected when compared to other GCK proteins.

The enrichment of MAP4K3 shRNA in the untreated library raised the hypothesis that MAP4K3 suppression lead to an increase in proliferation. To address this question, a BrdU ELISA was performed and revealed that suppression of MAP4K3 conferred an increase of DNA synthesis. This data suggests that suppression of MAP4K3 confers an increase in cell proliferation; however, other markers of proliferation such as cell number and cell cycle rates have not been addressed. A regulatory role for MAP4K3 in proliferation is a novel function that has not previously been described. As the role of MAP4K3 in proliferation is novel, an understanding of the role of other GCK-I group kinases in proliferation and cell cycle will be discussed. GCKR (MAP4K5) has been selected from a high throughput vector based RNAi library screen studying the effect of shRNAs on mitosis using HT29 colon cancer cells (Moffat, Grueneberg et al. 2006). In this screen two independent targeting shRNAs for GCKR were found to increase the rate of mitosis. In the same study, one shRNA targeting MAP4K3

was shown to confer an increase in the mitotic index but this result was not validated, as two or more independent shRNAs are needed to rule out non-specific effects. The mitotic index reflects the fraction of time that cells spend in mitosis versus the other stages of the cell cycle. An increased mitotic index can result from a lengthening of the mitotic phase (e.g., by arrest) or by a shortening of interphase. This study is the first link of GCKR to mitosis regulation. The phenotype of GCKR knock out mice has not been studied in regards to the effect on the cell cycle as the mice have just been described as viable (Shi, Huang et al. 2006). HPK1 (MAP4K1) is the most described GCK-1 group kinase and HPK1^{-/-} T cells have been found to be hyperproliferative in response to T-cell receptor stimulation (Shui, Boomer et al. 2007). This limited literature links the GCK-1 subfamily member HPK1 to the regulation of proliferation, which is consistent with the data presented here for MAP4K3.

Suppression studies of MAP4K3 have been recently described (Findlay, Yan et al. 2007). MAP4K3 was found to be activated by amino acids and to regulate the mTOR pathway. Suppression of MAP4K3 in HeLa cells caused a reduction in cell size. Smaller cell size is directly linked to mTOR deactivation as shown by the use of rapamycin (mTOR inhibitor) which leads to reduction in cell growth (Reiling and Sabatini 2006). It is therefore proposed that MAP4K3 is required for amino acids to activate S6K and overexpression of MAP4K3 induces the phosphorylation of the mTOR regulated inhibitor, 4E-BP1 (Findlay, Yan et al. 2007). This effect on mTOR is the proposed mechanism to explain the observation of reduced cell size.

This is a novel link of a GCK-I subfamily kinase to the regulation of the mTOR pathway and is the first link of a GCK kinase to affect cell size. Disruption of the S6K, target of mTOR, by knockout gene disruption of mice and flies generate animals significantly smaller in size with

smaller cells (Shima, Pende et al. 1998; Montagne, Stewart et al. 1999). There is no observation that HPK1 $-/-$ or GCKR $-/-$ KO mice have any irregularity in their size. Hippo, *Drosophila* Mst1 ortholog (GCK-II), restricts growth and cell proliferation while promoting apoptosis. The disruption of hippo in *Drosophila* results in bigger flies due to enhanced proliferation and suppression of apoptosis resulting in more cells (Hay and Guo 2003). This could be considered strikingly similar to the phenotype of MAP4K3 suppression in U2OS.

As the link of MAP4K3 suppression to cell size (Findlay, Yan et al. 2007) is a new observation no analysis using precise quantification, such as FACS, has been performed in this thesis but it should be noted that no change in MAP4K3 size was observed from visual observation down the light microscope from the gain and loss of function studies. This would be expected as MAP4K3 suppression in Hela cells leads to only a relative small reduction in cell size of 20%, 16% and 13% in G1, S and G2/M respectively. If MAP4K3 suppression results in a decrease in cell size, then the opposite phenotype of increased cell growth when MAP4K3 is overexpressed may be expected. For an example in the mTOR pathway, when S6K is overexpressed, it induces an increase in cell growth resulting in larger cells (Fingar, Salama et al. 2002). There is no description of MAP4K3 overexpressed phenotype in Findlay et al study. The gain of function analysis performed in this thesis clarifies the role of MAP4K3, as cell death is induced.

Alterations in cell size can result from changes in either cell growth rate or cell cycle progression. For example when the cell cycle is blocked, cells grow to an increased cell size; when the cell cycle accelerates in the face of an unchanged rate of cell growth, cells become smaller. An example is the overexpression of the cdk inhibitors p16 and p21, which confirms that in mammalian cells, growth continues and cell size increases when cell cycle progression

is blocked; therefore, the two processes are separable and distinct (McKilligin and Grainger 2001; Fingar, Salama et al. 2002). As MAP4K3 suppression induced an increase in proliferation in U2OS, if the respective growth rate remained the same the cells would become smaller. In the study by Findlay et al there was no analysis of proliferation rates on the HeLa cells where MAP4K3 was downregulated. If these cells were proliferating faster this could result in smaller cells due to a reduction in the time spent in interphase. The Findlay et al study shows a clear involvement of MAP4K3 in mTOR signalling with an analysis of the levels of S6K and 4E-BP1 phosphorylation following serum starvation in MAP4K3 siRNA cells. With this pathway, a clear mechanistic explanation for why the cells were smaller in size can be proposed. In this model, when MAP4K3 is suppressed, the proliferation rate would either be reduced or remain the same, as the mTOR pathway would be inhibited. U2OS cells following rapamycin treatment have a reduced cell size and reduced proliferation (Fingar, Salama et al. 2002). Therefore the observed phenotype of MAP4K3 suppression inducing proliferation is in contrast with the effect of inhibition of mTOR, suggesting that MAP4K3 does not affect this mechanism in U2OS cells. Further work to address this development of differing proposed functional roles of MAP4K3 would be to determine if suppression of MAP4K3 in U2OS leads to a change in cell size using FACS analysis and performing a second proliferation assay that measures a different marker of proliferation, or by the study of cell cycle changes. In this thesis I have not addressed the mechanism of why MAP4K3 suppression in U2OS induces an increase in proliferation and as such further investigation by analysis of expression of proteins that could be involved in this alteration could be pursued.

I have linked suppression of MAP4K3 to resistance to DNA damage induced cell death and enhanced proliferation. The failure to initiate apoptosis can be an important mechanism of

drug resistance in tumour cells (Igney and Krammer 2002) and cells from tumours can acquire an increase in proliferation and a decrease in apoptosis (Bergers, Hanahan et al. 1998). The role of MAP4K3 in both apoptosis and proliferation suggests a role for MAP4K3 as a putative tumour suppressor

It is difficult to reconcile the two different functions proposed for MAP4K3. MAP4K3 could be a regulator of cell survival that is activated by amino acid pro-growth stimuli and by UV pro-apoptotic stimuli, with the overexpression in U2OS cells inducing the pro-apoptotic function of MAP4K3. In this thesis I have presented data on both loss and gain of function analysis linking MAP4K3 to the regulation of apoptosis. To investigate how MAP4K3 may activate Bax, downstream signalling pathways of MAP4K3 overexpression were studied in detail in chapter 3.3 with specific emphasis on the MAPK pathways as MAP4K3 has been linked to activation of JNK.

Analysis of MAP4K3 dependent signal transduction pathways

As MAP4K3 suppression confers an increase in cell survival following UV treatment and induces cell death when overexpressed, the downstream signalling components involved in this process were investigated. From studies of the overexpressed protein in chapter 3.2, it has been determined that MAP4K3 induces the activation of Bax and caspases are required for MAP4K3 induced cell death. The aim of this section of the thesis was to investigate the signalling components that could lead to activation of Bax. As MAP4K3 has been shown to activate JNK (Deiner, Wang et al. 1997) and as JNK is essential for activation of the intrinsic pathway following UV treatment (Davis 2000), the MAPK signalling pathways were studied. An additional question to address was if the pathways identified from the overexpression studies are affected following UV treatment by siRNA mediated suppression or dominant negative expression of MAP4K3.

The overexpression of MAP4K3 has been performed to investigate the downstream pathways that are activated by MAP4K3. These experiments were performed in two cell lines to investigate if the results are cell type specific. The 293 cell line was used to achieve high levels of transfection and U2OS cells were also used as the cell death phenotype has been characterised in this cell line. As MAP4K3 overexpression has been linked previously to the activation of JNK (Deiner, Wang et al. 1997), the phosphorylation state of ERK, p38 and JNK have been studied. From the overexpression study ectopic expression of full length MAP4K3 was found to induce p38 and JNK phosphorylation and this was dependent on the kinase activity of MAP4K3. The experiments presented in this thesis reveal that MAP4K3 Δ C was sufficient to induce p38 and JNK phosphorylation and this was again dependent on the kinase activity. The N-terminal deletion mutant of MAP4K3 missing the kinase domain was not able to induce an increase in phosphorylation levels of p38 and JNK. These experiments using the

deletion mutants of MAP4K3 show that the kinase domain and activity of MAP4K3 is essential for increases in (p)-JNK and (p)-p38. No induction of (p)-ERK was observed in the overexpression experiments using MAP4K3 which suggests that the overexpression of MAP4K3 does not affect the phosphorylation levels of endogenous ERK. Therefore MAP4K3 induces a specific increase of phosphorylation levels of the p38 and JNK stress response MAPK pathways and does not lead to a more general activation of MAPK pathways. A previous study overexpressed p38 and MAP4K3 followed by an in-vitro kinase assay of p38 using ATF-2 as a substrate. This study failed to detect any enhanced p38 activity (Deiner, Wang et al. 1997). In the results presented in this thesis, I have shown that overexpression of full length MAP4K3 and MAP4K3 Δ C induces endogenous p38 phosphorylation in 293 cells, which was measured using a (p)-p38 antibody that suggests a possible increase in activity of p38. The ectopic expression of MAP4K3 Δ C in U2OS cells induced an increase in (p)-JNK and (p)-p38. This shows that MAPK3 can induced p38 and JNK phosphorylation in two different cell lines. This reveals that in U2OS cells where MAP4K3 Δ C induces cell death, the induction of (p)-p38 and (p)-JNK occurs. The induction of p38 phosphorylation by MAP4K3 is a new link to the p38 MAPK pathway and therefore the phosphorylation level of p38 pathway proteins has been investigated further.

The results presented in this thesis show that the C-terminal deletion mutant of MAP4K3 (MAP4K3 Δ C) induced more (p)-JNK and (p)-p38 than the full length MAP4K3. This contradicts the previous study (Deiner, Wang et al. 1997) which found that a partial C-terminal deletion of MAP4K3 induced approximately 10 fold less JNK activation compared to the full length MAP4K3. This result lead to the conclusion in their study that both the kinase activity of MAP4K3 and the 362-844 amino acids in the C-terminus are required for the maximal activation of JNK (Figure 2.2). A possible explanation for this discrepancy is

the fact that a revised sequence of MAP4K3 was used in this project that has an N-terminus extension of 8 amino acids (Ramjaun, Angers et al. 2001) compared to the MAP4K3 sequence used in (Deiner, Wang et al. 1997). The biggest difference between the two C-terminal deletion mutants are that the previous study used a partial C-terminal mutant as the amino acids 845-894 of MAP4K3 were not removed (Deiner, Wang et al. 1997). This partial C-terminal deletion could then have affected downstream signalling components or had an inhibitory effect on the kinase activity. An alternative explanation could be that the different methods used could have altered the result, as double overexpression was used in the previous study (Deiner, Wang et al. 1997) compared to MAP4K3 overexpression in this study. The results presented in this thesis clearly show that the complete removal of the C-terminal domain induces a greater increase of endogenous (p)-JNK and (p)-p38 compared to the full length protein. It is attractive to speculate that this could be a consequence of the increase in protein expression of the C-terminal deletion mutant or the removal of an auto-inhibitory domain present in the C-terminus.

An issue that arises is the differential expression levels of the MAP4K3 mutants. The MAP4K3 K45E expresses at a lower level when compared to the wild type protein. As this is the control that determines if the kinase activity induces the downstream changes, the lower expression level could lead to a reduction in (p)-JNK levels. To counter this argument, the truncation mutants clearly show that the protein lacking the kinase domain does not induce phosphorylation of downstream kinases and neither does the C-terminal kinase dead mutant. In the previous study (Deiner, Wang et al. 1997) the expression levels for the MAP4K3 and MAP4K3 kinase dead in 293 cells are differently expressed in the same order as observed in this project using a 5' FLAG tag fusion construct. This observation was not acknowledged or pursued further in the paper. The study by Findlay and colleagues did not observe a difference

in expression of the MAP4K3 wild type compared to the inactive kinase protein in 293 cells. A different mutation was performed at the conserved DFG motif of MAP4K3 to generate the kinase inactive protein. The DFG motif is the putative magnesium interacting site of MAP4K3 with alteration leading to inactivation of the catalytic activity. The reason why the Findlay study does not detect the altered expression levels of the MAP4K3 kinase dead as observed in this project is unknown but it should be noted that in their study, the MAP4K3 kinase dead expression levels were only shown following serum starvation of 293 cells.

MAP4K3 has been shown to activate the mTOR pathway therefore the phosphorylation state of S6K has also been investigated. Phosphorylation of Thr389, most closely correlates with p70 kinase activity in vivo (Weng, Kozlowski et al. 1998). In the study by Findlay et al, co-overexpression experiments using S6K and MAP4K3 were used to show an increase of activity of S6K by using a phospho-specific antibody for Thr389 and by an in-vitro kinase assay. In this thesis, no induction (p)-S6K at Thr389 was observed in conditions where robust phosphorylation of p38, JNK were detected, suggesting that under normal growth conditions the overexpression of MAP4K3 does not affect the phosphorylation level at Thr389 of endogenous S6K at this site. MAP4K3 in the experiments shown in this chapter can induce the endogenous p38 and JNK pathways but has no effect on endogenous phospho-S6K levels when cells are grown under complete growth conditions. With the knowledge acquired from this thesis, the effect of MAP4K3 overexpression leading to the phosphorylation of 4E-BP1, a component of the mTOR pathway, could be due to induction of the p38 pathway. The phosphorylation of 4E-BP1 leads to the dissociation of eIF-4E and this has been suggested to be mediated by a p38/MSK1 pathway in response to UV irradiation (Liu, Zhang et al. 2002). The cross talk between the stress response MAPK pathways and the pro-growth mTOR pathway following MAP4K3 overexpression has not been addressed in this thesis but could

entail the overexpression of MAP4K3 with the inhibition of p38 using a p38 chemical inhibitor to determine if 4E-BP1 phosphorylation is dependent on the p38 pathway.

The predominant mode of MAP kinase activation is by dual phosphorylation by MAP2Ks on the activation loop sites (Raman and Cobb 2003). The phospho-specific antibodies are an indicator of the activity of JNK and p38 as they bind phospho-Thr and Tyr residues that are targets of the dual specificity mitogen-activated-protein-kinase-kinases. To further define the pathway that MAP4K3 induces, the MAPKKs that are upstream of JNK and p38 have been investigated. The MKKs that phosphorylate JNK are MKK4 and MKK7 while for p38 the upstream MKKs are MKK3 and MKK6. The phosphorylation levels of these MKKs were investigated following ectopic expression of MAP4K3. The C-terminal deletion mutant was found to increase the phosphorylation of MKK4, MKK7 and MKK3/MKK6 using antibodies against the Ser and Thr within the activation loop of the MAP kinase kinase family that are crucial for the kinase activity (Raman and Cobb 2003). This places MAP4K3 upstream of MKK in the MAPK signalling pathway. This result agrees with the previous study of the role of MAP4K3 in JNK pathway, which using dominant negative co-transfections placed MAP4K3 upstream of MKK4 and MEKK1 (MKKK1) (Deiner, Wang et al. 1997).

To show in my experimental settings that MAP4K3 induces an increase in JNK and p38 activity, targets of these two kinases have been investigated. This will also define further the pathways that MAP4K3 is able to activate and identify proteins that could be involved in inducing the cell death. No change in the phosphorylation level of two targets of p38, ATF2 and MAPKAP kinase 2 were observed. An increase of the phospho-state of c-jun and phospho-stat-1, which are downstream targets of JNK and p38 respectively, was observed by overexpression of MAP4K3 Δ 343-874. The p-c-jun antibody used in this project binds to the

phosphorylated Ser-63 site. This is a site of JNK phosphorylation which results in increased transcription activity (Pulverer, Kyriakis et al. 1991). This is an important observation as the amino-terminal phosphorylation of c-Jun at Serine 63 and Serine 73 has been shown to be required for stress-induced apoptosis (Behrens, Sibilio et al. 1999). In the two studies using co-overexpression of JNK and MAP4K3, it has been observed that MAP4K3 induces an increase in JNK activity and an increase in JNK phosphorylation using a phospho-JNK specific antibody (Deiner, Wang et al. 1997; Ramjaun, Angers et al. 2001). Both of these studies used 293 cells and did not study endogenous p-c-jun levels. Therefore the data presented in this thesis of MAP4K3 Δ C overexpression leading to an increase of phosphorylation of endogenous c-Jun is a new observation.

The signal transducers and activators of transcription (Stat) factors are latent transcription factors in the cytoplasm that can become activated by various extracellular stimuli, including cytokines and growth factors that bind to specific cell surface receptors. Stat-1 is essential for interferon signalling, which can play critical roles in cell growth and death (Stephanou and Latchman 2005). The tyrosine phosphorylation of Stats at Tyr701 by JAKs is important for promoting Stat dimerisation, nuclear translocation, and DNA binding. The phosphorylation of serine 727 of Stat-1 occurs in the activation loop where phosphorylation leads to maximal transcriptional activity and is suggested to occur independently of tyrosine phosphorylation (Wen, Zhong et al. 1995; Kovarik, Stoiber et al. 1999; Kim and Lee 2007). p38 MAPK has been identified as the potential kinase responsible for serine phosphorylation of Stat-1 in response to stresses such as TNF- α , LPS, and UV irradiation (Kovarik, Stoiber et al. 1999; Decker and Kovarik 2000). The serine 727 phosphorylation of Stat-1 is required for the pro-apoptotic effects of Stat-1. An example of role in apoptosis is the use of Stat1-defective cardiac myocytes that have been found to be resistant to apoptosis induced by ischaemia

reperfusion injury or heat (Stephanou et al. 2001, 2002, Janjua et al. 2002). In this study I have shown that MAP4K3 Δ C is able to induce a phosphorylation cascade from the MKK3/6 to p38 and finally to the transcription factor Stat-1. Therefore the identification of Stat-1 phosphorylation leads to the suggestion that Stat-1 could be involved in the pro-apoptotic pathway induced by MAP4K3, as phosphorylation is required for the pro-apoptotic effects of Stat-1. Nevertheless it has been established that IFN- γ -stimulated serine phosphorylation of Stat-1 occurs independently of the p38 MAPK pathway. This study proposes that PKC- δ is the putative serine kinase for Stat-1 in response to both IFN- α/β and IFN- γ (Uddin, Sassano et al. 2002; Deb, Sassano et al. 2003). Additionally, PKC- δ has been also proposed to induce mitochondria dependent apoptosis that is potentially involved in serine phosphorylation of Stat-1 in response to LPS and etoposide (Rhee, Jones et al. 2003; DeVries, Kalkofen et al. 2004). Therefore the Stat-1 phosphorylation seen in the MAP4K3 overexpression study might not be due to a p38 dependent pathway. To clarify if Stat-1 phosphorylation is due a p38 pathway further experiments that could be performed would be the overexpression of MAP4K3 with the inhibition of p38 using a p38 chemical inhibitor to determine if Stat-1 phosphorylation is dependent on the p38 pathway.

As the overexpression of MAP4K3 induces the phosphorylation of two transcription factors at sites which increase the transcriptional activity, I have investigated the expression levels of target genes of the two transcription factors. In this study I have found no protein that is altered in expression by the increase of phosphorylation of the two identified transcription factors. A target gene of c-jun which has been studied is Bim which has no change in expression following MAP4K3 overexpression. For Stat-1 the target gene which has been studied is Bcl-2, which shows no increase in expression following the overexpression of

MAP4K3. Therefore in this thesis there is no evidence to show that the two transcriptional factors have altered activity.

Using both the U2OS and 293 cells, I have shown that MAP4K3 induces the JNK and p38 pathways in these cell lines. This data places MAP4K3 as an inducer of the JNK and p38 pathways as for each MAPK a target transcription factor has been shown to have an increased phosphorylation state and MAPKKs that have been activated. These results expand on the knowledge of MAP4K3 as an inducer of the JNK pathway and reveals that MAP4K3 can also induce the p38 pathway. MAP4K3 Δ C is a stronger inducer of the p38 and JNK pathways than full length protein and may explain why MAP4K3 Δ C has been shown to increase the phosphorylation state of upstream MKKs and downstream transcription factors. This leads to the hypothesis that the full length MAP4K3 would also be able to induce these downstream changes as p38 and JNK phosphorylation is observed, but in the experimental setting used the phosphorylation level of MKKs and transcription factors is below the experimental sensitivity. This could be overcome by co-overexpression experiments of the MAP4K3 and the reporter protein.

The expression levels of p53 and p21 were investigated in this project to determine if the induction of these proteins occurs following MAP4K3 overexpression. p53 at the protein level was studied as p53 is induced and stabilised by a variety of different stresses and this can lead to cell cycle arrest, induction of DNA repair proteins and initiation of apoptosis (Harris and Levine 2005). Further p53 can activate the death receptor and mitochondrial pathways of apoptosis by the increased expression of apoptotic genes such as Bax and Fas (Vousden and Lu 2002). p21 is a cyclin dependent kinase inhibitor that inhibits the cyclin E/cdk2 and cyclin A/cdk2 kinases, preventing these kinases from promoting cell cycle

progression. No detectable changes in p21 and p53 were observed following MAP4K3 overexpression in 293 cells. This suggests that there is no involvement of p21 and p53 pathways in the MAP4K3 induced signal transduction pathways.

In order to study the level at which MAP4K3 regulates the cell death machinery, I examined the expression of several Bcl-2 family proteins. Bcl-2 is an anti-apoptotic protein that operates by inhibition of the Bax/Bak proteins (Cory and Adams 2002). The expression of Bcl-2 protein can be decreased or phosphorylation can occur leading to an increase in Bax activity. Additionally Bcl-2 can be sequestered by BH3 only proteins (Cory and Adams 2002).

Bax is a pro-apoptotic protein and following cell death stimuli, Bax undergoes a conformational change. This activation can occur with or without increases in the expression level of Bax. In this study, I did not observe differences in the protein expression levels of the Bcl-2 family members, Bcl-2 and Bax, between controls and MAP4K3 overexpression cells. This suggests that MAP4K3 overexpression does not lead to a decrease in the anti-apoptotic Bcl2 protein or an increase in the expression of the pro-apoptotic Bax. BH3 only proteins such as Bim, Puma and Bmf can lead to activation of the intrinsic pathway and the displacement theory suggests that BH3 only proteins bind directly to Bcl-2 which displaces the inactive Bax/Bak (Willis, Fletcher et al. 2007). BH3 only proteins following apoptotic stimuli can be phosphorylated or an increase in expression occurs leading to binding with Bcl-2 protein. For example, JNK has been proposed to phosphorylate Bim leading to activation of the intrinsic pathway of apoptosis (Lei and Davis 2003). In addition, the expression of Bim can be transcriptionally induced by JNK dependent activated c-Jun leading to the induction of apoptosis (Whitfield, Neame et al. 2001). No change in protein expression of the three BH3 only proteins assayed for following MAP4K3 overexpression in 293 cells was observed and

no phosphorylated Bim was detected. This reveals that induction of Bim, Puma and Bmf is not involved following MAP4K3 overexpression. This does not rule out the involvement of any of these BH3 only proteins, as changes in localisation can occur. An example is that in some cell types, Bim is sequestered to microtubule complexes and Bmf to the myosin V motor complex by different dynein light chains. UV-irradiation induces release of both Bim and Bmf by a process that may involve their phosphorylation (Cory and Adams 2002).

To investigate the importance of the regulation of MAP4K3 on the JNK and p38 pathways following UV treatment, siRNAs against MAP4K3 and dominant negative approaches were performed. A theory proposed to explain the differing functions of JNK is that the early transient phase of JNK activation (<1 hr) can signal cell survival, while the later and more sustained phase of JNK activation (1-6 hr) can mediate pro-apoptotic signalling following TNF α treatment (Chang, Kamata et al. 2006; Ventura, Hubner et al. 2006). Therefore in the study of suppression of MAP4K3, the time points were chosen to study the prolonged JNK activation that has been proposed to mediate apoptosis. The early JNK activation was not studied (less than 1 hour). No effect of MAP4K3 kinase dead and siRNA mediated suppression of MAP4K3 on JNK or p38 phosphorylation following UV treatment was observed. As siRNA mediated suppression of MAP4K3 leads to an increase of survival following UV-induced cell death this result of no effect on phospho-JNK and phospho-p38 is surprising as they are phosphorylated by the overexpressed MAP4K3. The data presented in this chapter that shows an effect of MAP4K3 on signalling pathways was with the overexpressed protein. As there was no data on the significance of MAP4K3 overexpression or MAP4K3 suppression on the phosphorylation levels of JNK or p38 in the experiments following UV treatment, the relevance of MAP4K3 regulation on UV induced p38 and JNK pathways remains unknown.

The overexpression of the GCK-1 group kinases, that include MAP4K3, GCKR, HPK1 and GCK, have been linked to the activation of the JNK pathway and not to p38 induction (Dan, Watanabe et al. 2001). HPK1 enhances JNK and, to a lesser extent, ERK and p38 MAP kinase activation in H₂O₂-treated EL-4 cells (Schulze-Luehrmann, Santner-Nanan et al. 2002). p38 activation is not described towards GCK-1 group kinase in transient overexpression experiments. This study shows a clear induction of both the p38 and JNK pathways following MAP4K3 overexpression. This is not an unexpected scenario as other GCK group kinases have been linked to both the induction of JNK and p38 following overexpression. These include MINK and Mst-1 as examples. MINK a group GCK-IV protein activates p38 and JNK stress response pathway in overexpression studies (Dan, Watanabe et al. 2000). While Mst1 a GCK-II protein activates MKK6, p38 MAPK, MKK7 and SAPK in co-transfection assays, suggesting that Mst1 may activate the JNK and p38 pathways (Graves, Gotoh et al. 1998).

The data presented in this thesis for the MAP4K3 protein kinase builds on the 1997 paper which linked MAP4K3 to activation of the JNK pathway and to the activation of endogenous MAP4K3 following UV and TNF α treatments. The phosphorylation cascade induced by MAP4K3 overexpression has been explored further and identifies JNK and p38 pathway components that are phosphorylated downstream of MAP4K3. The JNK pathway has been implicated in activation of Bax (Weston and Davis 2007) and experiments using p38 inhibitors have linked p38 to the activation of Bax (Van Laethem, Van Kelst et al. 2004). This leads to the hypothesis that the cell death induced by MAP4K3 overexpression could be due to a p38 and/or JNK dependent pathway. A question that arises from this thesis is that as MAP4K3 can induce the phosphorylation of p38 and JNK does this lead to the cell death that

is induced by MAP4K3 overexpression. To address the hypothesis that MAP4K3 induced cell death is JNK and/or p38 dependent the following experiments could be performed. The inhibition of JNK or p38 activity could be performed using the appropriate chemical inhibitors and these inhibitors could be included following transient transfection with cell death measured by chromatin condensation. Another possibility would be to perform siRNA mediated suppression of JNK1/JNK2 or p38alpha followed by MAP4K3 overexpression and cell death measurements. These two experiments would determine if p38 and JNK pathways are essential for MAP4K3 induced cell death. In summary this chapter describes how overexpression of MAP4K3 leads to a phosphorylation cascade for both the JNK and p38 kinase pathways, with the kinase domain and activity of MAP4K3 required for this activation to occur.

Proteasomal regulation of MAP4K3

Previously I have shown that ectopic expression of several MAP4K3 deletion fragments resulted in different expression levels (see chapter 3.3). This could be caused by differing stability of the encoded proteins. The MAP4K3 polypeptide contains two PEST domains. PEST domains are short sequences (10–60 residues) enriched in proline (P), glutamic /aspartic acid (E), serine (S) and threonine (T) residues. Proteins with PEST domains are frequently targets of degradation by the ubiquitin-proteasome pathway (Rechsteiner and Rogers 1996) and as GCK, a GCK-1 group protein, has been found to be ubiquitin-proteasome degraded, this type of regulation was investigated for MAP4K3. Degradation of a protein via the ubiquitin-proteasome pathway involves two discrete steps. The protein is tagged with multiple ubiquitin molecules, followed by the degradation of the tagged protein by the 26S proteasome complex (Glickman and Ciechanover 2002). The work described in this thesis has investigated the two steps of proteasomal degradation by inhibition of the proteasome and co-immunoprecipitation of MAP4K3 and HA-ubiquitin.

The results presented in chapter 3.4 suggest that the 26S proteasome degrades MAP4K3, as a proteasome inhibitor stabilises MAP4K3 expression levels. This degradation could be ubiquitin mediated as the co-overexpression studies with HA-ubiquitin reveal that MAP4K3 co-immunoprecipitates with the HA tagged ubiquitin. This result does not rule out the possibility that a binding partner of MAP4K3 or a non-specific protein that is immunoprecipitated in both the N-terminal and C-terminal fractions is the protein that is ubiquitinated. The immunoprecipitate for GFP contains HA-ubiquitin in all the MAP4K3 mutants including the MAP4K3 Δ C that contains no defined binding domains. This could suggest that the HA-Ub binds directly to MAP4K3. For example Endophilin A1 is the only described protein that binds to MAP4K3 and this was determined by overexpressing both

MAP4K3 and Endophilin A1 (Ramjaun, Angers et al. 2001). In this study the proline rich regions encoded in the C-terminus of MAP4K3 were shown to bind to the SH3 domains of Endophilin A1 indicating that Endophilin A1 would not be expected to co-immunoprecipitate with the N-terminus of MAP4K3. This is an important observation as Itch, an HECT type E3 ligase, has been found to bind to the SH3 domains of Endophilin A1 leading to the ubiquitination of this protein (Angers, Ramjaun et al. 2004).

There is no consensus as to the specificity of the internal lysine residues that are targeted by ubiquitin. In some cases distinct lysines are required, while in others there is little or no specificity. In the case of PEST domains, the lysine residues in the vicinity of a specific PEST degradation signal can serve as ubiquitin attachment sites (Kornitzer et al., 1994). For MAP4K3, both the N-terminal and C-terminal fraction of the protein appear to be targeted to the proteasome. This may involve poly-ubiquitination of lysine residues that are contained within both the fragments. This leads to the hypothesis that for MAP4K3, no single specific lysine residue is required for ubiquitin mediated proteasome degradation to occur.

MAP4K3 contains two PEST domains in the C-terminal regulatory domain. PEST domains are found in many short-lived eukaryotic proteins such as myc, fos, c-jun and p53 and were proposed to play a role in their degradation (Rechsteiner and Rogers 1996). Removal or disruption of the PEST sequence can increase the half-life of a protein whereas insertion or creation of a new PEST sequence within a PEST sequence-free protein can decrease this half-life. For example, the deletion of a 27 residue PEST sequence from the carboxyl terminus of c-Fos increases its stability considerably (Tsurumi, Ishida et al. 1995). However, in general, PEST domains have not been found to have a direct functional role and therefore PEST domains can be considered a way to correlate the primary structure of a protein to its

stability within the cell (Rechsteiner and Rogers 1996). MAP4K3 in this thesis was considered to be ubiquitin-proteasome pathway degraded and this was observed for all the MAP4K3 deletion mutants. This suggests that the PEST domain of MAP4K3 is not essential for the ubiquitin mediated proteasome degradation. Nonetheless the MAP4K3 Δ C fragment does not contain the PEST domain and is expressed at a higher level than the full length protein, while the MAP4K3 Δ N fragment is expressed at a lower level than the full length protein. This evidence suggests a possible role of the PEST domains in conferring a reduction in stability, but other possibilities include binding proteins or the lysine residues within the C-terminal region that could have a role in MAP4K3 stability. GCK and GCKR have been studied for ubiquitination with no experiments performed on the function of the PEST domains. The isoform of MAP4K3 used in this experiment does not contain exon 13 resulting in loss of the first PEST domain. This suggests the first PEST domain is not essential for MAP4K3 proteasome mediated degradation.

Ubiquitin has seven lysine residues, which can be used for polymerization (Hochstrasser 2006). Two major forms of polyubiquitin chains have been characterized, in which the isopeptide bond linkages involve either Lys48 or Lys63. Lys48-linked polyubiquitin tagging is mostly used to target proteins for degradation by the proteasome, whereas Lys63-linked polyubiquitination has been linked to numerous cellular events that do not rely on degradative signalling via the proteasome (Hochstrasser 2006). Both GCK and GCKR are ubiquitinated with TNF inducing Lys63-linked ubiquitination of GCKR and subsequent GCKR oligomerization. GCK is exclusively Lys48-linked ubiquitinated and is degraded by the proteasome. In this section, MAP4K3 is ubiquitinated and stabilized by inhibitors of the proteasome, indicating that MAP4K3 is subject to proteasomal turnover and as such the comparison to GCK ubiquitin mediated proteasome degradation will be discussed in detail. In

resting cells, GCK is rapidly turned over, due to GCK kinase-dependent ubiquitination and degradation by the proteasome. Agonists such as poly(IC) and LPS, activate GCK in a TRAF6-dependent manner, by transiently stabilizing the ubiquitinated GCK polypeptide. The agonist activation of GCK involves TRAF6-dependent transient stabilization of the GCK polypeptide rather than an increase in kinase activity. (Zhong and Kyriakis 2004). From the experiments performed in this thesis I have not investigated which lysine on ubiquitin is used to form the polyubiquitin chain. A notable difference between MAP4K3 and GCK are that the kinase dead MAP4K3 is maintained at a lower level than the wild type protein, suggesting more degradation, whereas for GCK the proteasome degradation is dependent on the kinase activity.

In most cases the proteasome cleaves protein substrates into small peptides, usually 3-22 amino acid residues in length (Kisselev, Akopian et al. 1999). In this project it has been observed that overexpression of full length MAP4K3 and MAP4K3 fragments can lead to the formation of smaller GFP proteins than predicted. These possible degradation products are more than 22 amino acids in length as predicted by their observed size and the degradation products are still present following proteasome inhibition. These two pieces of evidence suggest that the degradation products are not a result of proteasomal degradation.

A controversial topic in the literature is that calpains may cleave proteins near regions containing PEST sequences (Rechsteiner & Rogers, 1996). It is proposed that these regions increase the local Ca^{2+} concentration and, in turn, activate calpains. The evidence for this is mixed, with studies indicating that PEST sequences do not influence substrate susceptibility to calpain proteolysis (Molinari, Anagli et al. 1995) while two more recent studies show that the PEST domain of I κ B α is necessary and sufficient for *in vitro* degradation by μ -calpain

(Shumway, Maki et al. 1999) and the two PEST motifs of CaV β 3 subunit regulate the Ca²⁺/calpain-mediated cleavage of this protein (Sandoval, Oviedo et al. 2006). The involvement of calpains in cleavage of GCK-1 family of proteins has not been described. Cleavage of the GCK-1 protein, HPK1 has been shown to be mediated by caspases (Chen, Meyer et al. 1999). The cleavage site of caspases in HPK1 is not conserved in MAP4K3 and cleavage by caspases has not been addressed for MAP4K3 in this project.

In this project I have characterised a protein kinase that induces cell death and is regulated by the proteasome. The ubiquitin proteasome system is important in regulating the degradation of many key regulatory molecules involved in apoptosis. These include p53, p73, mdm2, I κ B α , Bax and caspases (Melino 2005) with proteasome inhibitors inducing cell death. This section in summary suggests that MAP4K3 protein levels could be controlled post-translationally through ubiquitin proteasomal-dependent degradation.

Analysis of MAP4K3 levels in normal and tumour tissues

Tumour growth can be in part caused by an increase in cell population and enhanced resistance to apoptosis (Evan and Vousden 2001). Results described in chapter 3.2 show that MAP4K3 downregulation leads to an increase in cell survival following DNA-damage induced cell death and separately shows an increase in DNA synthesis, a marker for cell proliferation. This leads to the hypothesis that loss of function of MAP4K3 in cancer could occur. To investigate if MAP4K3 is downregulated or mutated in cancer, *in-silico* and experimental techniques were employed.

A variety of genome (DNA) defects are the underlining cause of human cancer (Haber and Settleman 2007). Genetic mutations are caused by genomic instability which can occur at the level of the chromosome or the nucleotide. Alterations at the nucleotide level include subtle changes in gene sequences or regulatory domains. Chromosome level changes can include changes in chromosome number or translocations (Lengauer, Kinzler et al. 1998).

At the nucleotide level the detection of small nucleotide changes within genes (intragenic mutations) that lead to loss of function or gain of function has been pursued by DNA-sequencing studies that are aimed at identifying these genes as the target of a mutational event (Sjoblom, Jones et al. 2006; Greenman, Stephens et al. 2007). In this project using bioinformatics searches of the literature I have investigated whether DNA encoding for MAP4K3 is mutated in cancer. The published literature suggests that MAP4K3 DNA is not mutated in cancer (Sjoblom, Jones et al. 2006; Greenman, Stephens et al. 2007).

Along with single nucleotide mutations, various abnormalities may be transmitted from a cancer cell to its progeny. The genetic modifications include deletion or amplification of

chromosome fragments, which often contain many genes, making it difficult to identify the specific genes targeted by these events. Translocations of genes lead to the fusion of DNA fragments from different chromosomal regions, either causing aberrant expression of a normal gene or creating an abnormal fusion protein. Finally epigenetic silencing involves heritable modifications of histones and nucleotides in regulatory regions of genes, leading to suppression of gene expression in the absence of DNA mutations (Haber and Settleman 2007). The gene expression levels can be altered by these genetic modifications. In this thesis I have investigated the link between MAP4K3 expression levels and cancer progression.

To investigate if MAP4K3 expression was reduced in tumour samples compared to normal tissue samples, bioinformatic searches and experimental analysis was carried out. The bioinformatics searches were performed using the GeneLogic and Oncomine databases and revealed that MAP4K3 expression levels are significantly altered in a variety of different tumour types. As such, the results from this analysis failed to show a robust link between MAP4K3 downregulation and cancer progression. The GeneLogic database had two different types of ovarian epithelial tumours where downregulation of MAP4K3 was detected. To confirm this data QRT-PCR on ovarian samples was performed to validate the Affymetrix study from the gene logic database. The lifetime risk of developing ovarian cancer is approximately 1 in 48 for women in England and Wales (CRUK). Ovarian cancer can be broken down into the following three subgroups according to the kind of cells from which they are formed; epithelial tumours arise from cells that line or cover the ovaries; germ cell tumours originate from cells that are destined to form eggs within the ovaries; and sex cord-stromal cell tumours begin in the connective cells that hold the ovaries together. Common epithelial tumours begin in the surface epithelium of the ovaries and account for about 90% of all ovarian cancers. They are divided into a number of subtypes; serous, endometrioid,

mucinous, and clear cell tumours. Serous tumours are the most widespread forms of ovarian cancer and account for 40% of epithelial tumours. Approximately 20% of ovarian epithelial tumours are Endometrioid. Mucinous tumours make up about 1% of epithelial tumours and clear cell tumours account for about 6% of common epithelial tumours. The GeneLogic database had samples of Adenocarcinoma, clear cell type (6) and papillary serous type (33) showing downregulation of MAP4K3 mRNA of 1.59 and 1.41 respectively compared to the control. The Origene cDNA panel used in this thesis contains control tissue and samples of grade I to IV ovarian tumours. The cDNA panel contains 41 ovarian epithelial tumours including 24 serous, 8 endometrioid, 4 mucinous, and 5 unclassified tumours of the ovary. This study of the expression level of MAP4K3 mRNA showed that MAP4K3 was significantly upregulated compared to the control tissue, with no significant increase in expression following increase in tumour grade. The serous adenocarcinomas from the GeneLogic data, showed downregulation however the Origene cDNA panel containing ovarian cancer samples showed upregulation of MAP4K3 but the Origene cDNA panel consisted of 58% serous ovarian carcinoma. The grade III/IV patient samples comprised 88% serous ovarian carcinoma and showed an increase in expression of MAP4K3 indicating the GeneLogic and Origene results were not analogous and this result was not affected by different ovarian cancer types. No conclusions are possible from the ovarian cancer data as contradictory results were observed from the GeneLogic affymetrix array and the study presented in this thesis. Therefore this leads to the hypothesis that MAP4K3 mRNA levels are not consistently up or downregulated in tumours suggesting that suppression of MAP4K3 mRNA is not an important step in tumorigenesis for ovarian cancer.

Final Discussion

Apoptosis is a highly dynamic and conserved process by which metazoan cells commit cellular suicide (Yuan 1996). Defects in the apoptosis-inducing pathways can eventually lead to expansion of a population of neoplastic cells (Evan and Vousden 2001). Additionally the resistance of tumour cells to apoptosis can also augment the escape of tumour cells from surveillance by the immune system (Igney and Krammer 2002). Moreover, because chemotherapy and irradiation act primarily by inducing apoptosis, defects in the apoptotic pathway can make cancer cells resistant to therapy. Therefore the resistance to apoptosis constitutes an important clinical problem (Igney and Krammer 2002) and as such the regulation of apoptosis following DNA damage stimuli has been investigated in this project.

The aim of this project was to identify and characterise novel cell death regulators. To identify cell death regulators, an RNAi screen was performed using a vector based RNAi library with UV irradiation used to induce cell death. This screen was performed in a pool format with the expression of the shRNA determined by sequencing. The screen revealed that an shRNA targeting MAP4K3 was the most highly expressed following UV-irradiation. The use of three independent siRNAs against MAP4K3 revealed that suppression of MAP4K3 induces an increase in cell survival following UV and cisplatin induced cell death. The involvement of MAP4K3 in the regulation of cell survival following UV treatment complements the study that shows UV activates endogenous MAP4K3 (Deiner, Wang et al. 1997). Using overexpression studies I have linked MAP4K3 to the activation of the intrinsic pathway of apoptosis and shown that the kinase domain and activity are essential for the maximal induction of cell death. The cell death induced by MAP4K3 has been considered to be apoptosis as caspases are required and chromatin condensation occurs. The cell death has been further described as being dependent on the mitochondrial pathway of apoptosis by the

ability of Bclxl to rescue the cell death. Additionally MAP4K3 was observed to induce Bax conformation change and clustering which is further evidence suggesting that MAP4K3 induces the mitochondrial pathway of apoptosis. These results using gain of function complement the results from suppression of MAP4K3 and suggest that MAP4K3 is a cell death regulator. This leads to the proposed pathway for MAP4K3 induced cell death as shown on Figure 4.1

To investigate the signalling pathways that could lead to the activation of cell death by MAP4K3 overexpression, the p38 and JNK pathways have been investigated. The results presented in this thesis add to the previous study on MAP4K3 (Deiner, Wang et al. 1997) by revealing that MAP4K3 can induce the p38 pathway in addition of the JNK pathway and this induction is dependent on the kinase domain and kinase activity. The ectopic expression of MAP4K3 Δ C has been found to induce the phosphorylation of the c-Jun transcription factor, a target of JNK, and also induce the phosphorylation of Stat-1, which can be phosphorylated by p38. Therefore downstream transcription factors that could have a role in the induction of cell death have been identified as increased in phosphorylation following MAP4K3 overexpression. In this project I have not addressed if the cell death induced by MAP4K3 is dependent on the JNK or p38 pathways and this is an important question for research on MAP4K3 dependent cell death. The posttranslational regulation of ectopically expressed MAP4K3 was investigated by use of a proteasome inhibitor which suggested that MAP4K3 is degraded by the proteasome. I have evidence suggesting that MAP4K3 is degraded by an ubiquitin proteasomal pathway.

As the suppression of MAP4K3 results in an increase in proliferation and cell survival following DNA damage induced apoptosis, the relevance of the *in-vitro* data was investigated

by comparing the mRNA expression levels of MAP4K3 in cancer patient samples compared to control tissue. This resulted in the conclusion that MAP4K3 mRNA levels are not consistently altered in cancer. In light of the data suggesting MAP4K3 is proteasome degraded, the protein levels of MAP4K3 could be a direction from which to study the expression levels from cancer samples. This would require the generation of a specific MAP4K3 antibody which was lacking in this project.

In summary, in this thesis I have identified and further characterised MAP4K3 as a novel cell death regulator. Therefore the initial aims of the project have been successfully achieved with the further characterisation taken place. This characterisation suggests that MAP4K3 induces apoptosis by activation of the intrinsic pathway and I have identified signalling components that could determine how MAP4K3 induces cell death.

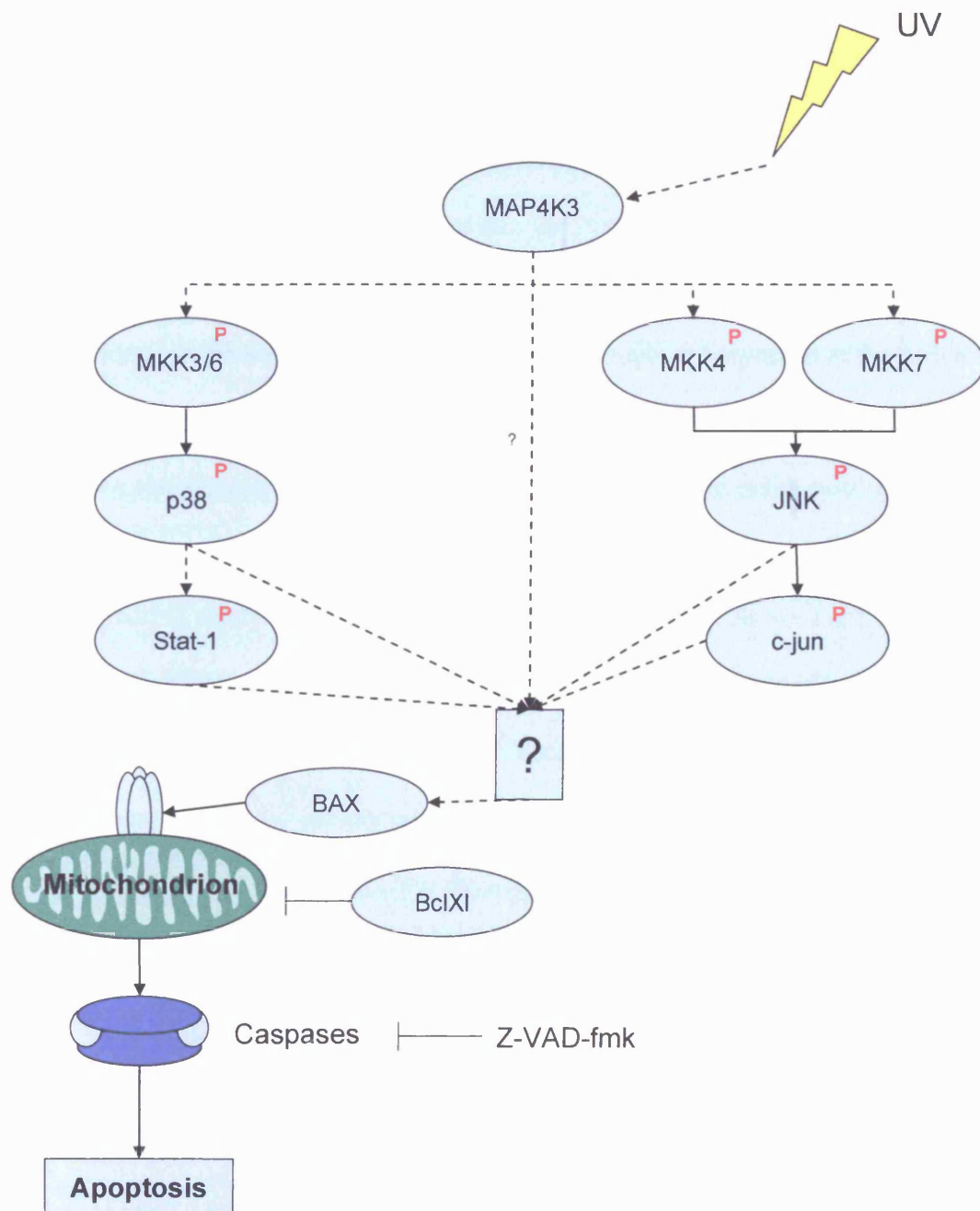


Figure 4.1: Proposed model for MAP4K3 involvement in the regulation of cell death

Endogenous MAP4K3 has been shown to be activated by UV light (Deiner, Wang et al. 1997) and in this thesis I have shown that suppression of MAP4K3 protects against UV induced cell death. Experiments involving the overexpression of MAP4K3 suggest that it induces the mitochondrial pathway of apoptosis by the activation of Bax. The mechanism of induction of Bax activation has not been determined in this project and on the diagram this is signified by a question mark. The JNK and p38 pathways that can lead to the activation of Bax have been identified in this project to be induced following overexpression of MAP4K3. Therefore MAP4K3 has been proposed to be a novel cell death regulator.

Further Work

In a previous study involving MAP4K3, there is data suggesting that MAP4K3 can autophosphorylate (Deiner, Wang et al. 1997). To further characterise MAP4K3, a study to examine the role of phosphorylation at several sites in terms of the effects on kinase activation and cell death could be performed. An example of mapping the sites of phosphorylation on a Ste20 kinase protein is with Mst-1 (Glantschnig, Rodan et al. 2002). This study demonstrated a role for Mst-1 intermolecular autophosphorylation of the activation loop in subdomain VIII on kinase activity. Alignment of Mst-1 subdomain VIII with MAP4K3 shows conservation in MAP4K3 of the phospho-regulated residues of Mst-1. Site-directed mutagenesis of Mst-1 Thr183 to alanine demonstrated its crucial role in kinase activation, eliminating catalytic activity to 1-3% and this mutant was shown not to induce cell death. The kinase subdomain VIII of MAP4K3 and Mst-1 share sequence homologue with Ser170 of MAP4K3 aligning with Mst-1 Thr183 site. Site directed mutations of Ser170 of MAP4K3 to alanine could be performed with downstream changes in phosphorylation of JNK/p38 to determine activity changes and the amount of cell death would be quantified. A second approach would be the generation of phospho-specific antibodies to probe for putative phosphorylation at Ser170 of MAP4K3.

In 2001, a screen using a cDNA expression library to identify binding partners of Endophilin A1 identified MAP4K3 as a novel binding partner. This result was then to validate using co-overexpression experiments to suggest binding of MAP4K3 to Endophilin A1 (Ramjaun, Angers et al. 2001). Therefore there is only one known binding partner for MAP4K3. To address this, a future experiment that could identify novel binding partners of MAP4K3 could be performed using tandem affinity purification (TAP) (Rigaut, Shevchenko et al. 1999). The TAP method would involve the fusion of the TAP tag to MAP4K3 and the introduction of the

plasmid into cells. The TAP tag encodes a calmodulin binding peptide (CBP), a TEV protease cleavage site, and Protein A and can be used to recover tagged protein with high efficiency and high purity via a two step affinity protocol. The fusion protein and associated components are recovered from cell extracts by affinity selection on an IgG matrix. After washing, the TEV protease is added to release the bound material by cleavage at the TEV cleavage site on the TAP tag. The eluted product is incubated with calmodulin-coated beads in the presence of calcium. This second affinity step is required to remove the TEV protease as well as traces of contaminants remaining after the first affinity selection. After washing, the bound material is released with EGTA and mass spectroscopy would then be used to identify bound proteins by MALDI analysis and/or MS/MS sequencing. This affinity purification technique could lead to the identification of novel binding partners that are either involved in the regulation of MAP4K3 activity or on the expression level such as possible E3 ligases that are involved in the proteasome mediated degradation of MAP4K3. If the protein that is identified by affinity purification is an E3 ligase, then experiments would include investigating if the E3 ligase affects the protein expression levels of MAP4K3.

The identification of a MAP4K3 substrate could be crucial in determining how overexpression of MAP4K3 leads to the activation of the JNK and p38 pathways. In most cases, the interaction between a kinase and a substrate is transient and as such the tandem affinity purification of MAP4K3 would not be expected to identify substrates. Substrates could be identified through the “bump and hole” technique (Shah, Liu et al. 1997). This technique requires the mutation of the ATP binding pocket of the kinase to enable it to utilise specific ATP analogues. The mutation creates a hole where the amine residue of ATP usually sits and allows the kinase to use ATP analogues that contain large hydrophobic moieties which wild kinases are unable to utilise. This does not appear to affect kinase activity or

substrate preferences. Therefore in-vivo labelling assays using the specific mutated kinase in combination with an ATP analogue should allow specific labelling of direct kinase substrates when the mutated kinase is overexpressed (Shah, Liu et al. 1997; Habelhah, Shah et al. 2001).

The role of MAP4K3 suppression in conferring a tumorigenesis phenotype has not been fully addressed in this thesis. An example of a future assay is the clonogenicity of shRNA mediated MAP4K3 suppressed cells following DNA damage stimuli. Another assay would be growth in soft agar of shRNA mediated suppressed MAP4K3 cells to determine if the anchorage-independent growth of U2OS cells is altered.

References

- Aas, T. (1996). "Specific P53 mutations are associated with de novo resistance to doxorubicin in breast cancer patients." *Nature Med.* **2**: 811-814.
- Adams, J., V. J. Palombella, et al. (1999). "Proteasome inhibitors: a novel class of potent and effective antitumor agents." *Cancer Res* **59**(11): 2615-22.
- Adrain, C. and S. J. Martin (2001). "The mitochondrial apoptosome: a killer unleashed by the cytochrome seas." *Trends Biochem Sci* **26**(6): 390-7.
- Ahn, S. H., W. L. Cheung, et al. (2005). "Sterile 20 kinase phosphorylates histone H2B at serine 10 during hydrogen peroxide-induced apoptosis in *S. cerevisiae*." *Cell* **120**(1): 25-36.
- Al-Mohanna, M. A., P. S. Manogaran, et al. (2004). "The tumor suppressor p16(INK4a) gene is a regulator of apoptosis induced by ultraviolet light and cisplatin." *Oncogene* **23**(1): 201-12.
- Allan, L. A. and M. Fried (1999). "p53-dependent apoptosis or growth arrest induced by different forms of radiation in U2OS cells: p21WAF1/CIP1 repression in UV induced apoptosis." *Oncogene* **18**(39): 5403-12.
- Allen, M., L. Svensson, et al. (2000). "Deficiency of the stress kinase p38alpha results in embryonic lethality: characterization of the kinase dependence of stress responses of enzyme-deficient embryonic stem cells." *J Exp Med* **191**(5): 859-70.
- Angers, A., A. R. Ramjaun, et al. (2004). "The HECT domain ligase itch ubiquitinates endophilin and localizes to the trans-Golgi network and endosomal system." *J Biol Chem* **279**(12): 11471-9.
- Ashrafi, K., F. Y. Chang, et al. (2003). "Genome-wide RNAi analysis of *Caenorhabditis elegans* fat regulatory genes." *Nature* **421**(6920): 268-72.
- Avraham, H., S. Y. Park, et al. (2000). "RAFTK/Pyk2-mediated cellular signalling." *Cell Signal* **12**(3): 123-33.
- Baer, M., T. W. Nilsen, et al. (1990). "Structure and transcription of a human gene for H1 RNA, the RNA component of human RNase P." *Nucleic Acids Res* **18**(1): 97-103.
- Bakiri, L., D. Lallemand, et al. (2000). "Cell cycle-dependent variations in c-Jun and JunB phosphorylation: a role in the control of cyclin D1 expression." *Embo J* **19**(9): 2056-68.
- Beardmore, V. A., H. J. Hinton, et al. (2005). "Generation and characterization of p38beta (MAPK11) gene-targeted mice." *Mol Cell Biol* **25**(23): 10454-64.
- Behrens, A., W. Jochum, et al. (2000). "Oncogenic transformation by ras and fos is mediated by c-Jun N-terminal phosphorylation." *Oncogene* **19**(22): 2657-63.
- Behrens, A., M. Sibilina, et al. (1999). "Amino-terminal phosphorylation of c-Jun regulates stress-induced apoptosis and cellular proliferation." *Nat Genet* **21**(3): 326-9.
- Benedict, M. A., Y. Hu, et al. (2000). "Expression and functional analysis of Apaf-1 isoforms. Extra Wd-40 repeat is required for cytochrome c binding and regulated activation of procaspase-9." *J Biol Chem* **275**(12): 8461-8.
- Bergers, G., D. Hanahan, et al. (1998). "Angiogenesis and apoptosis are cellular parameters of neoplastic progression in transgenic mouse models of tumorigenesis." *Int J Dev Biol* **42**(7): 995-1002.
- Bernards, R., T. R. Brummelkamp, et al. (2006). "shRNA libraries and their use in cancer genetics." *Nat Methods* **3**(9): 701-6.
- Berns, K., E. M. Hijmans, et al. (2004). "A Large-Scale RNAi Screen in Human Cells Identifies New Components of the p53 Pathway." *Nature* **428**: 431-437.

- Berns, K., E. M. Hijmans, et al. (2004). "A large-scale RNAi screen in human cells identifies new components of the p53 pathway." *Nature* **428**(6981): 431-7.
- Bernstein, E., A. Caudy, et al. (2001). "Role for a bidentate ribonuclease in the initiation step of RNA interference." *Nature* **409**: 363-366.
- Bode, A. M. and Z. Dong (2003). "Mitogen-activated protein kinase activation in UV-induced signal transduction." *Sci STKE* **2003**(167): RE2.
- Bouck, N., V. Stellmach, et al. (1996). "How tumors become angiogenic." *Adv Cancer Res* **69**: 135-74.
- Brancho, D., N. Tanaka, et al. (2003). "Mechanism of p38 MAP kinase activation in vivo." *Genes Dev* **17**(16): 1969-78.
- Breitschopf, K., E. Bengal, et al. (1998). "A novel site for ubiquitination: the N-terminal residue, and not internal lysines of MyoD, is essential for conjugation and degradation of the protein." *Embo J* **17**(20): 5964-73.
- Brummelkamp, T. R. and R. Bernards (2003). "New tools for functional mammalian cancer genetics." *Nat Rev Cancer* **3**(10): 781-9.
- Brummelkamp, T. R., R. Bernards, et al. (2002). "Stable suppression of tumorigenicity by virus-mediated RNA interference." *Cancer Cell* **2**(3): 243-7.
- Brummelkamp, T. R., R. Bernards, et al. (2002). "A System for Stable Expression of Short Interfering RNAs in Mammalian Cells." *Science* **296**: 550-553.
- Brummelkamp, T. R., A. W. Fabius, et al. (2006). "An shRNA barcode screen provides insight into cancer cell vulnerability to MDM2 inhibitors." *Nat Chem Biol* **2**(4): 202-6.
- Cerutti, L., N. Mian, et al. (2000). "Domains in gene silencing and cell differentiation proteins: The novel PAZ domain and redefinition of the piwi domain. ." *Trends Biochem. Sci.* **25**: 481-482.
- Chadee, D. N., T. Yuasa, et al. (2002). "Direct activation of mitogen-activated protein kinase kinase kinase MEKK1 by the Ste20p homologue GCK and the adapter protein TRAF2." *Mol Cell Biol* **22**(3): 737-49.
- Chai, J., C. Du, et al. (2000). "Structural and biochemical basis of apoptotic activation by Smac/DIABLO." *Nature* **406**(6798): 855-62.
- Chang, L., H. Kamata, et al. (2006). "The E3 ubiquitin ligase itch couples JNK activation to TNFalpha-induced cell death by inducing c-FLIP(L) turnover." *Cell* **124**(3): 601-13.
- Chau, V., J. W. Tobias, et al. (1989). "A multiubiquitin chain is confined to specific lysine in a targeted short-lived protein." *Science* **243**(4898): 1576-83.
- Chen, J. and G. Fang (2001). "MAD2B is an inhibitor of the anaphase-promoting complex." *Genes Dev* **15**(14): 1765-70.
- Chen, L., S. N. Willis, et al. (2005). "Differential targeting of prosurvival Bcl-2 proteins by their BH3-only ligands allows complementary apoptotic function." *Mol Cell* **17**(3): 393-403.
- Chen, Y. R., C. F. Meyer, et al. (1999). "Caspase-mediated cleavage and functional changes of hematopoietic progenitor kinase 1 (HPK1)." *Oncogene* **18**(51): 7370-7.
- Cheung, H. W., A. C. Chun, et al. (2006). "Inactivation of human MAD2B in nasopharyngeal carcinoma cells leads to chemosensitization to DNA-damaging agents." *Cancer Res* **66**(8): 4357-67.
- Chin, A. I., J. Shu, et al. (1999). "TANK potentiates tumor necrosis factor receptor-associated factor-mediated c-Jun N-terminal kinase/stress-activated protein kinase activation through the germinal center kinase pathway." *Mol Cell Biol* **19**(10): 6665-72.
- Ciechanover, A., A. Orian, et al. (2000). "Ubiquitin-mediated proteolysis: biological regulation via destruction." *BioEssays* **22**(5): 442-451.

- Cogoni, C. and G. Macino (1999). "Gene silencing in *Neurospora crassa* requires a protein homologous to RNA-dependent RNA polymerase." *Nature* **399**(6732): 166-9.
- Cory, S. and J. M. Adams (2002). "The Bcl2 family: regulators of the cellular life-or-death switch." *Nat Rev Cancer* **2**(9): 647-56.
- CRUK (2007). "Cancer Research UK News and Resources web site." <http://info.cancerresearchuk.org/cancerstats>: CancerStats.
- Dalmay, T., A. Hamilton, et al. (2000). "An RNA-dependent RNA polymerase gene in *Arabidopsis* is required for posttranscriptional gene silencing mediated by a transgene but not by a virus." *Cell* **101**(5): 543-53.
- Dan, I., S. E. Ong, et al. (2002). "Cloning of MASK, a novel member of the mammalian germinal center kinase III subfamily, with apoptosis-inducing properties." *J Biol Chem* **277**(8): 5929-39.
- Dan, I., N. M. Watanabe, et al. (2000). "Molecular cloning of MINK, a novel member of mammalian GCK family kinases, which is up-regulated during postnatal mouse cerebral development." *FEBS Lett* **469**(1): 19-23.
- Dan, I., N. M. Watanabe, et al. (2001). "The Ste20 group kinases as regulators of MAP kinase cascades." *Trends Cell Biol* **11**(5): 220-30.
- Danial, N. N. and S. J. Korsmeyer (2004). "Cell death: critical control points." *Cell* **116**(2): 205-19.
- Davies, H., C. Hunter, et al. (2005). "Somatic mutations of the protein kinase gene family in human lung cancer." *Cancer Res* **65**(17): 7591-5.
- Davis, R. J. (2000). "Signal transduction by the JNK group of MAP kinases." *Cell* **103**(2): 239-52.
- De Chiara, G., M. E. Marcocci, et al. (2006). "Bcl-2 Phosphorylation by p38 MAPK: identification of target sites and biologic consequences." *J Biol Chem* **281**(30): 21353-61.
- Deak, M., A. D. Clifton, et al. (1998). "Mitogen- and stress-activated protein kinase-1 (MSK1) is directly activated by MAPK and SAPK2/p38, and may mediate activation of CREB." *Embo J* **17**(15): 4426-41.
- Deb, D. K., A. Sassano, et al. (2003). "Activation of protein kinase C delta by IFN-gamma." *J Immunol* **171**(1): 267-73.
- Decker, T. and P. Kovarik (2000). "Serine phosphorylation of STATs." *Oncogene* **19**(21): 2628-37.
- Deiner, K., X. S. Wang, et al. (1997). "Activation of the c-Jun N-Terminal Kinase Pathway by a Novel Protein Kinase Related to Human Germinal Center Kinase." *Proceedings of the National Academy of Science USA* **94**: 9692-9697.
- DeMartino G and Slaughter C (1999). "The Proteasome, a Novel Protease Regulated by Multiple Mechanisms." *The Journal of Biological Chemistry* **274**(32): 22123-22126.
- Derijard, B., J. Raingeaud, et al. (1995). "Independent human MAP-kinase signal transduction pathways defined by MEK and MKK isoforms." *Science* **267**(5198): 682-5.
- DeVries, T. A., R. L. Kalkofen, et al. (2004). "Protein kinase Cdelta regulates apoptosis via activation of STAT1." *J Biol Chem* **279**(44): 45603-12.
- Dewson, G., R. T. Snowden, et al. (2003). "Conformational change and mitochondrial translocation of Bax accompany proteasome inhibitor-induced apoptosis of chronic lymphocytic leukemic cells." *Oncogene* **22**(17): 2643-54.
- Di Fiore, P., J. Pierce, et al. (1987). "erbB-2 is a potent oncogene when overexpressed in NIH/3T3 cells." *Science* **237**: 178-82.
- Dolado, I., A. Swat, et al. (2007). "p38alpha MAP kinase as a sensor of reactive oxygen species in tumorigenesis." *Cancer Cell* **11**(2): 191-205.

- Dorsett, Y. and T. Tuschl (2004). "siRNAs: applications in functional genomics and potential as therapeutics." *Nat Rev Drug Discov* **3**(4): 318-29.
- Drogen, F., S. M. O'Rourke, et al. (2000). "Phosphorylation of the MEKK Ste11p by the PAK-like kinase Ste20p is required for MAP kinase signaling in vivo." *Curr Biol* **10**(11): 630-9.
- Du, C., M. Fang, et al. (2000). "Smac, a mitochondrial protein that promotes cytochrome c-dependent caspase activation by eliminating IAP inhibition." *Cell* **102**(1): 33-42.
- Du, H. and Y. Liang (2006). "Saccharomyces cerevisiae ste20 mutant showing resistance to glucose-induced cell death." *Yi Chuan Xue Bao* **33**(7): 664-8.
- Duncan, P. I., D. F. Stojdl, et al. (1998). "The Clk2 and Clk3 dual-specificity protein kinases regulate the intranuclear distribution of SR proteins and influence pre-mRNA splicing." *Exp Cell Res* **241**(2): 300-8.
- Dykxhoorn, D. M., C. D. Novina, et al. (2003). "Killing the messenger: short RNAs that silence gene expression." *Nat Rev Mol Cell Biol* **4**(6): 457-67.
- Eferl, R. and E. F. Wagner (2003). "AP-1: a double-edged sword in tumorigenesis." *Nat Rev Cancer* **3**(11): 859-68.
- Elbashir, S., J. Harborth, et al. (2001). "Duplexes of 21-nucleotide RNAs mediate RNA interference in cultured mammalian cells." *Nature* **24**(411): 494-498.
- Elbashir, S., W. Lendeckel, et al. (2001). "RNA interference is mediated by 21 and 22 nucleotide RNAs." *Genes & Development* **15**: 188-200.
- Engelberg, D. (2004). "Stress-activated protein kinases-tumor suppressors or tumor initiators?" *Semin Cancer Biol* **14**(4): 271-82.
- Evan, G. I. and K. H. Vousden (2001). "Proliferation, cell cycle and apoptosis in cancer." *Nature* **411**(6835): 342-8.
- Farber, J. L. and S. K. El-Mofty (1975). "The biochemical pathology of liver cell necrosis." *Am J Pathol* **81**(1): 237-50.
- FDA (2003). "United States Food and Drug Administration press release 13 May 2003." <http://www.fda.gov/bbs/topics/NEWS/2003/NEW00905.html>.
- Findlay, G. M., L. Yan, et al. (2007). "A MAP4 kinase related to Ste20 is a nutrient-sensitive regulator of mTOR signalling." *Biochem J* **403**(1): 13-20.
- Findley, H., L. Gu, et al. (1997). "Expression and regulation of BCL-2, BCL-XL, and BAX correlate with p53 status and sensitivity to apoptosis in childhood acute lymphoblastic leukemia." *Blood* **89**: 2986-2993.
- Fingar, D. C., S. Salama, et al. (2002). "Mammalian cell size is controlled by mTOR and its downstream targets S6K1 and 4EBP1/eIF4E." *Genes Dev* **16**(12): 1472-87.
- Finucane, D. M., E. Bossy-Wetzel, et al. (1999). "Bax-induced caspase activation and apoptosis via cytochrome c release from mitochondria is inhibitable by Bcl-xL." *J Biol Chem* **274**(4): 2225-33.
- Fire, A., S. Xu, et al. (1998). "Potent and specific genetic interference by double-stranded RNA in *Caenorhabditis elegans*." *Nature* **391**: 806-811.
- Foulds, L. (1954). "The experimental study of tumor progression: a review." *Cancer Res* **14**(5): 327-39.
- Geng, Y., E. N. Eaton, et al. (1996). "Regulation of cyclin E transcription by E2Fs and retinoblastoma protein." *Oncogene* **12**(6): 1173-80.
- Glantschnig, H., G. A. Rodan, et al. (2002). "Mapping of MST1 kinase sites of phosphorylation. Activation and autophosphorylation." *J Biol Chem* **277**(45): 42987-96.
- Glickman, M. and A. Ciechanover (2002). "The Ubiquitin-Proteasome Proteolytic Pathway." *Physiological Review* **82**: 373-428.

- Glickman, M. H., D. M. Rubin, et al. (1998). "The regulatory particle of the *Saccharomyces cerevisiae* proteasome." *Mol Cell Biol* **18**(6): 3149-62.
- Golstein, P. and G. Kroemer (2007). "Cell death by necrosis: towards a molecular definition." *Trends Biochem Sci* **32**(1): 37-43.
- Graves, J. D., Y. Gotoh, et al. (1998). "Caspase-mediated activation and induction of apoptosis by the mammalian Ste20-like kinase Mst1." *Embo J* **17**(8): 2224-34.
- Greenman, C., P. Stephens, et al. (2007). "Patterns of somatic mutation in human cancer genomes." *Nature* **446**(7132): 153-8.
- Groll, M., L. Ditzel, et al. (1997). "Structure of 20S proteasome from yeast at 2.4 Å resolution." *Nature* **386**(6624): 463-71.
- Habelhah, H., K. Shah, et al. (2001). "Identification of new JNK substrate using ATP pocket mutant JNK and a corresponding ATP analogue." *J Biol Chem* **276**(21): 18090-5.
- Haber, D. A. and J. Settleman (2007). "Cancer: drivers and passengers." *Nature* **446**(7132): 145-6.
- Hahn, W. C., C. M. Counter, et al. (1999). "Creation of human tumour cells with defined genetic elements." *Nature* **400**(6743): 464-8.
- Hakem, R., A. Hakem, et al. (1998). "Differential requirement for caspase 9 in apoptotic pathways in vivo." *Cell* **94**(3): 339-52.
- Hamilton, A. and D. Baulcombe (1999). "A species of small antisense RNA in posttranscriptional gene silencing in plants." *Science* **286**: 950-952.
- Hammond, S., E. Bernstein, et al. (2000). "An RNA directed nuclease mediates post transcriptional gene silencing in drosophila cell." *Nature* **404**: 293-296.
- Han, J., Y. Jiang, et al. (1997). "Activation of the transcription factor MEF2C by the MAP kinase p38 in inflammation." *Nature* **386**(6622): 296-9.
- Hanahan, D. and R. A. Weinberg (2000). "The hallmarks of cancer." *Cell* **100**(1): 57-70.
- Hao, W., T. Takano, et al. (2006). "Induction of apoptosis by the Ste20-like kinase SLK, a germinal center kinase that activates apoptosis signal-regulating kinase and p38." *J Biol Chem* **281**(6): 3075-84.
- Harris, S. L. and A. J. Levine (2005). "The p53 pathway: positive and negative feedback loops." *Oncogene* **24**(17): 2899-908.
- Hay, B. A. and M. Guo (2003). "Coupling cell growth, proliferation, and death. Hippo weighs in." *Dev Cell* **5**(3): 361-3.
- Herrera, R. E., V. P. Sah, et al. (1996). "Altered cell cycle kinetics, gene expression, and G1 restriction point regulation in Rb-deficient fibroblasts." *Mol Cell Biol* **16**(5): 2402-7.
- Hershko, A., H. Heller, et al. (1983). "Components of ubiquitin-protein ligase system. Resolution, affinity purification, and role in protein breakdown." *J Biol Chem* **258**(13): 8206-14.
- Hochstrasser, M. (2006). "Lingering mysteries of ubiquitin-chain assembly." *Cell* **124**(1): 27-34.
- Hoffman, L., G. Pratt, et al. (1992). "Multiple forms of the 20 S multicatalytic and the 26 S ubiquitin/ATP-dependent proteases from rabbit reticulocyte lysate." *J Biol Chem* **267**(31): 22362-8.
- Hsu, Y. T., K. G. Wolter, et al. (1997). "Cytosol-to-membrane redistribution of Bax and Bcl-X(L) during apoptosis." *Proc Natl Acad Sci U S A* **94**(8): 3668-72.
- Hsu, Y. T. and R. J. Youle (1998). "Bax in murine thymus is a soluble monomeric protein that displays differential detergent-induced conformations." *J Biol Chem* **273**(17): 10777-83.
- Hu, M. C., W. R. Qiu, et al. (1996). "Human HPK1, a novel human hematopoietic progenitor kinase that activates the JNK/SAPK kinase cascade." *Genes Dev* **10**(18): 2251-64.

- Huang, C., W. Y. Ma, et al. (1999). "p38 kinase mediates UV-induced phosphorylation of p53 protein at serine 389." *J Biol Chem* **274**(18): 12229-35.
- Huppi, K., S. E. Martin, et al. (2005). "Defining and assaying RNAi in mammalian cells." *Mol Cell* **17**(1): 1-10.
- Ichijo, H. (1999). "From receptors to stress-activated MAP kinases." *Oncogene* **18**(45): 6087-93.
- Igney, F. H. and P. H. Krammer (2002). "Death and anti-death: tumour resistance to apoptosis." *Nat Rev Cancer* **2**(4): 277-88.
- Igney, F. H. and P. H. Krammer (2002). "Immune escape of tumors: apoptosis resistance and tumor counterattack." *J Leukoc Biol* **71**(6): 907-20.
- Iwasaka, T., M. Oh-uchida, et al. (1993). "Correlation between HPV positivity and state of the p53 gene in cervical carcinoma cell lines." *Gynecol Oncol* **48**(1): 104-9.
- Jiang, Y., H. Gram, et al. (1997). "Characterization of the structure and function of the fourth member of p38 group mitogen-activated protein kinases, p38delta." *J Biol Chem* **272**(48): 30122-8.
- Johnson, G. L. and K. Nakamura (2007). "The c-jun kinase/stress-activated pathway: Regulation, function and role in human disease." *Biochim Biophys Acta*.
- Johnson, R. S., B. van Lingen, et al. (1993). "A null mutation at the c-jun locus causes embryonic lethality and retarded cell growth in culture." *Genes Dev* **7**(7B): 1309-17.
- Jurgensmeier, J. M., Z. Xie, et al. (1998). "Bax directly induces release of cytochrome c from isolated mitochondria." *Proc Natl Acad Sci U S A* **95**(9): 4997-5002.
- Kamata, H., S. Honda, et al. (2005). "Reactive oxygen species promote TNFalpha-induced death and sustained JNK activation by inhibiting MAP kinase phosphatases." *Cell* **120**(5): 649-61.
- Kamath, R. S., A. G. Fraser, et al. (2003). "Systematic functional analysis of the *Caenorhabditis elegans* genome using RNAi." *Nature* **421**(6920): 231-7.
- Kelland, L. R. (2000). "Preclinical perspectives on platinum resistance." *Drugs* **59 Suppl 4**: 1-8; discussion 37-8.
- Kerr, J. F. (2002). "History of the events leading to the formulation of the apoptosis concept." *Toxicology* **181-182**: 471-4.
- Kerr, J. F., A. H. Wyllie, et al. (1972). "Apoptosis: a basic biological phenomenon with wide-ranging implications in tissue kinetics." *Br J Cancer* **26**(4): 239-57.
- Kiefer, F., L. A. Tibbles, et al. (1996). "HPK1, a hematopoietic protein kinase activating the SAPK/JNK pathway." *Embo J* **15**(24): 7013-25.
- Kim, H. S. and M. S. Lee (2007). "STAT1 as a key modulator of cell death." *Cell Signal* **19**(3): 454-65.
- Kinzler, K. W. and B. Vogelstein (1996). "Lessons from hereditary colorectal cancer." *Cell* **87**(2): 159-70.
- Kisselev, A. F., T. N. Akopian, et al. (1999). "The sizes of peptides generated from protein by mammalian 26 and 20 S proteasomes. Implications for understanding the degradative mechanism and antigen presentation." *J Biol Chem* **274**(6): 3363-71.
- Kluck, R. M., E. Bossy-Wetzler, et al. (1997). "The release of cytochrome c from mitochondria: a primary site for Bcl-2 regulation of apoptosis." *Science* **275**(5303): 1132-6.
- Kothakota, S., T. Azuma, et al. (1997). "Caspase-3-generated fragment of gelsolin: effector of morphological change in apoptosis." *Science* **278**(5336): 294-8.
- Kovarik, P., D. Stoiber, et al. (1999). "Stress-induced phosphorylation of STAT1 at Ser727 requires p38 mitogen-activated protein kinase whereas IFN-gamma uses a different signaling pathway." *Proc Natl Acad Sci U S A* **96**(24): 13956-61.

- Kyriakis, J. M. (1999). "Signaling by the germinal center kinase family of protein kinases." *J Biol Chem* **274**(9): 5259-62.
- Lei, K. and R. J. Davis (2003). "JNK phosphorylation of Bim-related members of the Bcl2 family induces Bax-dependent apoptosis." *Proc Natl Acad Sci U S A* **100**(5): 2432-7.
- Lengauer, C., K. W. Kinzler, et al. (1998). "Genetic instabilities in human cancers." *Nature* **396**(6712): 643-9.
- Lennon, G., C. Auffray, et al. (1996). "The I.M.A.G.E. Consortium: an integrated molecular analysis of genomes and their expression." *Genomics* **33**(1): 151-2.
- Lev, S., H. Moreno, et al. (1995). "Protein tyrosine kinase PYK2 involved in Ca(2+)-induced regulation of ion channel and MAP kinase functions." *Nature* **376**(6543): 737-45.
- Li, K., Y. Li, et al. (2000). "Cytochrome c deficiency causes embryonic lethality and attenuates stress-induced apoptosis." *Cell* **101**(4): 389-99.
- Lindsten, T., A. J. Ross, et al. (2000). "The combined functions of proapoptotic Bcl-2 family members bak and bax are essential for normal development of multiple tissues." *Mol Cell* **6**(6): 1389-99.
- Liu, G., Y. Zhang, et al. (2002). "Phosphorylation of 4E-BP1 is mediated by the p38/MSK1 pathway in response to UVB irradiation." *J Biol Chem* **277**(11): 8810-6.
- Liu, J., M. A. Carmell, et al. (2004). "Argonaute2 is the catalytic engine of mammalian RNAi." *Science* **305**(5689): 1437-41.
- Lowe, S. W. and A. W. Lin (2000). "Apoptosis in cancer." *Carcinogenesis* **21**(3): 485-95.
- Lowe, S. W., H. E. Ruley, et al. (1993). "p53-dependent apoptosis modulates the cytotoxicity of anticancer agents." *Cell* **74**(6): 957-67.
- MacKeigan, J. P., L. O. Murphy, et al. (2005). "Sensitized RNAi screen of human kinases and phosphatases identifies new regulators of apoptosis and chemoresistance." *Nat Cell Biol* **7**(6): 591-600.
- MacLaren, A., E. J. Black, et al. (2004). "c-Jun-deficient cells undergo premature senescence as a result of spontaneous DNA damage accumulation." *Mol Cell Biol* **24**(20): 9006-18.
- Martinez, J. and T. Tuschl (2004). "RISC is a 5' phosphomonoester-producing RNA endonuclease." *Genes Dev* **18**(9): 975-80.
- Martinou, J. C. and D. R. Green (2001). "Breaking the mitochondrial barrier." *Nat Rev Mol Cell Biol* **2**(1): 63-7.
- McKay, B. C., C. Becerril, et al. (2001). "P53 plays a protective role against UV- and cisplatin-induced apoptosis in transcription-coupled repair proficient fibroblasts." *Oncogene* **20**(46): 6805-8.
- McKilligin, E. and D. J. Grainger (2001). "Cell volume and rate of proliferation, but not protein expression pattern, distinguish pup/intimal smooth muscle cells from subcultured adult smooth muscle cells." *Cell Prolif* **34**(5): 275-92.
- Meister, G., M. Landthaler, et al. (2004). "Human Argonaute2 Mediates RNA Cleavage Targeted by miRNAs and siRNAs." *Molecular Cell* **15**: 185-197.
- Melino, G. (2005). "Discovery of the ubiquitin proteasome system and its involvement in apoptosis." *Cell Death Differ* **12**(9): 1155-7.
- Moffat, J., D. A. Grueneberg, et al. (2006). "A lentiviral RNAi library for human and mouse genes applied to an arrayed viral high-content screen." *Cell* **124**(6): 1283-98.
- Moffat, J. and D. M. Sabatini (2006). "Building mammalian signalling pathways with RNAi screens." *Nat Rev Mol Cell Biol* **7**(3): 177-87.
- Molinari, M., J. Anagli, et al. (1995). "PEST sequences do not influence substrate susceptibility to calpain proteolysis." *J Biol Chem* **270**(5): 2032-5.
- Montagne, J., M. J. Stewart, et al. (1999). "Drosophila S6 kinase: a regulator of cell size." *Science* **285**(5436): 2126-9.

- Moriguchi, T., F. Toyoshima, et al. (1996). "Purification and identification of a major activator for p38 from osmotically shocked cells. Activation of mitogen-activated protein kinase kinase 6 by osmotic shock, tumor necrosis factor-alpha, and H₂O₂." *J Biol Chem* **271**(43): 26981-8.
- Morrison, D. K. and R. J. Davis (2003). "Regulation of MAP kinase signaling modules by scaffold proteins in mammals." *Annu Rev Cell Dev Biol* **19**: 91-118.
- Mudgett, J. S., J. Ding, et al. (2000). "Essential role for p38alpha mitogen-activated protein kinase in placental angiogenesis." *Proc Natl Acad Sci U S A* **97**(19): 10454-9.
- Musti, A. M., M. Treier, et al. (1997). "Reduced ubiquitin-dependent degradation of c-Jun after phosphorylation by MAP kinases." *Science* **275**(5298): 400-2.
- Nechushtan, A., C. L. Smith, et al. (1999). "Conformation of the Bax C-terminus regulates subcellular location and cell death." *Embo J* **18**(9): 2330-41.
- Nijman, S. M., M. P. Luna-Vargas, et al. (2005). "A genomic and functional inventory of deubiquitinating enzymes." *Cell* **123**(5): 773-86.
- Nolan Lab Group, S. (2007). "Genetic Screens in Mammalian Cells using Retroviruses " <http://www.stanford.edu/group/nolan/screens/screens.html>.
- Norbury, C. J. and B. Zhivotovsky (2004). "DNA damage-induced apoptosis." *Oncogene* **23**(16): 2797-808.
- Okigaki, M., C. Davis, et al. (2003). "Pyk2 regulates multiple signaling events crucial for macrophage morphology and migration." *Proc Natl Acad Sci U S A* **100**(19): 10740-5.
- Olayioye, M. A. (2001). "Update on HER-2 as a target for cancer therapy: intracellular signaling pathways of ErbB2/HER-2 and family members." *Breast Cancer Res* **3**(6): 385-9.
- Paddison, P. J., A. A. Caudy, et al. (2002). "Short hairpin RNAs (shRNAs) induce sequence-specific silencing in mammalian cells." *Genes Dev* **16**(8): 948-58.
- Pfaffl, M. W. (2001). "A new mathematical model for relative quantification in real-time RT-PCR." *Nucleic Acids Res* **29**(9): e45.
- Pickart, C. and M. Eddins (2004). "Ubiquitin: structures, functions, mechanisms." *Biochimica et Biophysica*
- Porras, A., S. Zuluaga, et al. (2004). "P38 alpha mitogen-activated protein kinase sensitizes cells to apoptosis induced by different stimuli." *Mol Biol Cell* **15**(2): 922-33.
- Pothof, J., G. van Haaften, et al. (2003). "Identification of genes that protect the *C. elegans* genome against mutations by genome-wide RNAi." *Genes Dev* **17**(4): 443-8.
- Pulverer, B. J., J. M. Kyriakis, et al. (1991). "Phosphorylation of c-jun mediated by MAP kinases." *Nature* **353**(6345): 670-4.
- Raman, M. and M. H. Cobb (2003). "MAP kinase modules: many roads home." *Curr Biol* **13**(22): R886-8.
- Ramjaun, A. R., A. Angers, et al. (2001). "Endophilin regulates JNK activation through its interaction with the germinal center kinase-like kinase." *J Biol Chem* **276**(31): 28913-9.
- Rampino, N. (1997). "Somatic frameshift mutations in the BAX gene in colon cancers of the microsatellite mutator phenotype." *Science* **275**: 967-969.
- Rechsteiner, M. and S. W. Rogers (1996). "PEST sequences and regulation by proteolysis." *Trends Biochem Sci* **21**(7): 267-71.
- Reed, J. C., J. M. Jurgensmeier, et al. (1998). "Bcl-2 family proteins and mitochondria." *Biochim Biophys Acta* **1366**(1-2): 127-37.
- Reiling, J. H. and D. M. Sabatini (2006). "Stress and mTOR signaling." *Oncogene* **25**(48): 6373-83.
- Renan, M. J. (1993). "How many mutations are required for tumorigenesis? Implications from human cancer data." *Mol Carcinog* **7**(3): 139-46.

- Rhee, S. H., B. W. Jones, et al. (2003). "Toll-like receptors 2 and 4 activate STAT1 serine phosphorylation by distinct mechanisms in macrophages." *J Biol Chem* **278**(25): 22506-12.
- Rhodes, D. R., S. Kalyana-Sundaram, et al. (2007). "Oncomine 3.0: genes, pathways, and networks in a collection of 18,000 cancer gene expression profiles." *Neoplasia* **9**(2): 166-80.
- Rigaut, G., A. Shevchenko, et al. (1999). "A generic protein purification method for protein complex characterization and proteome exploration." *Nat Biotechnol* **17**(10): 1030-2.
- Rouse, J., P. Cohen, et al. (1994). "A novel kinase cascade triggered by stress and heat shock that stimulates MAPKAP kinase-2 and phosphorylation of the small heat shock proteins." *Cell* **78**(6): 1027-37.
- Sakahira, H., M. Enari, et al. (1998). "Cleavage of CAD inhibitor in CAD activation and DNA degradation during apoptosis." *Nature* **391**(6662): 96-9.
- Sanchez, I., R. T. Hughes, et al. (1994). "Role of SAPK/ERK kinase-1 in the stress-activated pathway regulating transcription factor c-Jun." *Nature* **372**(6508): 794-8.
- Sandoval, A., N. Oviedo, et al. (2006). "Two PEST-like motifs regulate Ca²⁺/calpain-mediated cleavage of the CaVbeta3 subunit and provide important determinants for neuronal Ca²⁺ channel activity." *Eur J Neurosci* **23**(9): 2311-20.
- Sanger "The Cancer Genome Project." <http://www.sanger.ac.uk/genetics/CGP/>.
- Savill, J. and V. Fadok (2000). "Corpse clearance defines the meaning of cell death." *Nature* **407**(6805): 784-8.
- Scavo, L. M., R. Ertsey, et al. (1998). "Apoptosis in the development of rat and human fetal lungs." *Am J Respir Cell Mol Biol* **18**(1): 21-31.
- Scheffner, M., J. M. Huibregtse, et al. (1993). "The HPV-16 E6 and E6-AP complex functions as a ubiquitin-protein ligase in the ubiquitination of p53." *Cell* **75**(3): 495-505.
- Scheffner, M., U. Nuber, et al. (1995). "Protein ubiquitination involving an E1-E2-E3 enzyme ubiquitin thioester cascade." *Nature* **373**(6509): 81-3.
- Scherer, D. C., J. A. Brockman, et al. (1995). "Signal-induced degradation of I kappa B alpha requires site-specific ubiquitination." *Proc Natl Acad Sci U S A* **92**(24): 11259-63.
- Schlesinger, D. H., G. Goldstein, et al. (1975). "The complete amino acid sequence of ubiquitin, an adenylate cyclase stimulating polypeptide probably universal in living cells." *Biochemistry* **14**(10): 2214-8.
- Schreiber, M., A. Kolbus, et al. (1999). "Control of cell cycle progression by c-Jun is p53 dependent." *Genes Dev* **13**(5): 607-19.
- Schulze-Luehrmann, J., B. Santner-Nanan, et al. (2002). "Hematopoietic progenitor kinase 1 supports apoptosis of T lymphocytes." *Blood* **100**(3): 954-60.
- Schwarz, A., R. Bhardwaj, et al. (1995). "Ultraviolet-B-induced apoptosis of keratinocytes: evidence for partial involvement of tumor necrosis factor-alpha in the formation of sunburn cells." *J Invest Dermatol* **104**(6): 922-7.
- Sells, M. A., U. G. Knaus, et al. (1997). "Human p21-activated kinase (Pak1) regulates actin organization in mammalian cells." *Curr Biol* **7**(3): 202-10.
- Shah, K., Y. Liu, et al. (1997). "Engineering unnatural nucleotide specificity for Rous sarcoma virus tyrosine kinase to uniquely label its direct substrates." *Proc Natl Acad Sci U S A* **94**(8): 3565-70.
- Sharp, P., C. Novina, et al. (2003). "Killing the Messenger: Short RNAs that Silence Gene Expression." *Nature Reviews Molecular Cell Biology* **4**: 457-467.
- Shay, J. W. and S. Bacchetti (1997). "A survey of telomerase activity in human cancer." *Eur J Cancer* **33**(5): 787-91.

- Shi, C. S., N. N. Huang, et al. (2006). "The mitogen-activated protein kinase kinase kinase GCKR positively regulates canonical and noncanonical Wnt signaling in B lymphocytes." *Mol Cell Biol* **26**(17): 6511-21.
- Shi, C. S. and J. H. Kehrl (2003). "Tumor necrosis factor (TNF)-induced germinal center kinase-related (GCKR) and stress-activated protein kinase (SAPK) activation depends upon the E2/E3 complex Ubc13-Uev1A/TNF receptor-associated factor 2 (TRAF2)." *J Biol Chem* **278**(17): 15429-34.
- Shi, C. S., A. Leonardi, et al. (1999). "TNF-mediated activation of the stress-activated protein kinase pathway: TNF receptor-associated factor 2 recruits and activates germinal center kinase related." *J Immunol* **163**(6): 3279-85.
- Shi, C. S., J. M. Tuscano, et al. (1999). "GCKR links the Bcr-Abl oncogene and Ras to the stress-activated protein kinase pathway." *Blood* **93**(4): 1338-45.
- Shi, Y. (2002). "Mechanisms of caspase activation and inhibition during apoptosis." *Mol Cell* **9**(3): 459-70.
- Shibata, S., S. Kyuwa, et al. (1994). "Apoptosis induced in mouse hepatitis virus-infected cells by a virus-specific CD8⁺ cytotoxic T-lymphocyte clone." *J Virol* **68**(11): 7540-5.
- Shima, H., M. Pende, et al. (1998). "Disruption of the p70(s6k)/p85(s6k) gene reveals a small mouse phenotype and a new functional S6 kinase." *Embo J* **17**(22): 6649-59.
- Shui, J. W., J. S. Boomer, et al. (2007). "Hematopoietic progenitor kinase 1 negatively regulates T cell receptor signaling and T cell-mediated immune responses." *Nat Immunol* **8**(1): 84-91.
- Shumway, S. D., M. Maki, et al. (1999). "The PEST domain of IkappaBalpha is necessary and sufficient for in vitro degradation by mu-calpain." *J Biol Chem* **274**(43): 30874-81.
- Sijen, T., J. Fleenor, et al. (2001). "On the role of RNA amplification in dsRNA-triggered gene silencing." *Cell* **107**(4): 465-76.
- Sjoblom, T., S. Jones, et al. (2006). "The consensus coding sequences of human breast and colorectal cancers." *Science* **314**(5797): 268-74.
- Soengas, M. S. (2001). "Inactivation of the apoptosis effector Apaf-1 in malignant melanoma." *Nature* **409**: 207-211.
- Song, J. J., S. K. Smith, et al. (2004). "Crystal structure of Argonaute and its implications for RISC slicer activity." *Science* **305**(5689): 1434-7.
- Sporn, M. B. (1996). "The war on cancer." *Lancet* **347**(9012): 1377-81.
- Stark, G., M. Kerr, et al. (1998). "How cells respond to interferons." *Annual Review of Biochemistry* **67**: 227-264.
- Stein, B., H. Brady, et al. (1996). "Cloning and characterization of MEK6, a novel member of the mitogen-activated protein kinase kinase cascade." *J Biol Chem* **271**(19): 11427-33.
- Stephanou, A. and D. S. Latchman (2005). "Opposing actions of STAT-1 and STAT-3." *Growth Factors* **23**(3): 177-82.
- Strange, K., J. Denton, et al. (2006). "Ste20-type kinases: evolutionarily conserved regulators of ion transport and cell volume." *Physiology (Bethesda)* **21**: 61-8.
- Strasser, A., A. W. Harris, et al. (1990). "Novel primitive lymphoid tumours induced in transgenic mice by cooperation between myc and bcl-2." *Nature* **348**(6299): 331-3.
- Strasser, A., L. O'Connor, et al. (2000). "Apoptosis signaling." *Annu Rev Biochem* **69**: 217-45.
- Sulston, J. E. and H. R. Horvitz (1977). "Post-embryonic cell lineages of the nematode, *Caenorhabditis elegans*." *Dev Biol* **56**(1): 110-56.
- Suzuki, M., R. J. Youle, et al. (2000). "Structure of Bax: coregulation of dimer formation and intracellular localization." *Cell* **103**(4): 645-54.

- Tahbaz, N., F. A. Kolb, et al. (2004). "Characterization of the interactions between mammalian PAZ PIWI domain proteins and Dicer." *EMBO Rep* **5**(2): 189-94.
- Teitz, T. (2000). "Caspase-8 is deleted or silenced preferentially in childhood neuroblastomas with amplification of MYCN." *Nature Med* **6**: 529-535.
- Thornberry, N. A., T. A. Rano, et al. (1997). "A combinatorial approach defines specificities of members of the caspase family and granzyme B. Functional relationships established for key mediators of apoptosis." *J Biol Chem* **272**(29): 17907-11.
- Thrower, J. S., L. Hoffman, et al. (2000). "Recognition of the polyubiquitin proteolytic signal." *Embo J* **19**(1): 94-102.
- Tibbles, L. A. and J. R. Woodgett (1999). "The stress-activated protein kinase pathways." *Cell Mol Life Sci* **55**(10): 1230-54.
- Tomari, Y., C. Matranga, et al. (2004). "A protein sensor for siRNA asymmetry." *Science* **306**(5700): 1377-80.
- Tournier, C., C. Dong, et al. (2001). "MKK7 is an essential component of the JNK signal transduction pathway activated by proinflammatory cytokines." *Genes Dev* **15**(11): 1419-26.
- Tournier, C., P. Hess, et al. (2000). "Requirement of JNK for stress-induced activation of the cytochrome c-mediated death pathway." *Science* **288**(5467): 870-4.
- Tournier, C., A. J. Whitmarsh, et al. (1997). "Mitogen-activated protein kinase kinase 7 is an activator of the c-Jun NH2-terminal kinase." *Proc Natl Acad Sci U S A* **94**(14): 7337-42.
- Treier, M., L. M. Staszewski, et al. (1994). "Ubiquitin-dependent c-Jun degradation in vivo is mediated by the delta domain." *Cell* **78**(5): 787-98.
- Tsujimoto, Y., J. Cossman, et al. (1985). "Involvement of the bcl-2 gene in human follicular lymphoma." *Science* **228**(4706): 1440-3.
- Tsurumi, C., N. Ishida, et al. (1995). "Degradation of c-Fos by the 26S proteasome is accelerated by c-Jun and multiple protein kinases." *Mol Cell Biol* **15**(10): 5682-7.
- Tuschl, T. and A. Borkhardt (2002). "Small interfering RNAs: A Revolutionary tool for the analysis of gene function and gene therapy." *Molecular Interventions* **2**(3): 158-163.
- Uddin, S., A. Sassano, et al. (2002). "Protein kinase C-delta (PKC-delta) is activated by type I interferons and mediates phosphorylation of Stat1 on serine 727." *J Biol Chem* **277**(17): 14408-16.
- Van Laethem, A., S. Van Kelst, et al. (2004). "Activation of p38 MAPK is required for Bax translocation to mitochondria, cytochrome c release and apoptosis induced by UVB irradiation in human keratinocytes." *Faseb J* **18**(15): 1946-8.
- van Nocker, S., S. Sadis, et al. (1996). "The multiubiquitin-chain-binding protein Mub1 is a component of the 26S proteasome in *Saccharomyces cerevisiae* and plays a nonessential, substrate-specific role in protein turnover." *Mol Cell Biol* **16**(11): 6020-8.
- Ventura, A., A. Meissner, et al. (2004). "Cre-lox-regulated conditional RNA interference from transgenes." *Proc Natl Acad Sci U S A* **101**(28): 10380-5.
- Ventura, J. J., A. Hubner, et al. (2006). "Chemical genetic analysis of the time course of signal transduction by JNK." *Mol Cell* **21**(5): 701-10.
- Vermeulen, K., D. R. Van Bockstaele, et al. (2005). "Apoptosis: mechanisms and relevance in cancer." *Ann Hematol* **84**(10): 627-39.
- Vousden, K. H. and X. Lu (2002). "Live or let die: the cell's response to p53." *Nat Rev Cancer* **2**(8): 594-604.
- Wang, X. Z. and D. Ron (1996). "Stress-induced phosphorylation and activation of the transcription factor CHOP (GADD153) by p38 MAP Kinase." *Science* **272**(5266): 1347-9.

- Wen, Z., Z. Zhong, et al. (1995). "Maximal activation of transcription by Stat1 and Stat3 requires both tyrosine and serine phosphorylation." *Cell* **82**(2): 241-50.
- Weng, Q. P., M. Kozlowski, et al. (1998). "Regulation of the p70 S6 kinase by phosphorylation in vivo. Analysis using site-specific anti-phosphopeptide antibodies." *J Biol Chem* **273**(26): 16621-9.
- Weston, C. R. and R. J. Davis (2007). "The JNK signal transduction pathway." *Curr Opin Cell Biol* **19**(2): 142-9.
- Whitfield, J., S. J. Neame, et al. (2001). "Dominant-negative c-Jun promotes neuronal survival by reducing BIM expression and inhibiting mitochondrial cytochrome c release." *Neuron* **29**(3): 629-43.
- Willis, S. N., J. I. Fletcher, et al. (2007). "Apoptosis initiated when BH3 ligands engage multiple Bcl-2 homologs, not Bax or Bak." *Science* **315**(5813): 856-9.
- Wittenberg, C. and R. La Valle (2003). "Cell-cycle-regulatory elements and the control of cell differentiation in the budding yeast." *Bioessays* **25**(9): 856-67.
- Wolter, K. G., Y. T. Hsu, et al. (1997). "Movement of Bax from the cytosol to mitochondria during apoptosis." *J Cell Biol* **139**(5): 1281-92.
- Woo, M., R. Hakem, et al. (1998). "Essential contribution of caspase 3/CPP32 to apoptosis and its associated nuclear changes." *Genes Dev* **12**(6): 806-19.
- Wu, C., M. Whiteway, et al. (1995). "Molecular characterization of Ste20p, a potential mitogen-activated protein or extracellular signal-regulated kinase kinase (MEK) kinase kinase from *Saccharomyces cerevisiae*." *J Biol Chem* **270**(27): 15984-92.
- Wu, J. J., R. J. Roth, et al. (2006). "Mice lacking MAP kinase phosphatase-1 have enhanced MAP kinase activity and resistance to diet-induced obesity." *Cell Metab* **4**(1): 61-73.
- Xiong, W. and J. T. Parsons (1997). "Induction of apoptosis after expression of PYK2, a tyrosine kinase structurally related to focal adhesion kinase." *J Cell Biol* **139**(2): 529-39.
- Yang, D., C. Tournier, et al. (1997). "Targeted disruption of the MKK4 gene causes embryonic death, inhibition of c-Jun NH2-terminal kinase activation, and defects in AP-1 transcriptional activity." *Proc Natl Acad Sci U S A* **94**(7): 3004-9.
- Yang, D. D., C. Y. Kuan, et al. (1997). "Absence of excitotoxicity-induced apoptosis in the hippocampus of mice lacking the *Jnk3* gene." *Nature* **389**(6653): 865-70.
- Yiu, S. M., P. W. Wong, et al. (2005). "Filtering of ineffective siRNAs and improved siRNA design tool." *Bioinformatics* **21**(2): 144-51.
- Yoshida, H., Y. Y. Kong, et al. (1998). "Apaf1 is required for mitochondrial pathways of apoptosis and brain development." *Cell* **94**(6): 739-50.
- Yuan, J. (1996). "Evolutionary conservation of a genetic pathway of programmed cell death." *J Cell Biochem* **60**(1): 4-11.
- Zamore, P., T. Tuschl, et al. (2000). "RNAi: double stranded RNA directs the ATP dependent cleavage of mRNA at 21 to 23 nucleotide intervals." *Cell* **101**: 25-33.
- Zamore, P. D. (2002). "Ancient pathways programmed by small RNAs." *Science* **296**(5571): 1265-9.
- Zamzami, N. and G. Kroemer (2001). "The mitochondrion in apoptosis: how Pandora's box opens." *Nat Rev Mol Cell Biol* **2**(1): 67-71.
- Zarubin, T. and J. Han (2005). "Activation and signaling of the p38 MAP kinase pathway." *Cell Res* **15**(1): 11-8.
- Zenz, R., H. Scheuch, et al. (2003). "c-Jun regulates eyelid closure and skin tumor development through EGFR signaling." *Dev Cell* **4**(6): 879-89.
- Zhang, L., S. H. Yang, et al. (2007). "Rev7/MAD2B Links c-Jun N-Terminal Protein Kinase Pathway Signaling to Activation of the Transcription Factor Elk-1." *Mol Cell Biol* **27**(8): 2861-9.

-
- Zhang, Y., J. N. Blattman, et al. (2004). "Regulation of innate and adaptive immune responses by MAP kinase phosphatase 5." *Nature* **430**(7001): 793-7.
- Zhong, J. and J. M. Kyriakis (2004). "Germinal center kinase is required for optimal Jun N-terminal kinase activation by Toll-like receptor agonists and is regulated by the ubiquitin proteasome system and agonist-induced, TRAF6-dependent stabilization." *Mol Cell Biol* **24**(20): 9165-75.
- Zhou, B. B. and S. J. Elledge (2000). "The DNA damage response: putting checkpoints in perspective." *Nature* **408**(6811): 433-9.
- Zihni, C., C. Mitsopoulos, et al. (2006). "Prostate-derived sterile 20-like kinase 2 (PSK2) regulates apoptotic morphology via C-Jun N-terminal kinase and Rho kinase-1." *J Biol Chem* **281**(11): 7317-23.
- Zou, H., W. J. Henzel, et al. (1997). "Apaf-1, a human protein homologous to *C. elegans* CED-4, participates in cytochrome c-dependent activation of caspase-3." *Cell* **90**(3): 405-13.